AD_____

GRANT NUMBER DAMD17-94-J-4389

TITLE: Optimization of Technique Factors for Conventional Mammography

PRINCIPAL INVESTIGATOR: R. Edward Hendrick, Ph.D.

CONTRACTING ORGANIZATION: University of Colorado
Health Sciences Center
Denver, Colorado 80262

REPORT DATE: March 1998

TYPE OF REPORT: Final

PREPARED FOR: Commander
U.S. Army Medical Research and Materiel Command
Fort Detrick, Maryland 21702-5012

REPORT DOCUMENTATION PAGE

Form Approved
OMB No. 0704-0188

1. AGENCY USE ONLY *(Leave blank)*	2. REPORT DATE	3. REPORT TYPE AND DATES COVERED
	March 1998	Final (15 Aug 94 - 14 Feb 98)

4. TITLE AND SUBTITLE

Optimization of Technique Factors for Conventional Mammography

5. FUNDING NUMBERS

DAMD17-94-J-4389

6. AUTHOR(S)

R. Edward Hendrick, Ph.D.

7. PERFORMING ORGANIZATION NAME(S) AND ADDRESS(ES)

Univeristy of Colorado
Health Sciences Center
Denver, Colorado 80262

8. PERFORMING ORGANIZATION REPORT NUMBER

9. SPONSORING / MONITORING AGENCY NAME(S) AND ADDRESS(ES)

U.S. Army Medical Research and Materiel Command
Fort Detrick, Maryland 21702-5012

10. SPONSORING / MONITORING AGENCY REPORT NUMBER

11. SUPPLEMENTARY NOTES

12a. DISTRIBUTION / AVAILABILITY STATEMENT

Approved for public release; distribution unlimited

13. ABSTRACT *(Maximum 200 words)*

This final report presents progress achieved during a three and one-half year postdoctoral research project to determine the optimum technique factors for screen-film mammography. This work project has analyzed the effects of mammography film, processing conditions, and technique factor selection (target-filtration, kVp, and resultant film optical densities) on image contrast and low-contrast lesion detection. New methods of evaluating film, processing, and technique factors were developed, leading to new quality control tests and a simple set of rules for optimizing technique factors in screen-film mammography. These rules were applied to approximately two dozen clinical sites involved in the Colorado Mammography Advocacy Project (CMAP). Improved technique factors were recommended and the resulting improvement in image quality at CMAP sites has been evaluated.

14. SUBJECT TERMS		15. NUMBER OF PAGES
Breast Cancer	breast imaging technology mammography system performance mammography, image quality	100
		16. PRICE CODE

17. SECURITY CLASSIFICATION OF REPORT	18. SECURITY CLASSIFICATION OF THIS PAGE	19. SECURITY CLASSIFICATION OF ABSTRACT	20. LIMITATION OF ABSTRACT
Unclassified	Unclassified	Unclassified	Unlimited

FOREWORD

Opinions, interpretations, conclusions and recommendations are those of the author and are not necessarily endorsed by the U.S. Army.

____ Where copyrighted material is quoted, permission has been obtained to use such material.

____ Where material from documents designated for limited distribution is quoted, permission has been obtained to use the material.

__✓__ Citations of commercial organizations and trade names in this report do not constitute an official Department of Army endorsement or approval of the products or services of these organizations.

____ In conducting research using animals, the investigator(s) adhered to the "Guide for the Care and Use of Laboratory Animals," prepared by the Committee on Care and Use of Laboratory Animals of the Institute of Laboratory Resources, National Research Council (NIH Publication No. 86-23, Revised 1985).

____ For the protection of human subjects, the investigator(s) adhered to policies of applicable Federal Law 45 CFR 46.

____ In conducting research utilizing recombinant DNA technology, the investigator(s) adhered to current guidelines promulgated by the National Institutes of Health.

____ In the conduct of research utilizing recombinant DNA, the investigator(s) adhered to the NIH Guidelines for Research Involving Recombinant DNA Molecules.

____ In the conduct of research involving hazardous organisms, the investigator(s) adhered to the CDC-NIH Guide for Biosafety in Microbiological and Biomedical Laboratories.

R E Hendrick 3/12/98

PI - Signature Date

TABLE OF CONTENTS

INTRODUCTION

This final report summarizes work performed during a three-year postdoctoral fellowship grant on optimization of technical factors in screen-film mammography. This work has led to new techniques for analyzing film-processing contrast, new phantoms for evaluating mammography image quality, and extensive contrast-detail phantom results that have resulted in a simple prescription for selecting technique factors to optimize image contrast and low-contrast lesion detection in screen-film mammography.

Optimizing image quality in screen-film mammography requires separately optimizing several different components of the mammographic imaging system. These include, but are not limited to, maximizing film and processing contrast, setting the range of film optical densities to maximize low-contrast lesion detection, and selecting technique factors that maximize low-contrast lesion detection in clinical images. These topics are the subject of this research project and this report. Additional determinants of mammography image quality that are not the subject of this research project include positioning, compression, image noise, image artifacts, and clinical film viewing conditions.

This report is divided into three parts: 1) assessing film-processing contrast in mammography, 2) understanding the effects of clinical imaging conditions (such as film optical density, target-filter materials, and kVp) on image contrast and low-contrast lesion detection, and 3) assessing the effects of recommended technique factor changes on image quality at selected mammography sites. A separate subsection of this Introduction is included for each area. Each of these areas is dealt with separately in the Body of Report, with separate items in each of three sections: Methods, Results and Discussion sections.

1. Film and Processing Contrast

Light sensitometry is a useful quality control tool in mammography **[1-3]**. It involves exposing mammography film to a range of discrete light levels spanning the range of sensitivity of the mammography film. The processed sensitometric film contains a range of optical densities from minimum to maximum, with a sufficient number of intermediate optical density steps to characterize the response of the processed film to light exposure. The Hurter and Driffield (H&D) curve for the film (and processing) is produced by plotting the optical density of each step versus step number (or the logarithm of light exposure to each step). H&D curves predate x-ray imaging as a method of graphically describing the response of processed photographic emulsions to light exposure **[4]**.

In mammography, light sensitometry is used routinely as a quality control test to assess the constancy of film processing **[1,3].** By using the same sensitometer and densitometer and by using a single box of control film set aside for QC purposes (to eliminate possible film emulsion differences from batch to batch), changes in film processing conditions can be isolated. A sheet of control film is exposed using the same sensitometer and sensitometer settings each day mammography is performed. The film is processed immediately in the mammography film processor and optical densities are measured from selected steps on the film using the densitometer. Three sensitometric parameters are recorded each day: a mid-density step (the step with OD closest to 1.20), a density difference parameter (the OD difference between the step with OD closest to 2.20 and the step with OD closest to, but not less than, 0.45), and the base plus fog level (the OD in step 1). Measuring and plotting these three parameters allows a facility to monitor its film processing consistency from day to day. A crossover procedure from one box of control film to the next provides a method to remove the effects of different film emulsion batches, so that processor performance can be tracked over periods longer than the 100 day duration of one box of control film.

The daily processor sensitometry described above has become the standard in mammography QC, implemented in 1990 as a voluntary standard by the ACR Mammography Accreditation Program and adopted by reference as a required QC procedure under the Mammography Quality Standards Act (MQSA) Interim Rules **[5,6]**.

A weakness of routine processor sensitometry is that it assesses the constancy of film processing, but does not provide a method to determine the adequacy of film processing; that is, whether film processing conditions were set up properly for mammography film in the first place. In the past, mammography sites have had no way to assess the adequacy of film processing. We propose a sensitometric method based on the gamma plot to assess the adequacy of film processing. This method makes use of the fact that gamma plot results are largely unaffected by latent image fade and involves comparing gamma plots from sensitometric data from the site's processor to gamma plots from sensitometric data from a second processor optimized for the site's mammography film.

A second limitation of standard mammography QC procedures is that they do not monitor differences between control film and clinical film, nor do they monitor changes in the clinical film used for patient imaging at a facility. It has become obvious in recent years that the same mammography film type can exhibit substantial differences in sensitometric results from batch to batch. When film batches change, mammography sites can experience unexpected changes in clinical and phantom images that are not reflected in sensitometric results, since processor QC typically uses one film batch while clinical imaging uses

another. Failure to monitor changes in sensitometric performance from one batch of clinical film to another can leave site personnel surprised and puzzled when film quality changes due to emulsion changes. We provide a simple method to evaluate film emulsion changes from batch to batch, either between control film and clinical film or from one batch of clinical film to another. Unlike standard processor sensitometry, this procedure permits comparison of film contrast across the entire range of film optical densities.

A basic construct, which is not original with our work, is to plot 21-step sensitometry data in a manner that better describes the contrast properties of film and processing across the full range of optical densities. These curves have been used in the past to compare contrast from different films. The "gamma plot" or "contrast plot" does this by charting the point-to-point slope of the H&D curve between adjacent pairs of sensitometer steps, versus the average optical densities of each adjacent pair of steps. On a modern 21-step sensitometer, each step increases the light intensity output by a constant factor (approximately a square root of two) from that of the previous step. If only differences between optical densities at adjacent steps are considered, as they are in the vertical scale of the gamma plot, then those differences do not depend on the overall intensity of light output from the sensitometer; they depend only on the relative light output from step to step. As long as the relative light output from step to step keeps a constant factor (a square root of two), the gamma plot provides a reasonably sensitometer-invariant method of assessing film and processing performance, as will be demonstrated in this paper.

The hypothesis of our work on film-processing contrast is that gamma plots provide a useful quality control tool for monitoring film and processing in mammography. The gamma plot permits a method to monitor not only processing consistency, but also proper processor setup in the first place.

Gamma plots are useful because they:

1) Graphically depict the contrast produced by film and processing as a function of optical density. The height of the gamma plot curve represents the "local contrast": the amount of contrast at each optical density. This permits comparison of contrast from different film types, different film batches, and under different processing conditions over the entire range of film optical densities;

2) Provide a useful quality control tool for determining that processing is optimized for a given type of mammography film;

3) Graphically describe the range of optical densities over which maximum (or near maximum) contrast is achieved for the specific film and processing used. This can help guide automatic exposure control set-up and clinical technique factor selection;

4) Provide a useful way to compare one batch of film to another, for both control film and clinical film;

5) Provide a useful quality control tool for assessing the consistency of film contrast, including effects of both film emulsion and processing, over time;

6) Make use of data already acquired daily through processor sensitometry at every mammography facility in the U.S.;

7) Provide an assessment of film and processing that is reasonably invariant to the particular sensitometer and densitometer used, allowing comparison of film and processor performance without requiring internal standardization or calibration of sensitometers and densitometers.

Gamma plots, on the other hand, do not tell the user about:

1) Film and processing speed, since gamma plots are only based on OD differences, not on the magnitude of OD resulting from a known light exposure;

2) Screen properties, since screens are not included in gamma plot measurements;

3) The x-ray components of the imaging chain, since x-ray components are not included in gamma plot test methodology;

4) Image noise, since gamma plots are based on densitometry over large areas relative to the noise pattern in mammograms;

5) Image artifacts, unless processing artifacts are so substantial that they affect the accuracy of film sensitometry.

A single parameter based on the gamma plot is proposed as a new quantity to summarize overall film and processing contrast. This parameter, called the gamma index, A_g, is the integrated area under the gamma plot curve. It provides a concise summary of contrast provided by both film and processing over the entire range of optical densities. The gamma index, along with the optical density at a mid-density step, can be measured and charted as an overall monitor of film and processing performance.

2. Technique Factor Selection

Conventional screen-film mammography with dedicated mammography equipment is the accepted method of screening for breast cancer in women 40 years of age and over and is the primary diagnostic tool for the evaluation of

suspicious breast findings **[7]**. In 1992, it was estimated that 23.5 million mammograms were performed, approximately 99% of them using screen-film image receptors **[8].** The use of mammography has increased in the intervening years. At the same time, xeromammographic image receptors have been replaced by screen-film image receptors. Since full-field digital mammography has yet to be approved for clinical use by the FDA, screen-film mammography is the predominant clinical tool for screening and diagnostic mammography.

Recent innovations in mammography equipment, such as the addition of alternative target-filter materials to units in clinical service, have increased the range of technique factors selectable by the user **[9]**. At the same time, recent innovations in films and processing have increased the contrast and decreased the latitude of screen-film image receptors, making appropriate technique factor selection by the user even more crucial **[10].**

Previous authors have noted the problem of underexposure of mammograms and the effect of low optical densities on lesion detection in mammography **[11,12]**. In 1992, Law noted that approximately 15% of breasts in the UK Breast Screening Program of women 50-65 showed a dense structure of area 10 cm^2 or greater that was underexposed by conventional mammography **[11].** Young, et.al., performed a retrospective review of the detection rate for small breast cancers (diameter < 10 mm) and average film optical densities at 31 screening centers involved in the UK National Breast Screening Program **[12].** They found a wide range of optical densities at participating sites, with an average detection rate for small breast cancers that was significantly higher (1.7 ± 1 per 1,000) at centers using average optical densities greater than 1.2, compared to the average detection rate (of 1.2 ± 1 per 1,000) for centers using average optical densities less than 1.2.

Other researchers have used contrast-detail (CD) phantoms of different designs to study the effects of film optical densities on detection. Robson, et.al., used a contrast-detail phantom consisting of a 3 cm Perspex phantom and 3 mm contrast-detail test object to optimize optical densities on two kinds of mammography film **[13]**. They found optimum optical densities to be 1.63 -1.80 for Kodak Min-RE and 1.68-2.02 for Fuji MI-NH/HR Mammo Fine film.

This work uses a new CD phantom to evaluate optimum technique factors in screen-film mammography. This new CD phantom consists of tissue-equivalent materials and is designed to span the range of typical breast compositions and compressed breast thicknesses. Our study also includes the use of relatively new Rhodium (Rh) target and filtration materials.

Our evaluation methods focus on the ability to detect relatively small, low-contrast lesions rather than higher contrast calcifications. The primary reason for

focusing on low-contrast masses rather than calcifications is that approximately two-thirds of invasive breast cancers are detected as low-contrast masses rather than as calcifications **[14].** The smallest detail in the CD phantom is 0.25 mm, typical of the size of a larger microcalcification. Technique factors optimized for the detection of low-contrast lesions will serve well in the detection of higher contrast microcalcifications. User-selectable technique factors (target/filtration, kVp, and mAs) do not have significant effects on the limiting spatial resolution of screen-film mammography systems, so optimizing techniques for low-contrast lesion detection will not adversely affect the detection of calcifications. In fact, it can be argued that optimizing techniques such as film optical densities for the detection of small, low-contrast lesions also will improve the detection of higher-contrast calcifications. The techniques developed and employed in this work can equally well be applied to the optimization of lesion detection in full-field digital mammography, as well as to compare low-contrast lesion detection in screen-film and digital mammography. Work in those areas is in progress.

3. Effects of Recommended Technique Factor Changes

The Colorado Mammography Advocacy Project (CMAP) is a State of Colorado project that provides screening mammography at 38 sites within the Denver metropolitan area and maintains follow-up data of mammography outcomes for over 250,000 women. Between 1989 and late 1995, as part of the quality assurance of CMAP, UCHSC Radiological Sciences provided medical physics surveys of CMAP sites. A total of 207 mammography surveys were conducted over the six year period. In addition to standard ACR medical physics QC tests, standardized data were collected on processor performance, consistency of AEC performance, resulting optical densities, and resulting exposure times using the sites' clinical technique factors for 2, 4, and 6 cm thick breasts. After 1993, improved technique factors were recommended on mammography units where optical densities were too low (<1.20) for any breast thickness, where optical densities were not consistent across breast thicknesess (within a range of 0.30), or where exposure times were excessively long (> 2 seconds) for any breast thickness. In cases where these technique errors existed, a new technique chart was developed and posted on the units. This subset of CMAP sites was used to assess the effect of recommending improved technique factors by comparing subsequent site visit measurement results to previously measured results for the same unit or site.

BODY OF REPORT

This report consists of three separate sections with three subsections each:

I. METHODS

1. Film and Processing Contrast

A. Theory: Light sensitometry using a 21 step sensitometer yields optical density values for each of 21 steps on the processed mammography film: OD_i, i=1,2,...,21. The H&D curve plots $y_i = OD_i$ versus step number $x_i = i$ (or $x_i = \log(E_i)$, where E_i is the light exposure to the film under step i).

The gamma plot is constructed by plotting a different set of (x_i, y_i) pairs from the same data. In the gamma plot, yi is the slope of the H&D curve from point to point:

$$y_i = \frac{OD_{i+1} - OD_i}{\log_{10}(\text{sqrt}(2))}, \qquad [1]$$

the point-to-point change in y on the H&D curve being the difference between optical densities at adjacent steps, delta $y = OD_{i+1} - OD_i$, the point-to-point change in x on the H&D curve being the difference in the logarithm of light exposure from step to step: delta $x = \log_{10}(E_{i+1}) - \log10(E_i) = \log_{10}(E_{i+1}/E_i) = \log_{10}(\text{sqrt}(2))$. The x_i coordinate in the gamma plot is the average of optical densities at the two adjacent steps:

$$x_i = \frac{OD_{i+1} + OD_i}{2} \qquad [2]$$

for i=1, 2, ...,20, so that the slope of the H&D curve is attributed to an optical density point midway between the two adjacent points on the H&D curve.

Gamma plots more fully represent film and processing contrast over the full range of optical densities, but are more difficult to plot over time as an indicator of processor performance than simple sensitometric parameters such as mid-density or density difference. Therefore, a single parameter is proposed to characterize film contrast over the full range of optical densities. The film-processing contrast index, A_g, is defined as the area under the gamma plot curve:

$$A_g = \text{integral}_{OD_{min}}^{OD_{max}} \gamma\,(OD)d(OD), \qquad [3]$$

where OD_{min} is the base plus fog optical density of the film and OD_{max} is the maximum optical density of the film. A_g can be determined in closed form from the 21 optical density steps read from the sensitometric strip by assuming a linear interpolation between adjacent gamma plot points (or a trapezoidal approximation for the area under the gamma plot curve), yielding:

$$A_g = \frac{1}{4\log_{10}(\mathrm{sqrt}(2))} \sum_{i=1}^{19} (OD_{i+2}-OD_i)^2 . \qquad [4]$$

The sum in Eq. [4] combines the areas of the 19 trapezoids formed from the 20 gamma plot points. Interpolation between gamma plot points can be other than linear, including cubic spline interpolation using the information from a set of 4 adjacent gamma plot points and least square fits to the entire set of 20 gamma plot points. The effect of different methods of interpolating between gamma plot points on A_g was investigated.

B. Experiments: Six commonly used types of mammography film were exposed using the same 21-step sensitometer. Films were processed using the same processing conditions with 90-second total processing time, as specified by each film manufacturer. H&D curves and gamma plots were compared for each of the six film types to assess contrast over the full range of optical densities from each film. The gamma plot contrast index, A_g, was calculated for each film type using linear interpolation between gamma plot points. Conventional sensitometric parameters also were calculated: the mid-density (MD), density difference (DD), and base plus fog (B+F) as defined by the ACR QC Manuals. To permit comparison between films where the MD or DD steps shift from one film to another (because of the OD prescriptions in the ACR definition), the optical density from a single step and the density difference between two fixed steps are also listed for each film.

Sources of normal variations in gamma plots using the same film and processing conditions were determined. Sample variations of gamma plots were determined by sensitometric exposure of ten consecutive films from the same film emulsion batch. The ten films were processed under identical processing conditions by processing films in the same processor, temperature, and chemistry within a few minutes of each other. Normal temporal variations of gamma plots were determined by taking one gamma plot each week for ten weeks from a processor determined to be "in control" by standard processor sensitometry. In each case, mean gamma plot curves were constructed by averaging the vertical heights of the ten individual gamma plot curves at each OD value assuming linear interpolation between adjacent gamma plot points. Gamma plot curves representing one standard deviation above and below each

mean gamma plot curve were determined by establishing the symmetric vertical range of contrast values that included 68.3% of the individual gamma plot points at each OD value.

To investigate the range of gamma plots and A_g values obtained from clinical sites, we analyzed sensitometric strips obtained from 209 medical physics surveys conducted at 74 mammography sites in Colorado between 1990 and 1995. Each set of sensitometer data was obtained with the same sensitometer and densitometer, using the site's clinical film and processing.

The dependence of gamma plots on the specific sensitometer used was established by exposing films from the same film batch using 8 different 21-step sensitometers, processing each strip in the same manner in the same processor within a few minutes of each other. The dependence of gamma plots on the specific densitometer used was established by measuring ODs of the 21-steps of a single sensitometer strip using 9 different densitometers. In each case, gamma plots were superimposed on the same graph for comparison to the sample variations and temporal variations determined above.

The effect of latent image fade on gamma plots was studied using two different types of mammography film (Kodak MRH-1 and Min R-2000). Films from the same emulsion batch and box for each film type were exposed 1, 2, 3, 4, and 7 days prior to processing, along with a film exposed immediately before processing; gamma plots, A_g, MD, DD, and B+F values were compared for each film.

The effect of film fog on gamma plots was studied using a single type of mammography film (Kodak Min R-2000). Films from the same emulsion batch and box were exposed by a sensitometer and then placed on a darkroom counter directly beneath and approximately 4 feet from a ceiling-mounted darkroom safelight for 1, 2, 4, 8, and 16 minutes; an additional film was exposed by the sensitometer and processed immediately without exposure to the darkroom safelight. The resulting gamma plots, A_g, and conventional sensitometric parameters were compared for each film.

The effects of different developer chemistry conditions on gamma plots were studied by producing sensitometric strips with old chemistry, fresh chemistry without starter, fresh chemistry with starter, and fresh chemistry plus starter after 1, 2, and 5 days of "seasoning", which consisted of running a normal mammography schedule of approximately 20 patients (80-100 films) per day. All films were taken from the same emulsion batch.

The effect on gamma plots and A_g values of different emulsion batches of the same film type (Kodak Min R-2000) were studied by exposing films using the same sensitometer and by processing both films simultaneously in the same

processor.

The effect on gamma plots and A_g values of different emulsion batches of the same film type (Kodak Min R-2000) were studied by producing gamma plots using the same sensitometer and by processing films from three different emulsion batches one after another in the same processor.

The effects of processor developer temperature on gamma plots, A_g values, and conventional sensitometric parameters were studied by exposing films from the same box by a sensitometer and processing films at the recommended developer temperature and at 1°C steps from 25°C to 40°C.

2. Technique Factor Selection

A contrast-detail (CD) phantom of our own design was used to quantitatively evaluate image quality over a range of compressed breast thicknesses (2-6 cm) and compositions (100% fatty, 70% fatty/30% glandular, 50% fatty/50% glandular, and 30% fatty/70% glandular). The CD phantom consisted of a 9 by 9 array of low-contrast circular test objects milled into a D-shaped 1 cm thick section of breast equivalent material, to which additional 1 cm thick sections of D-shaped breast materials of different compositions were added to give the total thicknesses and compositions listed above. Each row of the CD pattern contained 9 objects at a fixed level of contrast with object diameters ranging from 0.25 mm to 4 mm. Subject contrast had nine different levels, ranging from 0.29% to 3.95%, quantitated as the attenuation difference between object and background ($e^{\mu t}$-1, where μ is the attenuation coefficient of the phantom BR-12 material at 19 keV effective beam energy, t is the thickness difference between object and background in the phantom) **(Figure 1)**.

Medical physicists were trained in scoring the CD phantom under standardized viewing conditions that included the use of completely masked CD phantom images and low ambient room light. Reviewers were instructed to read the phantom starting with the row of objects with highest contrast, and reading from largest to smallest detectable object in that row. An object was judged as "detected" if it occurred in the correct location, was generally round in shape, and was more visible than artifactual "objects" occurring elsewhere in the CD phantom, but not in the locations of the 81 test objects. Comparison of detected objects against artifacts elsewhere in the phantom was used to guard against overscoring because of prior knowledge of the location of test objects in the phantom. Once an object was too faint to detect, was not generally round in shape, or was less conspicuous than artifactual objects in the background of the phantom, counting was stopped and the number of consecutively visible objects in that row was summed. Reviewers then moved on to the next row of objects at slightly lower contrast. Only integer scores were permitted for each row, the row score indicating the number of objects visible in that row.

The CD score for each reading of each image was determined by summing the area of detected objects in contrast-detail space **(Figure 2)**. Thus, the more low-contrast objects detected, the higher the CD score. If no objects in the CD phantom were detected, a minimum score of zero would result. If all 81 objects in the CD phantom were detected, a maximum score of 17.34 would result. In all screen-film experiments reported here (a total of over 800 readings), CD area scores ranged from 0 to 15.6. In screen-film experiments at fixed optical densities over all breast thicknesses and compositions, CD area scores ranged from 9.6 to 15.6.

Three independent sources of variation contribute to the uncertainty in CD area scores: between-reader (or inter-observer) variations, within-reader (or intra-observer) variations and sample variations **[15]**. In CD phantom experiments where N_S identical sample films were acquired under each exposure condition, with each film read N_i times by N_r independent reviewers, the total uncertainty in CD score would be:

$$\sigma_{total} = \{\sigma_S^2/N_S + \sigma_b^2/N_r + \sigma_W^2/(N_S N_r N_i)\}^{1/2}, \qquad [5]$$

where σ_S is the standard deviation in CD area due to sample variation, σ_b is the standard deviation in CD area due to inter-reader (between-observer) variation, and σ_W is the standard deviation in CD area due to intra-reader (within-observer) variation.

Experiment #1: Determining Uncertainties in CD Scores

Our first experiment was performed to determine the magnitude of each of these three sources of variation in CD area scores. We acquired five identically exposed images using a GE DMR mammography unit and Kodak Min R-2000 cassettes and film, with all film taken from the same emulsion batch and box. Each image was read three times by four different reviewers, each pair of readings by each reviewer separated by an interval of at least two weeks. To minimize recall bias, the five test images acquired under identical conditions were randomly interspersed with fifteen other images having a range of image quality and CD scores. Readers were required to score all twenty images and were blinded to the identity of the five images used to evaluate reader variation.

Within-reader standard deviation (σ_W) was determined by calculating the root mean squared (rms) variation in CD scores across multiple readings of the same film, then averaging over all five films and four reviewers. All multiple readings included within-reader variations, regardless of whether multiple samples, multiple readers, or multiple readings were involved.

Sample standard deviation (σ_S) was calculated by measuring rms deviation across the five multiple samples acquired under identical imaging conditions, averaged over all four readers and three readings, which measured:

$$S_{samples} = \{\sigma_S^2+\sigma_W^2\}^{1/2}. \quad [6]$$

σ_S was determined by subtracting σ_W (determined above) from the measured $S_{samples}$ in quadrature **[15]**.

Between-reader standard deviation (σ_b) was determined by calculating the rms deviation across different readers scoring each film, averaged over all five films and three readings, which measured:

$$S_{between} = \{\sigma_b^2+\sigma_W^2\}^{1/2}. \quad [7]$$

σ_b was determined by subtracting σ_W from the measured $S_{between}$ in quadrature.

The results of this initial experiment which determined σ_b, σ_W, and σ_S for screen-film mammography were used, along with Eq (1), to determine an efficient way to reduce uncertainties in CD scores in subsequent experiments.

All subsequent experiments involved acquisition of two identical images under each exposure condition, and reading of each acquired image independently by two reviewers. Reviewers were blinded to exposure conditions and images were mixed so that a reviewer would encounter a variety of images under different exposure conditions at each reading session to minimize scoring bias.

All image acquisitions were done on a GE-DMR mammography unit using Kodak Min R-2000 screens and film. Either a single cassette or a set of three cassettes of the same screen material matched for optical densities was used. Images were processed on a Kodak M6B processor with autoloading and Kodak chemistry.

Experiment #2: Effect of Optical Density on Low-contrast Lesion Detection

The second experiment investigated the effects of optical densities on low-contrast lesion detection. kVp was fixed (at 26), phantom thickness was fixed (at 6 cm) and simulated breast tissue composition was fixed (at 50% glandular/50% fat). Three different target-filtration combinations (Mo/Mo, Mo/Rh, and Rh/Rh) were used, acquiring two images at each of a number of different mAs values to span the range of film optical densities used in mammography.

Means and standard deviations of CD scores were determined from two independent reviews of each film for each target-filter and each optical density. Bonferroni t-tests were used to test for the significance of differences in CD scores among the three target-filter combinations.

Experiment #3: Effects of Target-filter and kVp on Low-contrast Lesion Detection

The third experiment, based on the results of the previous two, consisted of acquiring films at a fixed narrow range of optical densities (1.65-1.75) to maximize lesion detection as a function of OD and eliminate the effects of ODs on technique factor optimization. This experiment varied breast thickness (2, 4, and 6 cm), composition (0% glandular/100% fat, 30% glandular/70% fat, 50% glandular/50% fat, and 70% glandular/30% fat), target-filtration (Mo/Mo, Mo/Rh, and Rh/Rh), and kVp values (24-32 for Mo/Mo and Mo/Rh, 26-32 for Rh/Rh), with commensurate adjustment of mAs values to keep film optical densities constant. Again, two CD phantom images were acquired under each imaging condition and each CD phantom image was scored independently by two reviewers. Analysis of variance procedures with a standard software package (SAS) were used to study the effects of kVp and target-filtration on CD scores for each breast thickness and composition. mAs values were recorded to determine exposure times and breast doses for each exposure; average glandular doses for each exposure were calculated based on previously measured half-value layer (HVL) and exposure output values (in milliRoentgen/mAs) for each target-filter and kVp combination.

3. Effects of Recommended Technique Factor Changes

Results from medical physics surveys at CMAP sites between 1990 and 1996 were analyzed to determine trends in the quality of mammography over that time period. Data from 207 site surveys at 36 mammography sites were analyzed to assess trends toward improvement in mammography image quality. Data analyzed included phantom scores, film-processing A_g values (based on data acquired using the site's film and processing, but a single sensitometer and densitometer for all sites), film optical densities and exposure times for 2, 4, and 6 cm breasts using standardized 50% fatty/50% glandular breast tissue-equivalent BR-12 material.

Additional analysis was done to assess the effect of recommended improvements in image quality based on the technique factor concepts validated in this work. At sites surveyed since 1993, improved technique factors were recommended on mammography units where optical densities were too low (<1.20) for any breast thickness, where optical densities were not consistent across breast thicknesess (within a range of 0.30), or where exposure times were excessively long (> 2 seconds) for any breast thickness. At sites for which

improved technique factors were recommended, the effect of those improved technique factors was assessed based on the following year's site survey results for film optical densities and exposure times. Since the most critical test of the mammography system is its performance for thicker breasts, the film optical densities and exposure times for 6 cm thick breasts were analyzed.

II. RESULTS

1. Film and Processing Contrast

The H&D curves for six different mammography films processed under the same processing conditions are shown in **Figure 3**. The corresponding six gamma plot curves for these films under the same processing conditions are shown in **Figure 4**. Several results are apparent from these gamma plot curves. First, differences in the heights of these gamma plot curves indicate that there are substantial differences in the levels of contrast produced by different mammography films, even under the same processing conditions. Second, the different widths of different curves show that some films have broad optical density ranges over which nearly maximum contrast is preserved, while other films have relatively narrow ranges of maximum contrast. A narrow range of maximum contrast reflects a limited linear portion of the H&D curve. Third, different films have peak contrast occurring at different optical densities. For example, film Types 1 and 4 have maximum contrast at an optical density near 2.0, Types 2 and 3 have maxima at optical densities above 2.0, and Types 5 and 6 have maxima at optical densities below 2.0.

Fourth, and perhaps most importantly, **Figure 4** demonstrates that all mammography films operate at reduced contrast for optical densities below 1.2, with substantial reductions in contrast for optical densities below 1.0. The shape of the gamma plots for lower optical densities is the same regardless of the particular film used. Table 1 lists the integrated area under the entire gamma plot curve, A_g, for each of the mammography films included in **Figure 4**. Note the sizable differences between A_g values, with greater contrast over the full range of optical densities producing greater A_g.

Calculated A_g values listed in all tables were determined assuming a linear interpolation between gamma plot points. A_g values were also determined from data sets using other methods of interpolation between gamma plot points. Cubic spline interpolation between gamma plot points yielded A_g values approximately 1.1% higher than linear interpolation and 8th-10th order polynomial fits to gamma plot points yielded A_g values approximately 1% higher than the A_g values found using a linear interpolation. Differences in A_g caused by the interpolation method were found to be insignificant compared to differences due to film and processing conditions.

Table 1 also lists the mid-density (MD) for each film (the step closest to 1.20), and the optical density from a single step (step 11, which is the speed step in most cases) to permit comparison of ODs between films. The density difference (DD) as defined in the ACR QC Manuals (the difference between the step closest to 2.2 and the step closest to, but not less than, 0.45), and the density difference between two fixed steps (step 13- step 10) are also listed, to permit comparison between films. The base plus fog (B+F) of each film is also listed. There is no correlation between conventionally defined density difference and A_g values, due to the shifting of DD steps. There is a general correlation between step 13 - step 10 OD differences and A_g values; however, A_g values appear to characterize overall film contrast properties better than OD differences between fixed steps, which amount to summing the height of several (in this case three) points of the twenty making up the gamma plot curve.

Figure 5A illustrates the sample variation of gamma plots by displaying ten gamma plot curves acquired under identical processing conditions with one type of mammography film (Kodak MRH-1). **Figure 5B** illustrates the mean gamma plot curve for the ten films and the + one standard deviation gamma plot curves reflecting sample variation for film from the same emulsion batch processed under identical processing conditions.

Figure 6A and **6B** illustrate normal temporal variations of gamma plots acquired over a ten week period from a processor that was "in control" according to normal processor QC measures. Note that the + one standard deviation limits are wider in **Figure 6B** than in **Figure 5B**, reflecting the increased variation of processing conditions over time, even though the same film emulsion batch was used. **Table 2** lists the Ag, MD, DD, and B+F for the normal sample variations and temporal variations illustrated in **Figures 5** and **6**. For the ten films processed at the same time, the range of A_g values was 9.5 to 10.1 (mean A_g = 9.78, standard deviation = 0.17). For the ten films processed one week apart each, the range of A_g values was 9.8 to 11.1 (mean A_g = 10.55, standard deviation = 0.45).

The range of gamma plots occurring among 207 processors surveys at 38 mammography sites between 1990 and 1995 is shown by the two gamma plot curves in **Figure 7** and the data in **Table 3**. The minimum gamma plot A_g value was 3.7, the maximum A_g value was 14.6. The median A_g value among 207 sites was 8.9; the mean A_g was 9.4. These results demonstrate the significant range of film and processing contrast that exists among clinical mammography sites.

The effect on gamma plot curves of using different sensitometers is illustrated in **Figure 8**. Each of the eight curves in **Figure 8** was produced using a different 21-step sensitometer, while using the same film batch and processing conditions. The variation among the eight curves in **Figure 8** is slightly greater

than the sample variations illustrated in **Figure 5**, but less than the temporal variations among "in control" processing shown in **Figure 6**.

Figure 9 shows nine gamma plot curves determined from the same sensitometry film using nine different densitometers. The variations among seven of the nine are insignificant, being comparable to the range of sample variations of gamma plot curves illustrated in **Figure 5**; two densitometers, however, gave significantly different gamma plot results, due to densitometer inaccuracies. These two densitometers (D1 and D7) were found to yield inaccurate results for optical densities above 2.0 and were recommended for repair.

These results suggest that gamma plot curves are relatively invariant to the particular 21-step sensitometer used, but may be affected by inaccurate densitometer performance. **Table 4** lists the A_g, MD, DD, and B+F values for the eight different sensitometers and nine different densitometers whose performance is illustrated in **Figures 8** and **9**. While MD and step 11 OD values fluctuated widely (due to different light output from different sensitometers), and DD and step 13 - step 9 OD differences fluctuated, A_g values were reasonably consistent for the eight sensitometers (A_g range: 12.1 - 12.9) and for the seven densitometers (A_g range 12.0 - 12.5) that were performing correctly.

The effect of a delay between film exposure and processing on gamma plots is shown in **Figures 10** and **11**. These results show that "latent image fade" had insignificant effects on film contrast for Min R-2000 film and had only a minor effect on film contrast for MRH-1 film. Interestingly, a delay between film exposure and processing actually increased film contrast slightly for MRH- 1. **Table 5** lists the Ag, MD, DD, and B+F values for the latent image results illustrated in **Figures 10** and **11**. These results indicate that delays between film exposure and processing had an insignificant effect on image contrast for Min R-2000 film and had a slight effect on MRH-1 film.

The effects of darkroom fog on gamma plots, A_g, MD, DD, and B+F values are illustrated in **Figure 12** and **Table 6**. Substantial film fog did reduce film contrast and A_g values slightly, but had far less of an effect than film type, film emulsion differences, and processing conditions in most cases (see below). The subtle effects of film fog were apparent as an increase in step 11 optical densities, as an increase in step 13 - step 10 density differences, and as a slight increase in B+F OD values (**Table 6**), even though the overall effect of film fog was to reduce overall contrast. The effect of film fog on image contrast was most obvious by examining gamma plot curves and Ag values, not from analysis of conventional sensitometric parameters.

The effect of different developer chemistry conditions on gamma plots is illustrated in **Figure 13** and **Table 7**. Old chemistry and fresh chemistry plus

starter after 5 days of "seasoning" yielded nearly identical gamma plots. Fresh chemistry without starter yielded reduced contrast for lower optical densities and increased contrast for higher optical densities. Adding starter increased contrast for lower optical densities and lowered contrast for higher optical densities. Seasoning increased contrast across the entire mid-range of optical densities. Comparison of A_g values and density difference values for these different processing conditions demonstrates that A_g gives a more complete description of film contrast that DD or fixed step differences (step 13 - step 10).

Gamma plots for two different batches of the same type of mammography film (Kodak Min R-2000) are shown in **Figure 14**. These gamma plots show significant variations from batch to batch. The corresponding A_g, MD, DD, and B+F values for the two batches are given in **Table 8**. The differences in gamma plots between the two emulsions demonstrate that film contrast can differ significantly from batch to batch of the same type of mammography film. Those differences are apparent as differences in the height of gamma plot curves across the mid-range of optical densities. Those differences also are apparent as differences in A_g and DD values (between fixed steps) in Table 8, but are not apparent as differences in MD or B+F values.

The effect of developer temperature on gamma plots and summary parameters are illustrated in **Figures 15-17** and **Table 9**. As developer temperature increases from 25°C to 33°C, gamma plot curves and A_g values increase (**Figures 15** and **16**). Gamma plot curves and A_g values remain high and approximately constant for developer temperatures between 33°C and 37°C, and then decrease as developer temperature continues to increase. These results show optimization of film contrast at developer temperatures between 33°C and 37°C (**Figure 16**). Note the decrease in contrast at optical densities at and around 1.0 for these high developer temperatures (**Figure 15**). In contradistinction, fixed step ODs and fixed step OD differences continue to increase monotonically as developer temperature is increased from 25°C to 40°C (**Figure 17**). Conventionally defined MD and DD values cannot be used to analyze the effect of temperature because of the need to shift steps to keep the reference step for MD the step closest to 1.20 OD and the two reference steps for DD those closest to 2.20 and closest to, but not less than, 0.45 (**Table 9**).

2. Technique Factor Selection

Experiment #1: Determining Uncertainties in CD Scores

Reader performance studies of the contrast-detail (CD) phantom demonstrated that intra-reader variations were the greatest source of uncertainty and inter-reader variations the smallest source of uncertainty. For screen-film mammography with good image quality, a mean contrast-detail score of 12.3 was measured. For multiple images read by multiple readers multiple times,

intra-reader standard deviations were determined to be 0.49, sample variation standard deviations were determined to be 0.24, and inter-reader standard deviations were determined to be 0.05. These results were used in Eq (1) to predict the total variation in CD scores in the case of N_S identically acquired samples, each read by N_r readers N_i times. For $N_S = N_r = N_i = 1$, the three independent sources of variation add in quadrature, yielding $\sigma_{total} = 0.55$. **Table 10** shows the estimated total standard deviation (σ_{total}) based on increasing the number of identically acquired samples, number of readers of each sample, and number of independent readings of each sample by each reader. By acquiring two samples under each imaging conditions and having each sample read independently by two readers, Eq (1) predicts that σ_{total} will be reduced by 45%, to 0.30. Other methods to reduce scoring variations, such as a larger number of readers of a single image or more readings of a single image, are less efficient in reducing scoring uncertainties. Consequently, to reduce uncertainties in all subsequent CD experiments, two identically exposed films were acquired, with each film scored independently by two CD phantom readers.

Experiment #2: Effect of Optical Density on Low-contrast Lesion Detection

Using this multiple image, multiple reader strategy, we next acquired CD phantom images to study the effect of optical densities on low-contrast lesion detection for three different target-filtration combinations (Mo/Mo, Mo/Rh, and Rh/Rh) on a simulated 6 cm thick, 50% fat/50% glandular compressed breast. **Figure 18** compares CD scores versus optical density for the three target-filter combinations, showing the strong dependence of low-contrast lesion detection on optical densities and the lack of significant differences between results at the same optical density for different target-filter combinations. A sharp rise in CD scores was found as OD increases for low optical densities. A broad maximum in CD scores was found for ODs between approximately 1.2 and 2.5 and a rapid decrease in CD scores was found for ODs above 2.5-2.75. These low-contrast detection results generally conform to the shape of the gamma plot curve for the specific film used, indicating that impaired lesion detection at low and high ODs is a result of the reduced contrast in mammography film at low and high ODs.

The uncertainties displayed in **Figure 18** are the standard deviations based on acquisition of two images under each test condition and independent scoring of each image by two reviewers. Bonferroni t-tests were used to test for the significance of differences among the three target-filter combinations, indicating no statistically significant differences at the $p < 0.05$ level. Due to the phantom thickness and mAs limit on Mo/Mo exposures, average background ODs greater than 3.0 could not be produced for the Mo/Mo target-filter combination.

Experiment #3: Effects of Target-filter and kVp on Low-contrast Lesion Detection

Based on the test results of Experiment #2, all subsequent testing with different breast thicknesses and compositions was done at a narrow range of OD between1.65 and 1.75. This narrow range was picked to be near the center of the range of maximized low-contrast detection (1.2 – 2.5) to eliminate any possible dependence of low-contrast lesion detection on OD from technique optimization experiments. The results of these experiments, which varied compressed breast thicknesses, composition, target-filtration, and kVp, while altering mAs to maintain constant ODs of 1.65-1.75, are shown in **Figures 19A-F**. **Figure 19A** illustrates the effect of increasing kVp from 24 to 32 for Mo/Mo target-filtration and 100% fatty breasts of 2, 4, and 6 cm thicknesses. **Figure 19A** demonstrates that increasing kVp while keeping ODs fixed causes a slight, but statistically significant decrease in low-contrast lesion detection for each breast thickness. The same general trend applies to other breast compositions (**Figures 19B-D**) and other target-filter combinations, although the effect of kVp on CD scores was greater for Mo/Mo than for the other two target-filter combinations. CD scores for a 50%/50% breast imaged using Mo/Rh and Rh/Rh target-filter combinations are shown in **Figures 19E-F**. Data for other breast compositions using Mo/Rh and Rh/Rh are not shown, but follow similar trends.

Analysis of variance linear models revealed statistically significant effects on CD scores of kVp, target-filtration, breast thickness, and breast composition. The effect of kVp on CD score was highly significant ($p<0.0001$), even though the decrease in CD score with increasing kVp was small. Averaging over all target-filter combinations, breast thicknesses, and breast compositions, CD scores decreased by 0.1 per kVp.

The effect of target-filtration on CD score revealed a highly significant distinction between Mo/Mo and the other two target-filter combinations (Mo/Rh or Rh/Rh) for 2 and 4 cm thick breasts ($p<0.0001$). On average, CD scores were 0.44 higher for Mo/Mo than for Rh/Rh. No distinction was found between Mo/Mo and the other two target-filter combinations for 6 cm breasts. No significant distinction was found between Mo/Rh and Rh/Rh for any breast thickness ($p=0.194$).

As shown in **Figure 19**, there were significant distinctions among CD scores for 2, 4, and 6 cm breast thicknesses, especially for breasts with greater glandular content. The effect of breast thickness on CD scores was highly significant ($p<0.0001$) with increasing breast thickness causing lower CD scores due to more scattered radiation.

The effect of breast composition on CD scores was highly significant for 4 and 6 cm thick breasts, with decreasing CD scores for increasing breast

glandularity ($p<0.0001$). For thin (2 cm) breasts, CD scores were not significantly different for different tissue compositions ($p=0.196$).

Given that kVp has a significant effect on image contrast and CD scores, it would appear that use of the lowest possible kVp is preferable for a given breast thickness and composition. Higher kVp has a major effect on x-ray output, however, decreasing exposure time (or mAs) for fixed ODs as illustrated in **Figures 20A-C**. For example, imaging of a 6 cm breast with Mo/Mo at 26 kVp requires 73% higher mAs than at 28 kVp and nearly three times the mAs required at 30 kVp, assuming the same optical densities are obtained. Thus, the prescription of using the lowest possible kVp must be modified by the requirement that exposure times be kept reasonably short.

The choice of target-filter material also affects the mAs (and exposure time) required to obtain a fixed film optical density. Using the same kVp, the mAs required to obtain the same optical densities with Mo/Rh is up to 30% less than that required for Mo/Mo, while the mAs required for Rh/Rh is up to 50% less than that required for Mo/Mo (**Figure 20**). One factor working against lower exposure times with rhodium target material is the fact that mA values are typically 20-25% less than those for molybdenum target material, due to the lower melting point of rhodium. Thus, use of Rh/Rh will yield exposure times that are up to 35% shorter than those for Mo/Mo, and comparable to those for Mo/Rh, for thicker breasts.

The selection of target-filtration and kVp also affects breast dose. The average glandular doses to maintain the same optical density for a 50%/50% breast of 2 to 6 cm thickness for each target-filter combination are shown in **Figures 21A-C**. Raising kVp by 2 decreases breast dose by 15-20% for the same target-filter materials. Switching from Mo/Mo to Mo/Rh for a 6 cm thick breast lowers average glandular breast doses by approximately 20%, while switching from Mo/Mo to Rh/Rh for a 6 cm thick breast lowers average glandular dose by approximately 35%, for the same kVp values. We did not include doses for a 2 cm breast using Mo/Rh or Rh/Rh, since the entrance-exposure-to-dose conversion factors have not been determined for thin breasts with those target-filter combinations.

The film optical densities resulting from uniformly thick heterogeneous breasts of thickness ranging from 2-7 cm and compositions ranging from 100% fatty to 100% glandular tissue for different target-filter combinations and different AEC detector placements are shown in **Figures 22A-L**. Separate curves for MRH-1 film and Min R-2000 film are shown. Of particular note is that the higher contrast Min R-2000 film has a greater range of optical densities and greater loss of contrast at the lower and upper ends of the OD range, especially for thicker breasts and where the AEC detector responds to 100% fat or 100% glandular tissue. This indicates that AEC detector positioning is even more critical with Min R-2000 film than with previously used films and that some loss of contrast may

occur in using this film with thicker, highly heterogeneous breasts.

3. Effects of Recommended Technique Factor Changes

The measured A_g values from different sites are plotted against time in a scattergram (**Figure 23A**) which also includes a linear best fit parameterization of A_g versus time. Average A_g values are summarized year by year in **Figure 23B**. While the spread of A_g values in each year is great, there is a statistically significant trend of increased A_g over time ($p < 0.01$), demonstrating a general improvement in film and processing contrast at mammography sites between 1990 and 1995. **Figure 23C** indicates the changes in A_g values for sites with 3 surveys at the same site; **Figure 23D** shows the changes in A_g for sites with 4 or more surveys per site. The majority of sites showed improvements in A_g, not as a result of our site surveys but as a result of general improvements in film contrast and greater attention by mammography sites to film processing conditions **[16]**.

Figure 24A is a scattergram of film optical densities for a 6 cm thick breast at each of the 207 unit surveys performed. The linear best fit curve shows the trend toward increased average film optical densities over time ($p < 0.05$). **Figure 24B** shows the trend in film optical densities on a site-by site basis for the 35 sites at which improved technique charts were constructed and posted starting in 1993. Of the 35 sites, 27 showed increases in film OD for AEC exposures of 6 cm breasts between first and last measurements.

Figure 25A is a scattergram of exposure times for a 6 cm thick breast at each of the 207 unit surveys performed. The linear best fit curve shows the trend toward decreased average exposure time year by year ($p < 0.05$). **Figure 25B** shows the trend in exposure times on a site-by site basis for the 35 sites at which improved technique charts were constructed and posted starting in 1993. Of the 35 sites, 26 showed decreases in film exposure times for AEC exposures of 6 cm breasts between first and last measurements. Beyond mid-1994, no sites had exposure times in excess of 2.5-3.0 seconds and most were at 2 seconds or below.

These optical density and exposure time results suggest that the interventions made by the medical physicist at CMAP sites between 1993 and 1995, especially in recommending technique factors based on the image optimization ideas described above, led to measurable improvements in image quality over that time period.

IV. DISCUSSION

1. Film and Processing Contrast

These results suggest methods for sites to use gamma plots to determine if processing is "optimized" without the use of a standardized sensitometer and densitometer. The most reliable method is based on the minimal effect of latent image fade on gamma plots for some types of mammography film (see Figure 8). If a mammography site uses a film for which latent image fade is not significant, such as Kodak Min R-2000, the site can use one or more sheets of their own film, flash the film using their own sensitometer, place the exposed, unprocessed film into a light-tight envelope, and mail it overnight to the film manufacturer or another site for immediate processing under conditions optimized for that film type. The processed film can then be mailed back to the site and optical densities measured using the site's own densitometer. The gamma plot results from the film manufacturer's optimized processing can be compared to a gamma plot constructed using the site's processing, the same film batch and box, the same sensitometer, and the same densitometer.

If latent image changes are significant for the film of interest (as in Figure 9), this method can still be used to assess processing by intentionally scheduling the same time delay between exposure and processing at the site as occurs for the manufacturer's processing. If the site's processing is optimized, the two gamma plots should demonstrate a reasonable match.

Care should be taken in interpreting gamma plot results. Gamma plot differences on the order of those between means and standard deviations for normal temporal variations (Figure 4) should not be taken as significant differences. Differences on the order of those shown between gamma plot curves for different films (Figure 2 other than the differences between Dupont and 3M, which are the same film emulsions) are significant.

Gamma plots that show a spike and dip in either order, rather than a relatively smooth curve, usually reflect a reading error. If the error occurs only sporadically, it is likely to be due to misreading a single step OD. This can happen when the densitometer aperture is not positioned properly over a single step on the sensitometer strip. If the spike and dip occur in the same general location on every gamma plot, it can be due to sensitometer light output that is not consistent with a square root of two increase from step to step. This can be due to a defective optical step tablet in the sensitometer or due to non-uniform light output behind the step tablet, for example, due to a cracked glass window at one step location in the sensitometer.

Since gamma plots combine the effects of both film and processing, it is useful to establish QC procedures that separately isolate changes in film

emulsions from changes in film processing. As in conventional processor QC, gamma plots using the same box of properly stored control film isolate contrast changes caused by processing changes alone.

Comparison of gamma plots acquired using one or more sheets of film from each of two different batches, processed simultaneously, will reveal contrast differences between film batches. Contrast differences between films such as those shown in Figure 12, especially decreases in film contrast of that magnitude, indicate an unacceptable level of change from batch to batch. In such cases, the new batch of film should be returned and replaced by a batch with contrast more consistent with the previous film batch.

The most important quality control issue at any mammography site is how their clinical film and processing are performing each day. A gamma plot constructed from the 21-step sensitometer data obtained from exposure of the site's clinical film demonstrates film and processing contrast over the entire range of optical densities. The A_g value based on the clinical film and processing provides a single index of overall site contrast. Monitoring gamma plots or A_g values from clinical film on a daily basis not only permits a site to monitor processing consistency, but to monitor the adequacy of contrast due to both film and processing. Given the variations that have occurred among emulsion batches of the same film type in recent years, this may be a more important daily measurement than conventional processor sensitometry QC, which monitors processing consistency, but not clinical film consistency or adequacy.

Is a higher film contrast at a given optical density necessarily better? Theoretical modeling of the detection of microcalcifications or low-contrast lesions in a screen-film imaging system indicates that as the film contrast (or gamma) increases, both the radiographic contrast and the noise due to quantum mottle increase linearly with gamma **[17]**. If quantum mottle were the only source of image noise, these two factors would cancel one another in the detection signal-to-noise ratio, and the detection of objects would be independent of film gamma. Other sources of noise contribute to image noise, however: primarily film granularity noise and, to a lesser extent, screen noise, both of which are independent of film gamma. The full expression for the signal-to-noise ratio for object detection has the form:

$$SNR\,(G) = \frac{SC.\ \gamma.\log_{10}e}{[\sigma_s^{\,2} + \sigma_g^{\,2} + \sigma_q^{\,2}]^{1/2}} \qquad [5]$$

where SC is subject contrast of the object of interest, γ is the film gamma at the particular optical density of interest, and σ_s, σ_g, and σ_q are the rms density

fluctuations due to screen structure mottle, film granularity mottle, and quantum mottle respectively. σ_s and σ_g are independent of the film contrast, G, while σ_q depends linearly on G. As long as σ_s and σ_g are not negligible compared to σ_q, SNR will increase as film gamma increases. For Min-R screens and Min-R film, Barnes and Chakraborty determined that σ_g and σ_q were approximately equal, while σ_s was less than 10% of σ_g or σ_q. For Min-R screens and OM-1 film, σ_g was approximately one-half of σ_q, and σ_s was less than 10% of σ_q. The fact that σ_q is not the only source of image noise indicates that lesion detection will improve if a film with a higher gamma at a given optical density is used. These results also indicate that the SNR for object detection is improved by using film optical densities for which the film contrast (γ) is greater. These results are supported by the contrast-detail results presented in Section II of this report, which show that low-contrast lesion detection is improved by using films with higher gamma for the same optical density and by using film optical densities for which local film contrast is at or near maximum.

2. Technique Factor Selection

Our contrast-detail results are consistent with the results of Young, et.al, and Robson, et.al., in demonstrating the significant effect of film optical densities on low-contrast lesion detection **[12, 13]. Figure 18** best demonstrates this effect, showing that low-contrast lesion detection drops precipitously for optical densities below 1.0-1.2, regardless of target-filter combination. The farther below 1.0 optical densities fall, the greater the loss of contrast. This result applies locally to each region of a mammogram. Thus, underexposed regions of a mammogram suffer reduced contrast, while properly exposed areas of the same mammogram may have adequate contrast.

While the CD phantom results presented in this paper assess low-contrast lesion detection in only one type of mammography film (Kodak Min R-2000), we have obtained a similar dependence of lesion detection on OD in our previously used mammography film (Kodak MRH-1; results not shown here). We have also characterized film contrast in a wide variety of mammography film types of different manufacturers and have demonstrated that all current mammography film types lose contrast at optical densities below 1.0-1.2.

Our results with Min R-2000 film demonstrate that maximum lesion detection occurs at optical densities between 1.5 and 2.0. This is consistent with the findings of Robson, et.al., who found that peak detection in two other mammography films occurred at OD values between 1.6 and 2.0. The detailed contrast properties of mammography films differ somewhat from one film type to another, especially at higher OD values, but all currently used mammography

films have peak contrast at optical densities above 1.5. Therefore, as a general rule we recommend setting target background optical densities at 1.5-2.0. This means that AEC response to a uniform composition and thickness of breast equivalent phantom material should yield an OD between 1.5 and 2.0, regardless of simulated breast thickness.

Due to variations in both breast thickness and composition, mammograms contain a spectrum of optical densities. Consequently, not all tissues presented on a mammogram can be displayed at OD values that have maximum contrast. The best that can be expected is to image all breast tissues at OD values that preserve reasonable contrast by being in the mid-range of optical densities, where lesion detection is maximum (**Figure 18**). To avoid significant contrast loss, fibroglandular tissues should be imaged at optical densities at or above 1.0. Setting the target background OD at 1.5-2.0, along with proper AEC detector placement, is helpful in imaging fibroglandular tissues at OD values of 1.0 or greater. Similarly, fatty tissues should be imaged at optical densities that do not exceed the upper OD limit of high contrast for the particular film being used. In the case of Min R-2000, this upper limit of high contrast occurs at OD values between 2.5 and 2.75, but the upper limit differs from one type of mammography film to another. Viewing of films (or regions of films) having higher optical densities requires good viewing conditions: high luminance viewboxes (or a hotlight), low ambient room light, and good film masking.

Figure 19 indicates that for optimized ODs, lower kVp values slightly increase low-contrast lesion detection, while **Figures 20 and 21** indicate that lower kVp substantially raises exposure time and breast dose. Longer exposure times significantly increase the probability of image blur due to motion. Moreover, exposure times longer than 3-4 seconds can result in automatic exposure control (AEC) termination of exposure by backup timer, yielding an underexposed film. As a general rule, exposure times in excess of approximately 2 seconds should be avoided, both to minimize patient motion and to prevent underexposure due to AEC backup timer termination. Thus, our recommendation for technique factor selection is to select kVp values that are as low as possible while ensuring that exposure times are less that approximately 2 seconds. The specific kVp selection for a given breast thickness and composition will vary from unit to unit depending on the unit's mA output and its entrance dose per mAs at the entrance surface of the breast. The minimum kVp keeping exposure time under 2 seconds also depends on the target-filter selection and on the speed of the film-screen-processing combination used at the mammography facility.

Consequently, rather than recommending a specific kVp for a given breast thickness and composition, the rule that we have provided is to select the lowest kVp that results in exposure times less than 2 seconds. Assuming appropriate film optical densities are being achieved, exposure times in excess of 2 seconds

are an indication that kVp has been set too low. This will normally occur for thicker and denser breasts, suggesting a technique revision to a more penetrating beam (Mo/Rh or Rh/Rh target-filter combination and/or higher kVp) to shorten exposure times. Switching to a more penetrating target-filter combination or raising kVp for the same target-filtration will decrease patient dose while shortening the exposure time.

On the other hand, extremely short exposure times (under 1/2 second) for thinner and fattier breasts (at appropriate film ODs) are an indication that beam quality can be lowered (by switching to Mo/Mo or to lower kVp values if Mo/Mo has been selected), thereby gaining some soft-tissue contrast and improving the detection of low-contrast lesions. For thin breasts, the breast dose will remain low even when a lower kVp is used.

The general approach of focusing on film optical densities and exposure times leads to the selection of more appropriate technique factors in mammography. It is aided by applying a film densitometer to clinical images to verify that film optical densities are at or above 1.0 throughout the breast, but especially in areas of greater fibroglandular content. It is further aided by mammography systems that flash or print out exposure times on film. Use of a densitometer and knowledge of film exposure times allow both the technologist and radiologist to assess quantitatively that they are optimizing mammographic technique by obtaining adequate optical densities with adequately short exposure times.

A SIMPLE PRESCRIPTION FOR OPTIMIZING MAMMOGRAPHY TECHNIQUES

Our experimental results lead to the following simple rules for maximizing the detection of low-contrast lesions in screen-film mammography:

1) Film ODs should be targeted at 1.5-2.0, so that film optical densities throughout the mammogram are 1.0 or greater.

2) Mo/Mo should be selected as the target-filter material for breasts less than 5.0 cm, Mo/Rh or Rh/Rh should be selected for breast thicknesses above 5.0 cm.

3) kVp should be varied with breast thickness, using lower kVp (22-25) for thin, fatty breasts and higher kVp (28-32) for thick, dense breasts. For each breast thickness, kVp settings should be as low as possible to maintain adequate optical densities, while keeping exposure times under 2.0 seconds.

4) film optical densities below 1.0 in any significant portion of the breast or exposure times longer than 2.0 seconds for any breast thickness or composition are indications of improper technique factor selection.

5) the use of Mo/Rh or Rh/Rh target-filter materials for breast thicknesses greater than 5 cm will decrease mAs by 30-50%, exposure times by 30-35%, and average glandular breast doses by 20-35%.

3. Effects of Recommended Technique Factor Changes

There is strong evidence of general improvement in image quality over time, as assessed by quantitative measurements of film-processing contrast (A_g values), film optical densities for 6 cm thick breasts, and exposure times for 6 cm thick breasts. These surrogate measures of image quality are certainly not the only measures that are possible or are important, but generally indicate greater attention to film-processing contrast and improvement in technique factor selection, especially for thicker breasts. It is likely that increases in A_g values reflect general improvements in film contrast and greater attention to processing conditions, while increased optical densities and decreased exposure times for thicker (6 cm) breasts reflect improvements in technique factors that were a direct result of the medical physicist testing and interventions.

CONCLUSIONS

This work has demonstrated that gamma plots provide a useful quality control tool for mammography, permitting sites to: 1) assess the adequacy of image contrast from film and processing, 2) assess the range of optical densities over which contrast is maintained, 3) have a simple way of comparing film and processing performance over the full range of optical densities. The summary parameter which this work introduces, A_g, provides a simple and convenient way of summarizing film and processing contrast over the full range of optical densities.

We have conducted a series of contrast-detail experiments that have determined optimum technique factors for image acquisition in screen-film mammography as a function of breast thickness and composition. Our results demonstrate the effects of optical density, target-filtration, and kVp on low contrast lesion detection at each breast thickness and composition. Our results lead to a set of simple rules that mammography sites can use to select and monitor technique factors that maximize cancer detection, while maintaining reasonably low breast doses, in all breasts.

This general prescription for improving mammography technique factors to maximize contrast while minimizing exposure time (and motion blurring) has been applied to site surveys conducted through CMAP since 1993 by providing revised technique charts that were more effective at maintaining adequately high optical densities while keeping exposure times under 2 seconds for all breast thicknesses. Analysis of CMAP site surveys demonstrates a general improvement in film-processing contrast, more consistent film optical densities, and reduced exposure times for thicker breasts.

REFERENCES

1. Hendrick RE, Bassett LW, Botsco MA, Butler PA, Dodd GD, et. al., Mammography quality control manual: radiologist's section, radiologic technologist's section, medical physicist's section, American College of Radiology, Revised Edition, 1994.

2. Gray JE, Winkler NT, Stears J, Frank ED. Quality control in diagnostic imaging. Baltimore, MD: University Park Press, 1983, p. 33-49.

3. Haus AG, Jaskulski SM. The basics of film processing in medical imaging. Madison, WI: Medical Physics Publishing Co., 1997.

4. Haus AG. Historical developments in film processing in medical imaging. In Haus AG, ed. Film processing in medical imaging. Madison, WI: Medical Physics Publishing Co., 1993. p. 1-16.

5. ACR Standards for the Performance of Screening Mammography, American College of Radiology, 1990.

6. Mammography facilities - requirements for accrediting bodies and quality standards and certification requirements; interim rules; 21 CFR Part 900, United States Federal Register, Washington, DC. Volume 58, No. 243, p. 67558-67572, 1993.

7. Bassett LW, Hendrick RE, Bassford TL, et.al. Quality Determinants of Mammography, Clinical Practice Guideline No. 13. AHCPR Publication No. 95-0632. Rockville, MD: Agency for Health Care Policy and Research, Public Health Service, U.S. Department of Health and Human Services. October 1994.

8. Houn F, Brown ML. Current practice of screening mammography in the United States: data from the National Survey of Mammography Facilities. Radiology 1994; 190: 209-215.

9. Yaffe MJ, Hendrick RE, Feig SA, Och J, Gagne R, Rothenberg LW, Ochs J, Gagne R. Recommended specifications for new mammography equipment: report of the ACR-CDC Focus Group on mammography equipment. Radiology 1995; 197: 19-26.

10. Haus AG: Technologic improvements in screen-film mammography. Radiology 1990; 174: 628-637.

11. Law J. Improved image quality for dense breasts in mammography. The British Journal of Radiology 1992; 65: 50-55.

12. Young KC, Wallis MG, Ramsdale ML. Mammographic film density and detection of small breast cancers. Clinical Radiology 1994; 49: 461-465.

13. Robson KJ, Kotre CJ, Faulkner K. The use of a contrast-detail tests object in the optimization of optical density in mammography. The British Journal of Radiology 1995; 68: 277-282.

14. Rothenberg LN, ed. NCRP Report No. 85: Mammography: A User's Guide, Bethesda, MD: National Council on Radiation Protection and Measurement, 1986.

15. Cohen G, McDaniel DL, Wagner LK. Analysis of variance in contrast-detail experiments. Medical Physics 1984; 11: 469-73.

16. Hendrick RE, Chrvala CA, Plott CM, et.al. Improvement in mammography quality control: 1987-1995. Accepted for publication in Radiology, December 1997.

17. Barnes GT, Chakraborty DP. Radiographic mottle and patient exposure in mammography. Radiology 1982; 145: 815-821.

APPENDIX

PUBLICATIONS AND ABSTRACTS

Submitted Publications:

Hendrick RE, Chrvala CA, Plott CA, Wilcox-Buchalla P, Jessop N, Cutter GA. Improvement in Mammography Quality Control, 1987-1995. Accepted for publication in Radiology, November 1997.

Hendrick RE, Berns E, Chorbajian B, Choi SK. Gamma plot: a new quality control tool in screen-film mammography. Submitted for publication in Radiology, November 1997.

Hendrick RE, Choi SK, Plott CA, Berns E, Chorbajian B, Cutter G. Optimization of technique factors in screen-film mammography. Submitted for publication in Radiology, December 1997.

Abstracts:

Hendrick RE, Choi SK, Plott CA, Berns E, Chorbajian B, Cutter G. Optimization of technique factors in screen-film mammography. Poster presentation, The Department of Defense Breast Cancer Research Program Meeting, Washington DC, October 31 - November 4, 1997.

Hendrick RE. Optimization of technique factors in screen-film mammography. Invited Refresher Course Presentation, RSNA/AAPM Symposium on New Directions in Breast Imaging, Radiological Society of North America Annual Meeting, Chicago, IL, December 1, 1997.

Personnel Supported by this Grant:

Carmine Plott, Ph.D. - postdoctoral fellow
Seoung (Kim) Choi, Ph.D. - postdoctoral fellow
Beth Chorbajian, M.S. - graduate student
Eric Berns, M.S. - graduate student and PRA

TABLE DESCRIPTIONS

Table 1: Conventional processor sensitometry data (MD = mid-density, DD = density difference, B+F = base plus fog) and A_g values for the six films processed under the same processing conditions in **Figures 3 and 4.** Because of the shift in steps due to the ACR definitions of MD and DD, optical densities corresponding to a single mid-density step and two fixed density difference steps are also given (step 11 and step 13-10).

Table 2: Conventional processor sensitometry data (MD = mid-density, DD = density difference, B+F = base plus fog) and A_g values for the ten films processed under the same processing conditions at the same time (see **Figure 5**) and the 10 films processed at a rate of 1 per week in an "in control" processor (see **Figure 6**).

Table 3: Conventional processor sensitometry data (MD = mid-density, DD = density difference, B+F = base plus fog) and A_g values for the best and worst film-processing contrast among 207 site surveys (see **Figure 7**).

Table 4: Conventional processor sensitometry data (MD = mid-density, DD = density difference, B+F = base plus fog) and A_g values for eight different sensitometers (**Figure 8**) and nine different densitometers (**Figure 9**).

Table 5: Conventional processor sensitometry data (MD = mid-density, DD = density difference, B+F = base plus fog) and A_g values for films processed immediately and at 1, 2, 3, 4, and 7 day intervals after exposure for two kinds of mammography film, Kodak Min R-2000 (**Figure 10**) and Kodak MRH-1 (**Figure 11**).

Table 6: Conventional processor sensitometry data (MD = mid-density, DD = density difference, B+F = base plus fog) and A_g values for films fogged with different exposure times to the ambient light in a darkroom, ranging from zero to 16 minutes exposure (**Figure 12**).

Table 7: Conventional processor sensitometry data (MD = mid-density, DD = density difference, B+F = base plus fog) and A_g values for films processed under different chemistry conditions, including fresh developer chemistry without and with starter, with additional seasoning over time after the addition of developer chemistry and starter (1 day, 2 days, 5 days) (**Figure 13**).

Table 8: Conventional processor sensitometry data (MD = mid-density, DD = density difference, B+F = base plus fog) and A_g values for two different emulsion

batches of the same type of mammography film (**Figure 14**).

Table 9: Conventional processor sensitometry data (MD = mid-density, DD = density difference, B+F = base plus fog) and A_g values for the same emulsion batch of mammography film processed at different developer temperatures ranging from 25 to 41 degrees Celsius (**Figures 15-17**).

Table 10: Theoretical estimate of total standard deviation (σ_{total}) for different numbers of readers (N_r), numbers of samples (N_s), and number of readings of each film by each reader (N_i).

Table 11: P-values for the significance of trends in decreasing contrast detail scores with increasing kVp values corresponding to the data in **Figures 19A-F**.

Table 1

Film	Ag	MD	step 11	DD	13-10	B+F
Type 1	11.8	0.99	0.99	1.76	1.76	0.21
Type 2	13.25	1.23	1.23	1.96	1.7	0.24
Type 3	12.72	1.2	1.2	1..92	1.66	0.24
Type 4	9.89	1.07	1.59	1.47	1.61	0.19
Type 5	7.54	1.44	0.61	1.76	1.02	0.21
Type 6	7.24	1.03	1.4	1.69	1.16	0.25

Table 2

	10 Films Developed @ same time						10 Films - 1 Per Week					
			step		steps				step		steps	
Film #	Ag	MD	10	DD	12-9	B+F	Ag	MD	10	DD	12-8	B+F
1	9.71	1.07	1.07	1.46	1.46	0.2	11.11	1.21	1.21	1.93	1.93	0.2
2	9.63	1.08	1.08	1.45	1.45	0.19	10.97	1.23	1.23	1.91	1.91	0.19
3	9.54	1.07	1.07	1.48	1.48	0.19	10.69	1.22	1.22	1.89	1.89	0.2
4	9.85	1.07	1.07	1.44	1.44	0.19	10.9	1.23	1.23	1.94	1.94	0.2
5	9.89	1.07	1.07	1.47	1.47	0.19	10.77	1.13	1.13	1.84	1.84	0.2
6	10	1.05	1.05	1.45	1.45	0.19	10.8	1.09	1.09	1.53	1.79	0.2
7	10.05	1.06	1.06	1.46	1.46	0.19	10.19	1.12	1.12	1.78	1.78	0.2
8	9.78	1.07	1.07	1.46	1.46	0.19	10.14	1.17	1.17	1.77	1.77	0.2
9	9.65	1.06	1.06	1.49	1.49	0.19	10.16	1.15	1.15	1.79	1.79	0.2
10	9.7	1.07	1.07	1.43	1.43	0.19	9.78	1.16	1.16	1.78	1.78	0.19
Mean	9.78						10.551					
Stdev	0.1655295						0.4454324					

Table 3

			Step		Steps	
	Ag	MD	11	DD	13-10	B+F
Best Ag	14.63	1.16	1.16	1.8	1.8	0.17
Worst Ag	3.74	1.16	0.58	1.56	0.76	0.16

Table 4

	Sensitometer		Step		Steps		Densitometer		Step		Steps	
Site	Ag	MD	11	DD	13-9	B+F	Ag	MD	11	DD	13-9	B+F
1	12.25	1.09	1.09	2.02	2.02	0.22	9.09	1.04	1.04	1.93	1.93	0.2
2	12.16	1.07	1.07	1.7	1.94	0.21	12.49	1.11	1.11	2.06	2.06	0.21
3	12.54	0.98	1.51	1.64	2.44	0.21	12.16	1.09	1.09	2.02	2.02	0.21
4	12.12	1.07	1.07	1.77	2.02	0.22	12.35	1.1	1.1	2.07	2.07	0.2
5	12.48	1.18	1.18	1.36	2.18	0.22	12.23	1.09	1.09	2.03	2.03	0.22
6	12.87	1.06	1.69	1.86	2.55	0.21	12.13	1.1	1.1	2.02	2.02	0.21
7	12.1	1.14	1.68	1.79	2.48	0.22	11.17	1.04	1.04	1.74	1.97	0.19
8							12.03	1.1	1.1	2.01	2.01	0.22
9	12.21	1.02	1.02	1.53	1.75	0.21	12.35	1.09	1.09	2.03	2.03	0.21

Table 5

	Latent-2000		Step		Steps		Latent MRH-1		Step		Steps	
Day	Ag	MD	12	DD	13-10	B+F	Ag	MD	11	DD	13-10	B+F
0	14.67	1.01	1.58	1.81	Same	0.21	9.34	1.12	1.63	1.73	1.56	0.2
1	15.63	1.44	1.44	1.72	1.72	0.21	9.83	1.42	1.42	1.48	1.48	0.2
2	15.42	1.46	1.46	1.75	1.75	0.21	9.83	1.37	1.37	1.48	1.48	0.2
3	14.93	1.45	1.45	1.73	1.73	0.21	9.81	1.29	1.29	2.01	2.01	0.2
4	15.22	0.94	1.51	1.77	1.77	0.21	9.9	1.26	1.26	1.99	1.99	0.2
7	15.28	0.92	1.48	1.78	1.78	0.21	10.37	1.23	1.23	1.73	2.01	0.2

Table 6

	Fogged Film		Step		Steps	
	Ag	MD	11	DD	13-10	B+F
No Fog	15.49	1.48	0.9	1.76	1.76	0.2
1 Min	15.03	0.95	0.95	1.78	1.78	0.21
2 Min.	14.72	0.99	0.99	1.82	1.82	0.21
4 Min.	14.53	1.04	1.04	1.86	1.86	0.21
8 Min.	14.71	1.17	1.17	1.3	1.93	0.21
16 Min.	14.2	1.35	1.35	1.45	2.05	0.23

Table 7

			Step		Steps	
	Ag	MD	11	DD	13-10	B+F
Old Chem	14.06	1.03	1.03	1.94	1.94	0.21
Fresh Chem. W/o Starter	14.4	1.26	1.26	1.39	1.95	0.21
Fresh Chem. W/ Starter	12.18	0.97	0.97	1.88	1.88	0.21
1 Day	13.22	0.99	0.99	1.93	1.93	0.2
2 Day	13.59	1.02	1.02	1.93	1.93	0.2
5 Day	13.87	1.01	1.01	1.92	1.92	0.2

Table 8

			Step		Steps	
	Ag	MD	11	DD	13-10	B+F
Emulsion1	13.38	0.97	0.97	1.91	1.91	0.21
Emulsion 2	10.99	0.96	0.96	1.67	1.67	0.21

Table 9

				Step		Steps	
Film #	Temp	Ag	MD	11	DD	12-9	B+F
1	25	8.91	0.98	0.64	1.51	0.66	0.21
2	26	9.6	1.05	0.69	1.85	0.72	0.21
3	27	9.75	1.2	0.76	2.01	0.85	0.2
4	28	10.18	1.27	0.82	1.42	0.9	0.2
5	29	10.65	1.37	0.88	1.48	0.97	0.2
6	30	10.67	1.42	0.9	1.5	1.01	0.2
7	31	11.06	0.9	0.95	1.8	1.07	0.21
8	32	10.92	1.09	1.09	1.96	1.18	0.21
9	33	11.39	1.16	1.16	2.05	1.24	0.21
10	34	11.22	1.25	1.25	1.32	1.32	0.21
11	35	11.03	1.3	1.3	1.36	1.36	0.21
12	36	11.1	1.36	1.36	1.57	1.38	0.22
13	37	11	0.99	1.44	1.63	1.42	0.22
14	38	10.08	1.03	1.51	1.72	1.5	0.22
15	39	10.26	1.14	1.65	1.82	1.57	0.24
16	40	9.43	1.21	1.75	1.84	1.6	0.25
17	41	9.93	1.31	1.83	1.34	1.63	0.25

Table 10

N_i = 1

	Nr =	1	2	3	4
Ns =	1	0.55	0.42	0.37	0.35
	2	0.39	0.3	0.26	0.24
	3	0.32	0.25	0.22	0.2
	4	0.28	0.21	0.2	0.17

N_i = 2

	Nr =	1	2	3	4
Ns =	1	0.42	0.35	0.32	0.3
	2	0.3	0.25	0.22	0.21
	3	0.25	0.2	0.18	0.17
	4	0.22	0.18	0.17	0.16

Table 11

P-Values

		2 cm	4 cm	6 cm
Mo/Mo	100% Fat	0.004	0.036	0.0003
	30% G / 70% F	0.126	0.01	0.0001
	50% G / 50% F	0.0195	0.0002	0.0001
	70% G / 30% F	0.114	0.051	0.0042
Mo/ Rh	50 % G/ 50% F	0.263	0.657	0.112
Rh/Rh	50 % G/ 50% F	0.985	0.554	0.681

FIGURE CAPTIONS

Figure 1A: The contrast-detail (CD) phantom developed and used in these experiments. The same 1-cm thick CD test pattern can be used with different compositions and thicknesses of breast-equivalent materials.

Figure 1B: Each point in the grid indicates the % contrast and size of one test object in the contrast-detail CD phantom (81 total objects).

Figure 2A: An x-ray image of the contrast-detail phantom.

Figure 2B: CD phantom scoring determines objects detected (larger points) compared to objects not detected (smaller points). The area of objects detected in size-contrast space (shaded area) is the CD score.

Figure 3: Hurter and Driffield (H&D) characteristic curves for six different brands of mammography film processed identically.

Figure 4: Gamma plot curves for the same six brands of mammography film included in Figure 1.

Figure 5A: Ten gamma plot curves from ten identical sensitometric films processed identically.

Figure 5B: The mean and one standard deviation curves from the ten films in A, illustrating the sample variation of gamma plot curves.

Figure 6A: Ten gamma plot curves, one per week for ten different weeks of sensitometry on an "in control" processor.

Figure 6B: The mean and one standard deviation curves from the ten films in A, illustrating normal temporal variations of gamma plot curves.

Figure 7: The best and worst gamma plot curves from 207 surveys of 38 mammography sites collected between 1990 and 1995. The best A_g value was 14.63, the worst was 3.74.

Figure 8: Gamma plot curves resulting from eight different sensitometers used on the same film batch and processor.

Figure 9: Gamma plot curves resulting from nine different densitometers used to read the same 21-step film strip.

Figure 10: Gamma plot curves illustrating the effects on contrast of 1, 2, 3, 4, and 7 days delay, compared to no delay, between film exposure and processing using Kodak Min R-2000 film.

Figure 11: Gamma plot curves illustrating the effects on contrast of 1, 2, 3, 4, and 7 days delay, compared to no delay, between film exposure and processing using Kodak MRH-1 film.

Figure 12: Gamma plot curves illustrating the effects on contrast of 1, 2, 4, 8, and 16 minutes of darkroom safelight exposure, compared to no exposure, in Kodak Min R-2000 film.

Figure 13: Gamma plot curves illustrating the effects on contrast of different processor chemistry conditions.

Figure 14: Gamma plot curves illustrating the contrast differences between two different batches of Kodak Min R-2000 film.

Figure 15: Gamma plot curves illustrating the effects on contrast of processor developer temperatures ranging from 25oC to 40oC.

Figure 16: The dependence of gamma plot Ag values on processor developer temperature.

Figure 17: The dependence of fixed step optical densities, optical density differences, and base plus fog values on processor developer temperature.

Figure 18: CD scores versus optical density for a 6 cm thick simulated compressed breast using 26 kVp and three different target-filter combinations.

Figure 19A: CD score versus kVp, keeping OD fixed, for 2, 4, and 6 cm breast thicknesses of 100% fatty breasts, Mo/Mo target-filter materials.

Figure 19B: CD score versus kVp, keeping OD fixed, for 2, 4, and 6 cm breast thicknesses of 30% glandular/70% fatty breasts, Mo/Mo target-filter materials.

Figure 19C: CD score versus kVp, keeping OD fixed, for 2, 4, and 6 cm breast thicknesses of 50% glandular/50% fatty breasts, Mo/Mo target-filter materials.

Figure 19D: CD score versus kVp, keeping OD fixed, for 2, 4, and 6 cm breast thicknesses of 70% glandular/30% fatty breasts, Mo/Mo target-filter materials.

Figure 19E: CD score versus kVp, keeping OD fixed, for 2, 4, and 6 cm breast thicknesses of 50% glandular/50% fatty breasts, Mo/Rh target-filter materials.

Figure 19F: CD score versus kVp, keeping OD fixed, for 4 and 6 cm breast thicknesses of 50% glandular/50% fatty breasts, Rh/Rh target-filter materials.

Figure 20A: mAs versus kVp, keeping OD fixed, for 2, 4, and 6 cm breast thicknesses of 50% glandular/50% fatty breasts, Mo/Mo target-filter materials.

Figure 20B: mAs versus kVp, keeping OD fixed, for 2, 4, and 6 cm breast thicknesses of 50% glandular/50% fatty breasts, Mo/Rh target-filter materials.

Figure 20C: mAs versus kVp, keeping OD fixed, for 2, 4, and 6 cm breast thicknesses of 50% glandular/50% fatty breasts, Rh/Rh target-filter materials.

Figure 21A: Average glandular dose versus kVp, keeping OD fixed, for 2, 4, and 6 cm breast thicknesses of 50% glandular/50% fatty breasts, Mo/Mo target-filter materials.

Figure 21B: Average glandular dose versus kVp, keeping OD fixed, for 4 and 6 cm breast thicknesses of 50% glandular/50% fatty breasts, Mo/Rh target-filter materials.

Figure 21C: Average glandular dose versus kVp, keeping OD fixed, for 4 and 6 cm breast thicknesses of 50% glandular/50% fatty breasts, Rh/Rh target-filter materials.

Figure 22A: Film optical densities resulting from AEC exposure of a uniform 2 cm thick tissue-equivalent phantom using a Mo/Mo target-filter combination and two film-screen combinations, Kodak Min R-2000 film and screens (solid curves) and MRH-1 film with Min R cassettes (dotted curves). The top pair of curves results from having the AEC detector set on 100% glandular tissues. The middle pair of curves results from having the AEC detector set on 50% glandular/50% fatty tissues, and the lowest pair of curves results from having the AEC detector set on 100% fatty tissues, all of the same 2 cm uniform thickness as the phantom.

Figure 22B: Film optical densities resulting from AEC exposure of a uniform 2 cm thick tissue-equivalent phantom using a Mo/Rh target-filter combination and two film-screen combinations, Kodak Min R-2000 film and screens (solid curves) and MRH-1 film with Min R cassettes (dotted curves). The top pair of curves results from having the AEC detector set on 100% glandular tissues. The middle pair of curves results from having the AEC detector set on 50% glandular/50% fatty tissues, and the lowest pair of curves results from having the AEC detector set on 100% fatty tissues, all of the same 2 cm uniform thickness as the phantom.

Figure 22C: Film optical densities resulting from AEC exposure of a uniform 2 cm thick tissue-equivalent phantom using a Rh/Rh target-filter combination and two film-screen combinations, Kodak Min R-2000 film and screens (solid curves) and MRH-1 film with Min R cassettes (dotted curves). The top pair of curves results from having the AEC detector set on 100% glandular tissues. The middle pair of curves results from having the AEC detector set on 50% glandular/50% fatty tissues, and the lowest pair of curves results from having the AEC detector set on 100% fatty tissues, all of the same 2 cm uniform thickness as the phantom.

Figure 22D: Film optical densities resulting from AEC exposure of a uniform 4 cm thick tissue-equivalent phantom using a Mo/Mo target-filter combination and two film-screen combinations, Kodak Min R-2000 film and screens (solid curves) and MRH-1 film with Min R cassettes (dotted curves). The top pair of curves results from having the AEC detector set on 100% glandular tissues. The middle pair of curves results from having the AEC detector set on 50% glandular/50% fatty tissues, and the lowest pair of curves results from having the AEC detector set on 100% fatty tissues, all of the same 4 cm uniform thickness as the phantom.

Figure 22E: Film optical densities resulting from AEC exposure of a uniform 4 cm thick tissue-equivalent phantom using a Mo/Rh target-filter combination and two film-screen combinations, Kodak Min R-2000 film and screens (solid curves) and MRH-1 film with Min R cassettes (dotted curves). The top pair of curves results from having the AEC detector set on 100% glandular tissues. The middle pair of curves results from having the AEC detector set on 50% glandular/50% fatty tissues, and the lowest pair of curves results from having the AEC detector set on 100% fatty tissues, all of the same 4 cm uniform thickness as the phantom.

Figure 22F: Film optical densities resulting from AEC exposure of a uniform 4 cm thick tissue-equivalent phantom using a Rh/Rh target-filter combination and two film-screen combinations, Kodak Min R-2000 film and screens (solid curves) and MRH-1 film with Min R cassettes (dotted curves). The top pair of curves results from having the AEC detector set on 100% glandular tissues. The middle pair of curves results from having the AEC detector set on 50% glandular/50% fatty tissues, and the lowest pair of curves results from having the AEC detector set on 100% fatty tissues, all of the same 4 cm uniform thickness as the phantom.

Figure 22G: Film optical densities resulting from AEC exposure of a uniform 6 cm thick tissue-equivalent phantom using a Mo/Mo target-filter combination and two film-screen combinations, Kodak Min R-2000 film and screens (solid curves) and MRH-1 film with Min R cassettes (dotted curves). The top pair of curves results from having the AEC detector set on 100% glandular tissues. The middle pair of curves results from having the AEC detector set on 50% glandular/50% fatty tissues, and the lowest pair of curves results from having the AEC detector set on 100% fatty tissues, all of the same 6 cm uniform thickness as the phantom.

Figure 22H: Film optical densities resulting from AEC exposure of a uniform 6 cm thick tissue-equivalent phantom using a Mo/Rh target-filter combination and two film-screen combinations, Kodak Min R-2000 film and screens (solid curves) and MRH-1 film with Min R cassettes (dotted curves). The top pair of curves results from having the AEC detector set on 100% glandular tissues. The middle pair of curves results from having the AEC detector set on 50% glandular/50% fatty tissues, and the lowest pair of curves results from having the AEC detector set on 100% fatty tissues, all of the same 6 cm uniform thickness as the phantom.

Figure 22I: Film optical densities resulting from AEC exposure of a uniform 6 cm thick tissue-equivalent phantom using a Rh/Rh target-filter combination and two film-screen combinations, Kodak Min R-2000 film and screens (solid curves) and MRH-1 film with Min R cassettes (dotted curves). The top pair of curves results from having the AEC detector set on 100% glandular tissues. The middle pair of curves results from having the AEC detector set on 50% glandular/50% fatty tissues, and the lowest pair of curves results from having the AEC detector set on 100% fatty tissues, all of the same 6 cm uniform thickness as the phantom.

Figure 22J: Film optical densities resulting from AEC exposure of a uniform 7 cm thick tissue-equivalent phantom using a Mo/Mo target-filter combination and two film-screen combinations, Kodak Min R-2000 film and screens (solid curves) and MRH-1 film with Min R cassettes (dotted curves). The top pair of curves results from having the AEC detector set on 100% glandular tissues. The middle pair of curves results from having the AEC detector set on 50% glandular/50% fatty tissues, and the lowest pair of curves results from having the AEC detector set on 100% fatty tissues, all of the same 7 cm uniform thickness as the phantom.

Figure 22K: Film optical densities resulting from AEC exposure of a uniform 7 cm thick tissue-equivalent phantom using a Mo/Rh target-filter combination and two film-screen combinations, Kodak Min R-2000 film and screens (solid curves) and MRH-1 film with Min R cassettes (dotted curves). The top pair of curves results from having the AEC detector set on 100% glandular tissues. The middle pair of curves results from having the AEC detector set on 50% glandular/50% fatty tissues, and the lowest pair of curves results from having the AEC detector set on 100% fatty tissues, all of the same 7 cm uniform thickness as the phantom.

Figure 22L: Film optical densities resulting from AEC exposure of a uniform 7 cm thick tissue-equivalent phantom using a Rh/Rh target-filter combination and two film-screen combinations, Kodak Min R-2000 film and screens (solid curves) and MRH-1 film with Min R cassettes (dotted curves). The top pair of curves results from having the AEC detector set on 100% glandular tissues. The middle pair of curves results from having the AEC detector set on 50% glandular/50% fatty tissues, and the lowest pair of curves results from having the AEC detector set on 100% fatty tissues, all of the same 7 cm uniform thickness as the phantom.

Figure 23A: A_g values measured at 207 different mammography sites between 1990 and late 1995 as part of the CMAP medical physics surveys. The solid curve represents a best linear fit of the A_g data versus time, indicating a statistically significant increase in film-processing contrast over time.

Figure 23B: Average A_g values measured at 207 different mammography sites year by year between 1990 and 1995 as part of the CMAP medical physics surveys. Error bars represent one standard deviation from the mean for each year.

Figure 23C: Changes in A_g values among 10 sites with 3 medical physics surveys conducted between 1990 and 1995.

Figure 23D: Changes in A_g values among 7 sites with 4 or more medical physics surveys conducted between 1990 and 1995. Taken collectively, these upward trends are significant.

Figure 24A: A scattergram of film optical densities resulting from exposure of a uniform 6 cm thick phantom consisting of breast equivalent BR-12 material using each site's clinical technique factors for a 6 cm thick breast. The solid curve represents a best linear fit of the OD data versus time, indicating a statistically significant increase in film optical densities over time.

Figure 24B: Trends as a function of time between January 1993 and December 1995 in film optical densities for a 6 cm thick breast phantom among the 35 sites with two or more measurements in that time period.

Figure 25A: A scattergram of exposure times resulting from a 6 cm thick breast equivalent phantom using each site's clinical technique factors. The solid curve represents a best linear fit of the exposure time data versus time, indicating a statistically significant decrease in exposure times.

Figure 25B: Trends as a function of time between January 1993 and December 1995 in exposure times for a 6 cm thick breast phantom among the 35 sites with two or more measurements in that time period.

Figure 1A

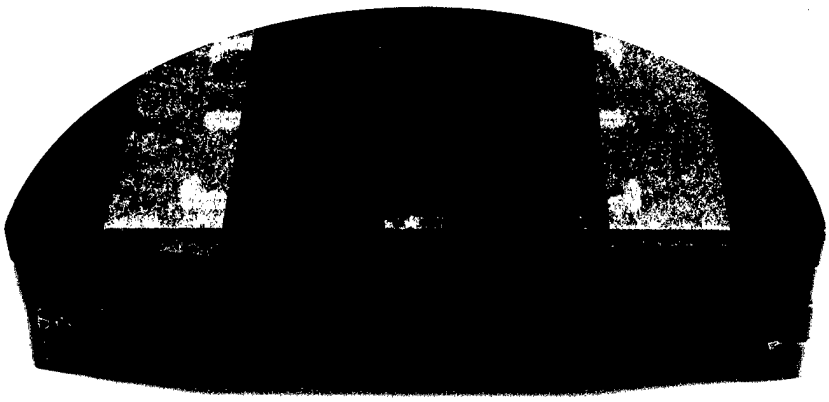

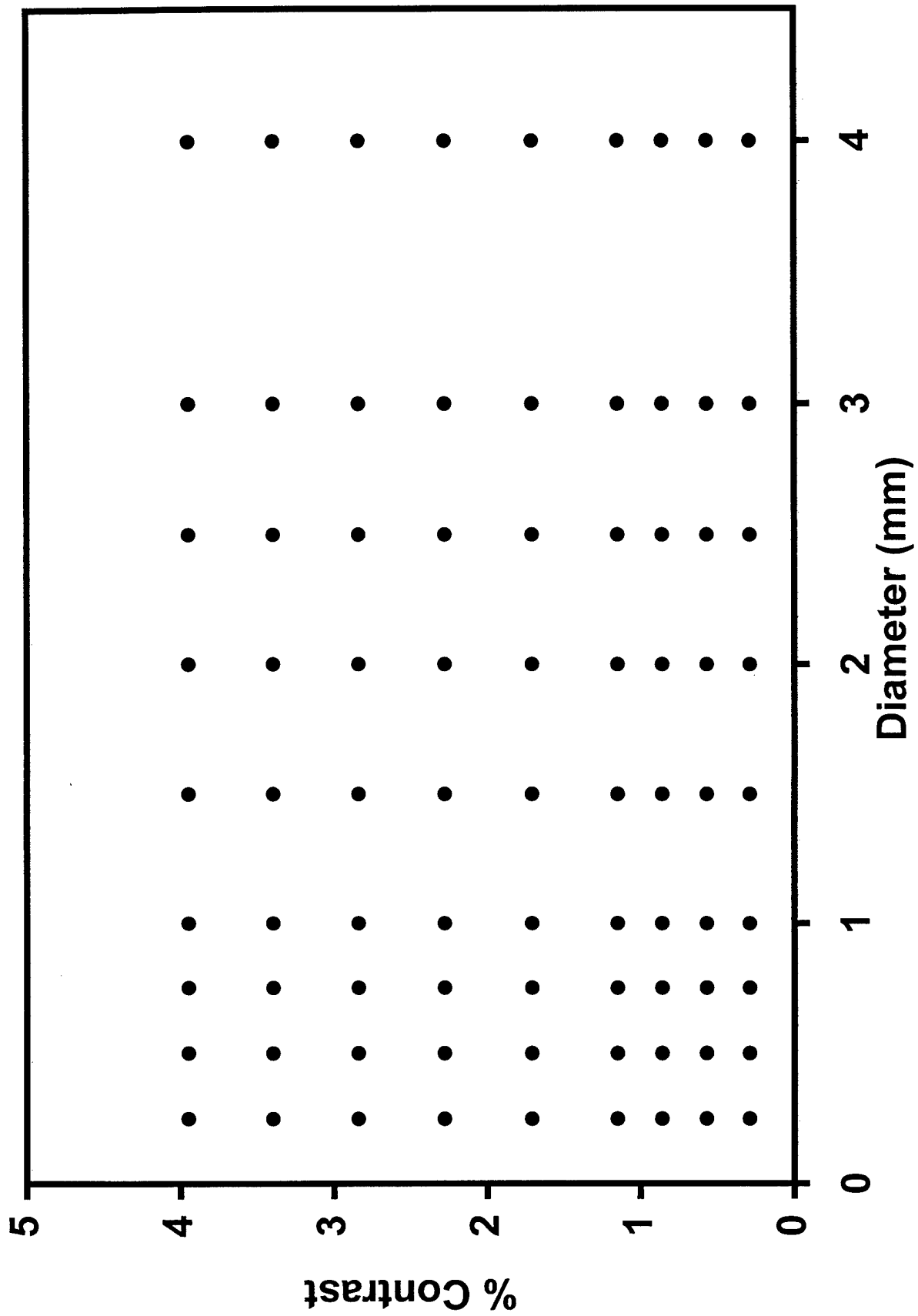

Figure 1B

Figure 2A

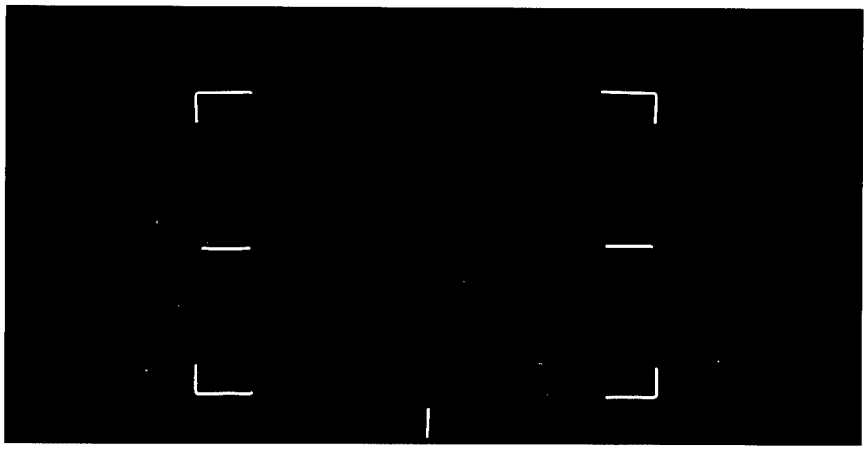

Figure 2B

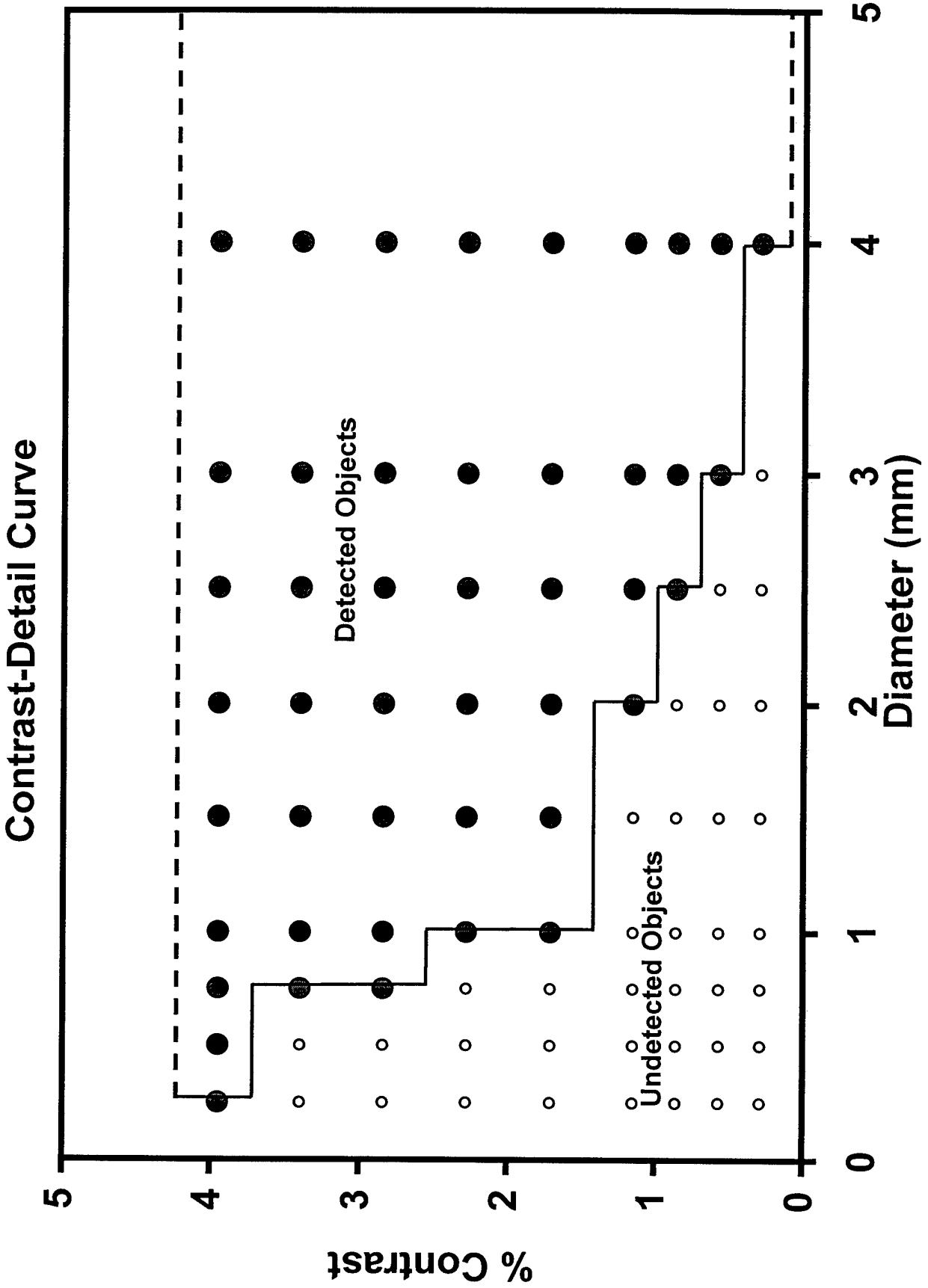
Contrast-Detail Curve
% Contrast
Diameter (mm)
Detected Objects
Undetected Objects
0
1
2
3
4
5

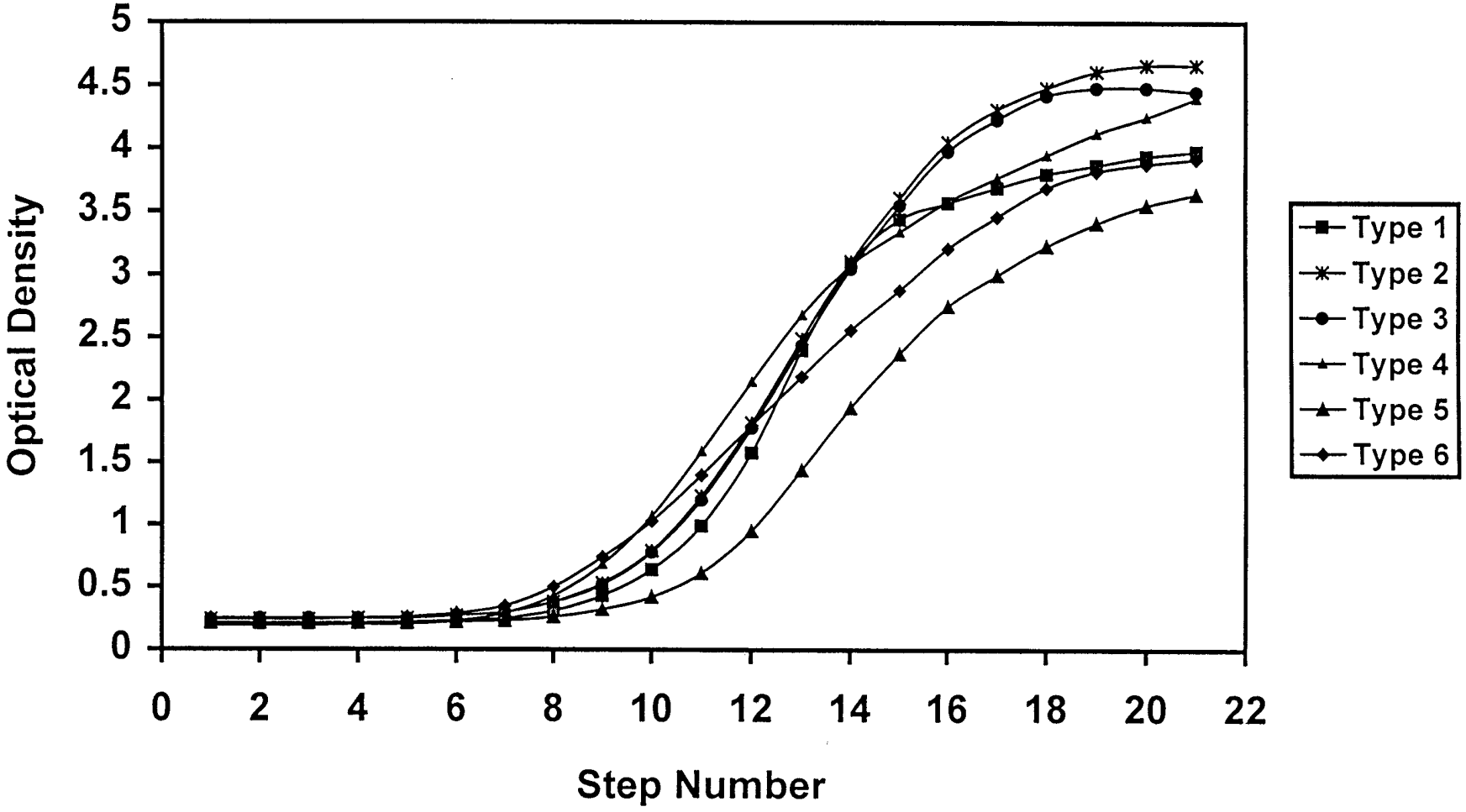
H&D Curves
Optical Density
5
4.5
4
3.5
3
2.5
2
1.5
1
0.5
0
0
2
4
6
8
10
12
14
16
18
20
22
Step Number
Type 1
Type 2
Type 3
Type 4
Type 5
Type 6

Figure 3

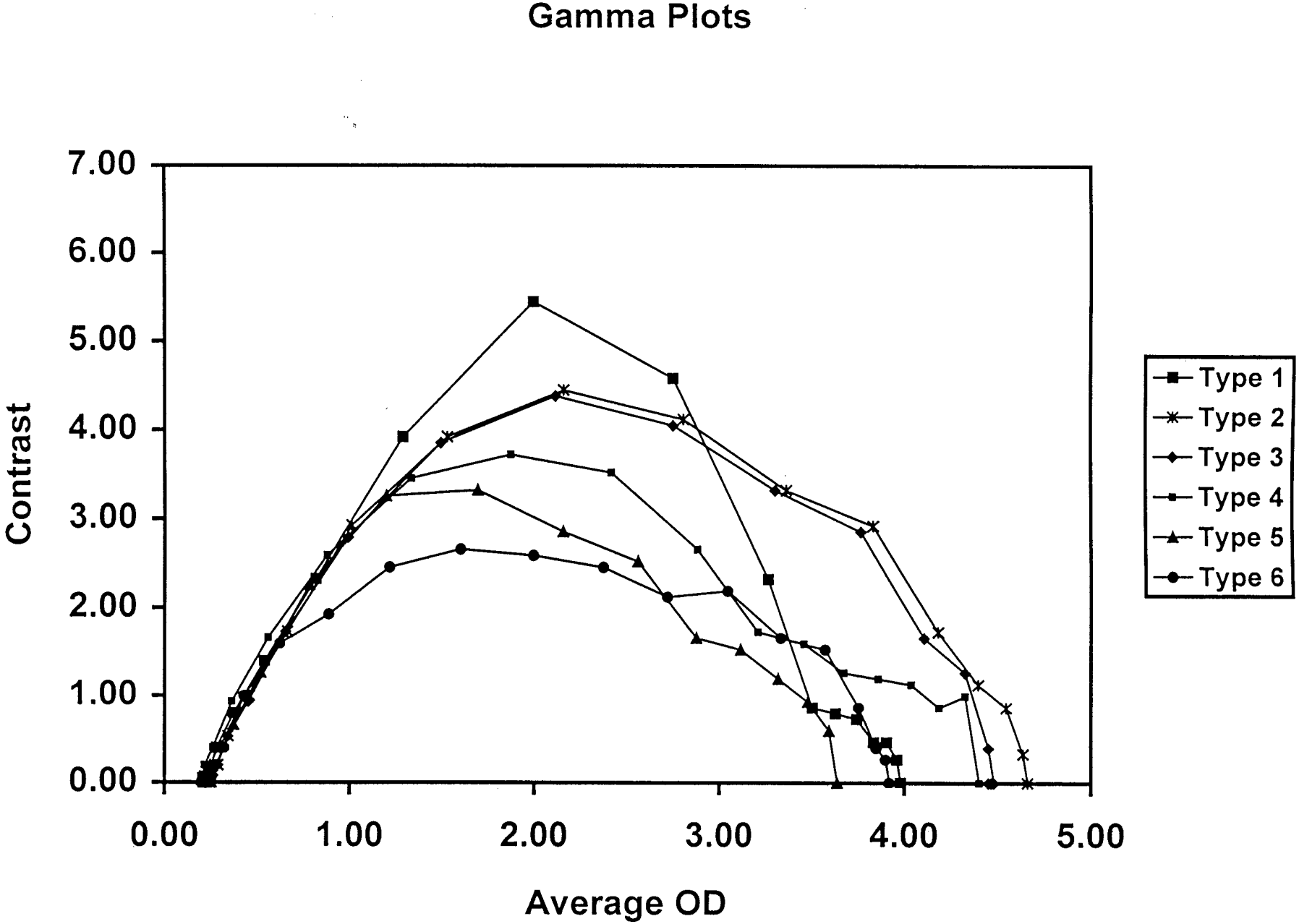
Gamma Plots
Contrast
7.00
6.00
5.00
4.00
3.00
2.00
1.00
0.00
0.00
1.00
2.00
3.00
4.00
5.00
Average OD
Type 1
Type 2
Type 3
Type 4
Type 5
Type 6

Figure 4

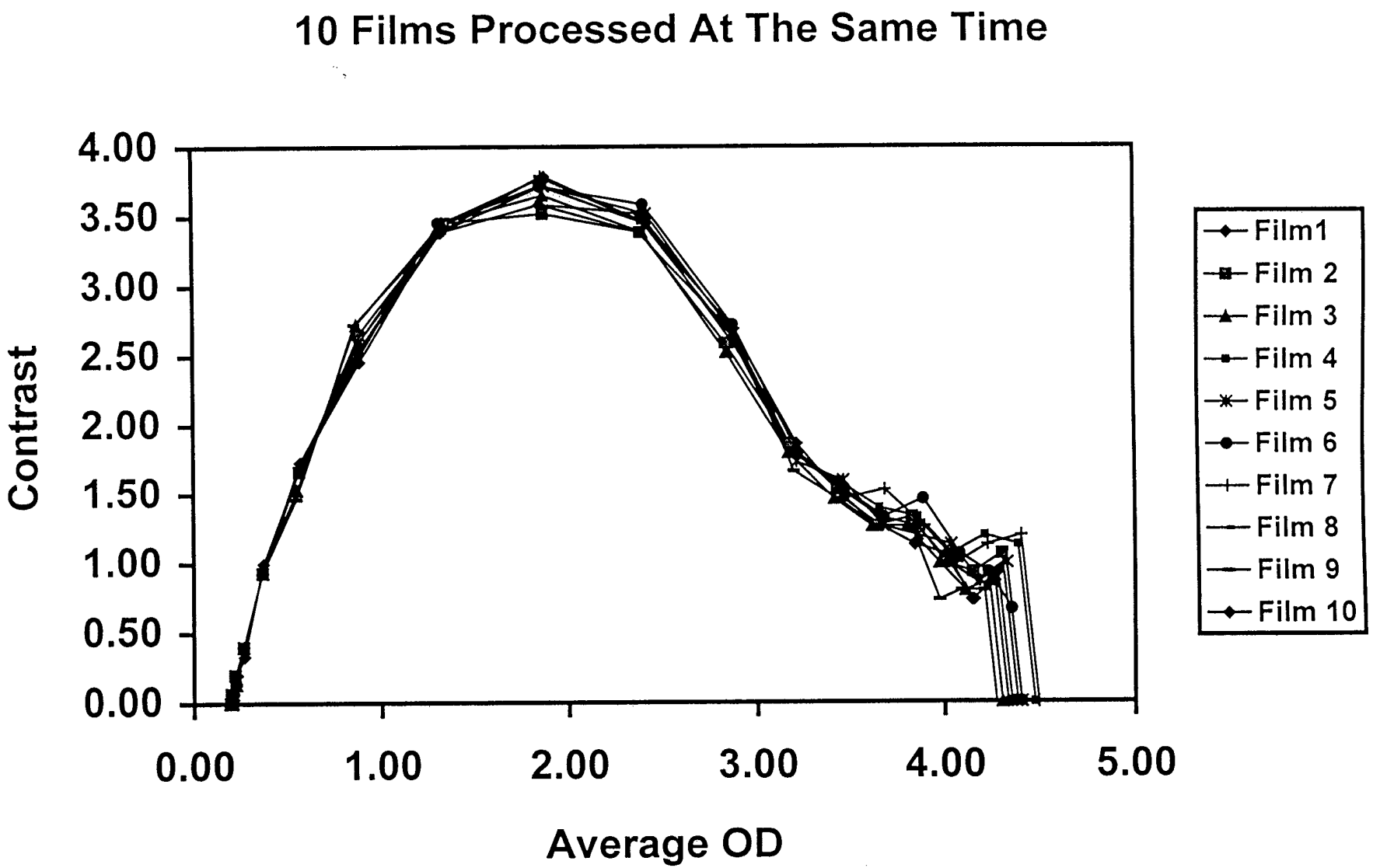
10 Films Processed At The Same Time
Contrast
4.00
3.50
3.00
2.50
2.00
1.50
1.00
0.50
0.00
0.00
1.00
2.00
3.00
4.00
5.00
Average OD
Film1
Film 2
Film 3
Film 4
Film 5
Film 6
Film 7
Film 8
Film 9
Film 10

Figure 5A

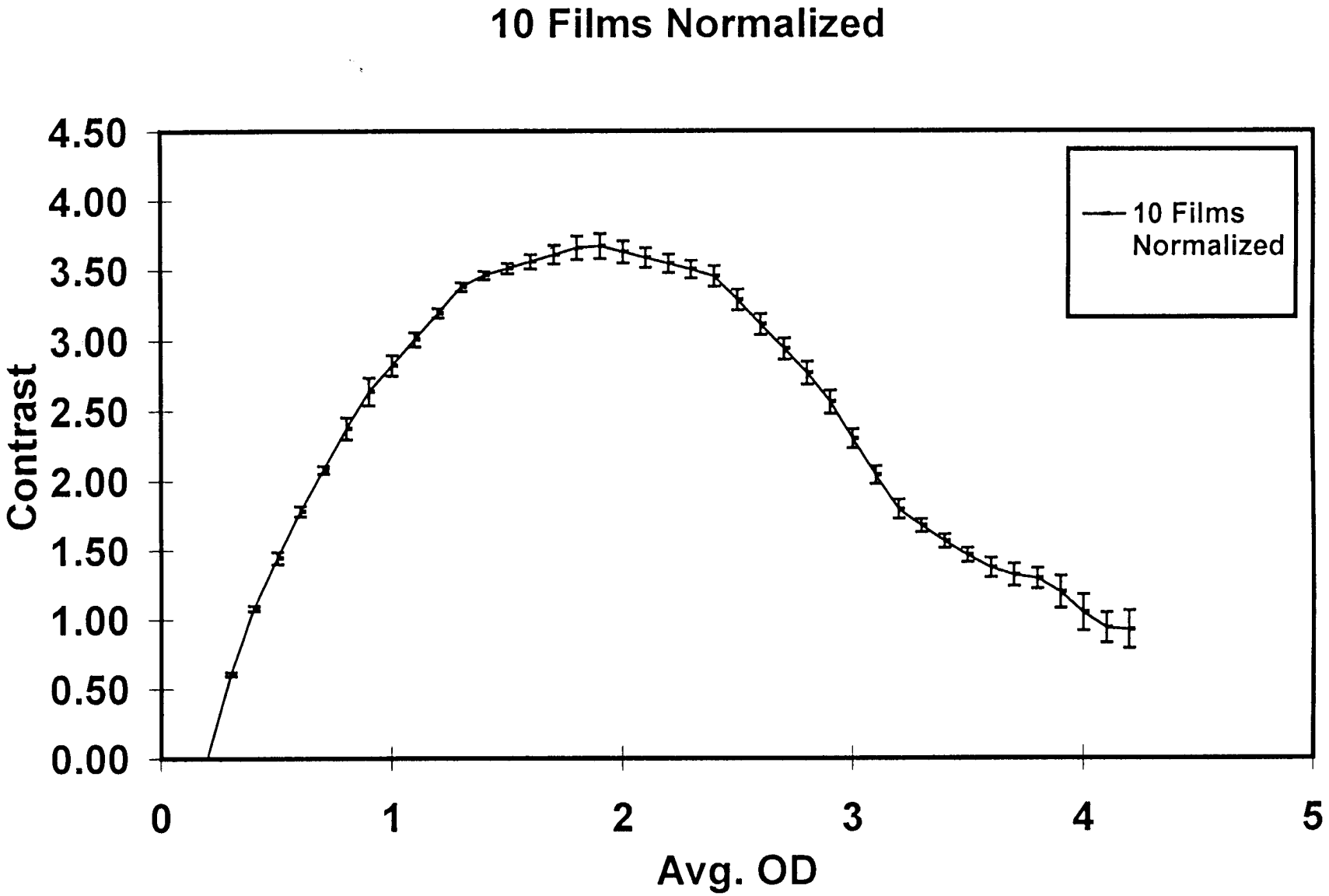
10 Films Normalized
Contrast
4.50
4.00
3.50
3.00
2.50
2.00
1.50
1.00
0.50
0.00
0
1
2
3
4
5
Avg. OD
10 Films Normalized

Figure 5B

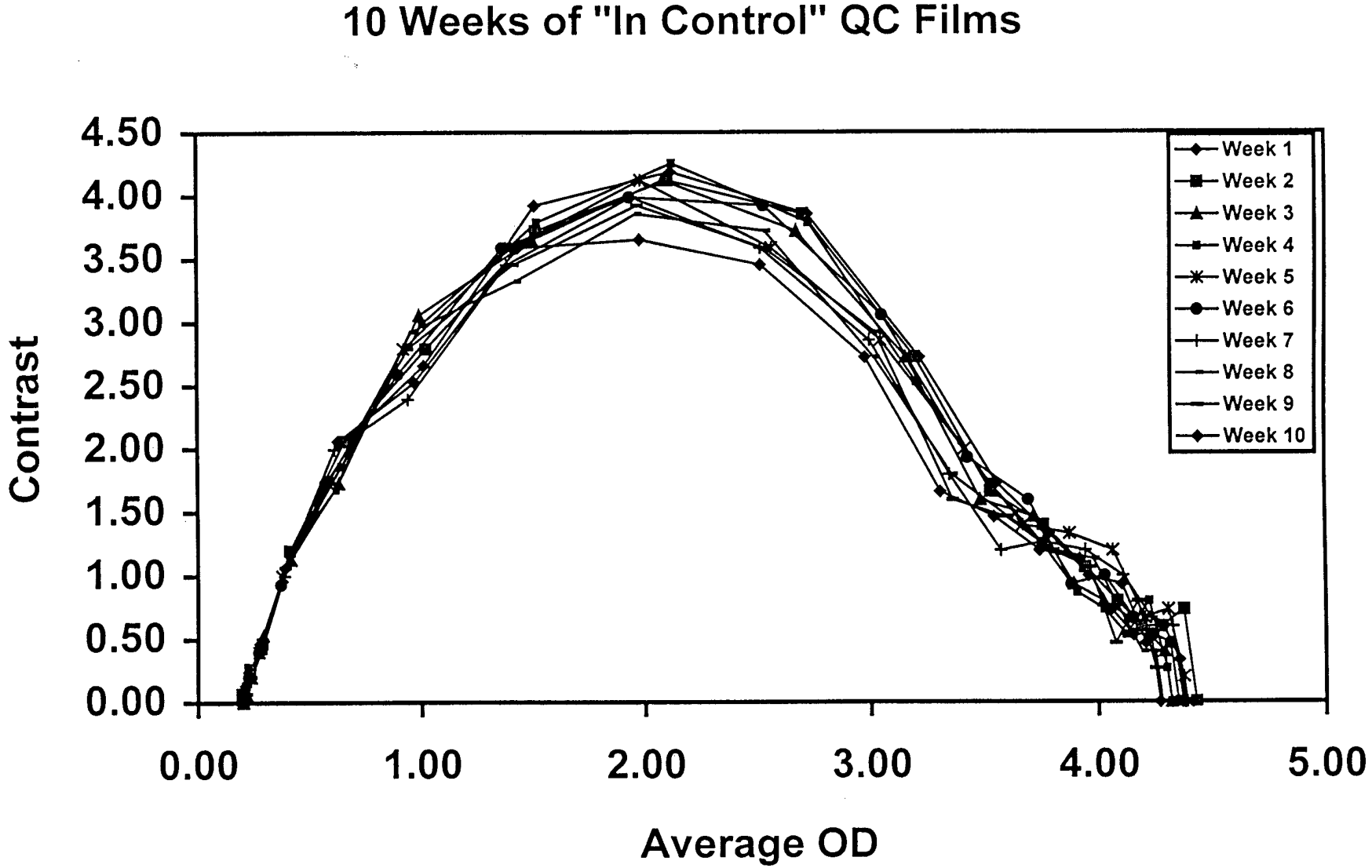
10 Weeks of "In Control" QC Films
Contrast
4.50
4.00
3.50
3.00
2.50
2.00
1.50
1.00
0.50
0.00
0.00
1.00
2.00
3.00
4.00
5.00
Average OD
Week 1
Week 2
Week 3
Week 4
Week 5
Week 6
Week 7
Week 8
Week 9
Week 10

Figure 6A

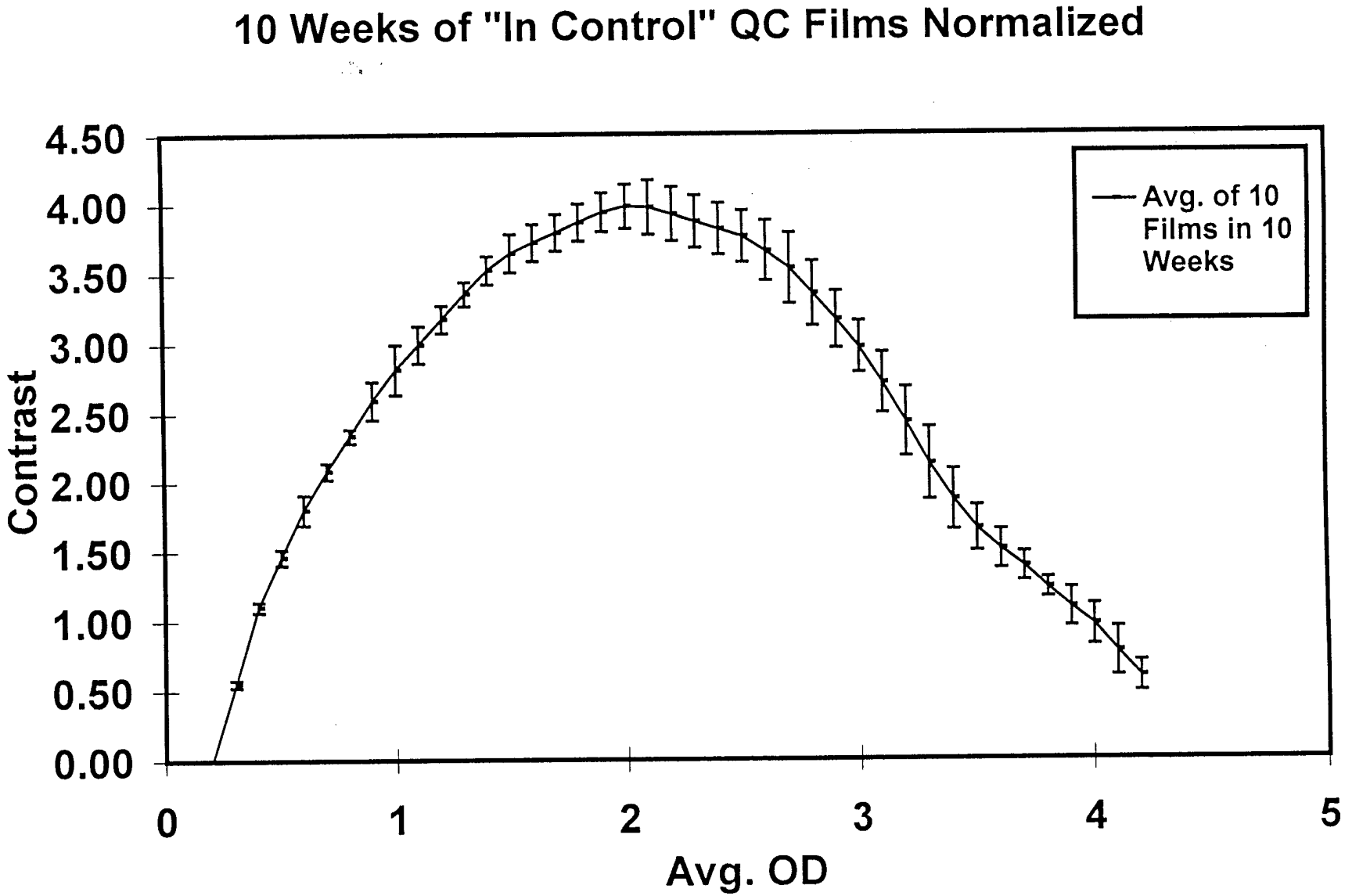
10 Weeks of "In Control" QC Films Normalized
Contrast
4.50
4.00
3.50
3.00
2.50
2.00
1.50
1.00
0.50
0.00
0
1
2
3
4
5
Avg. OD
Avg. of 10 Films in 10 Weeks

Figure 6B

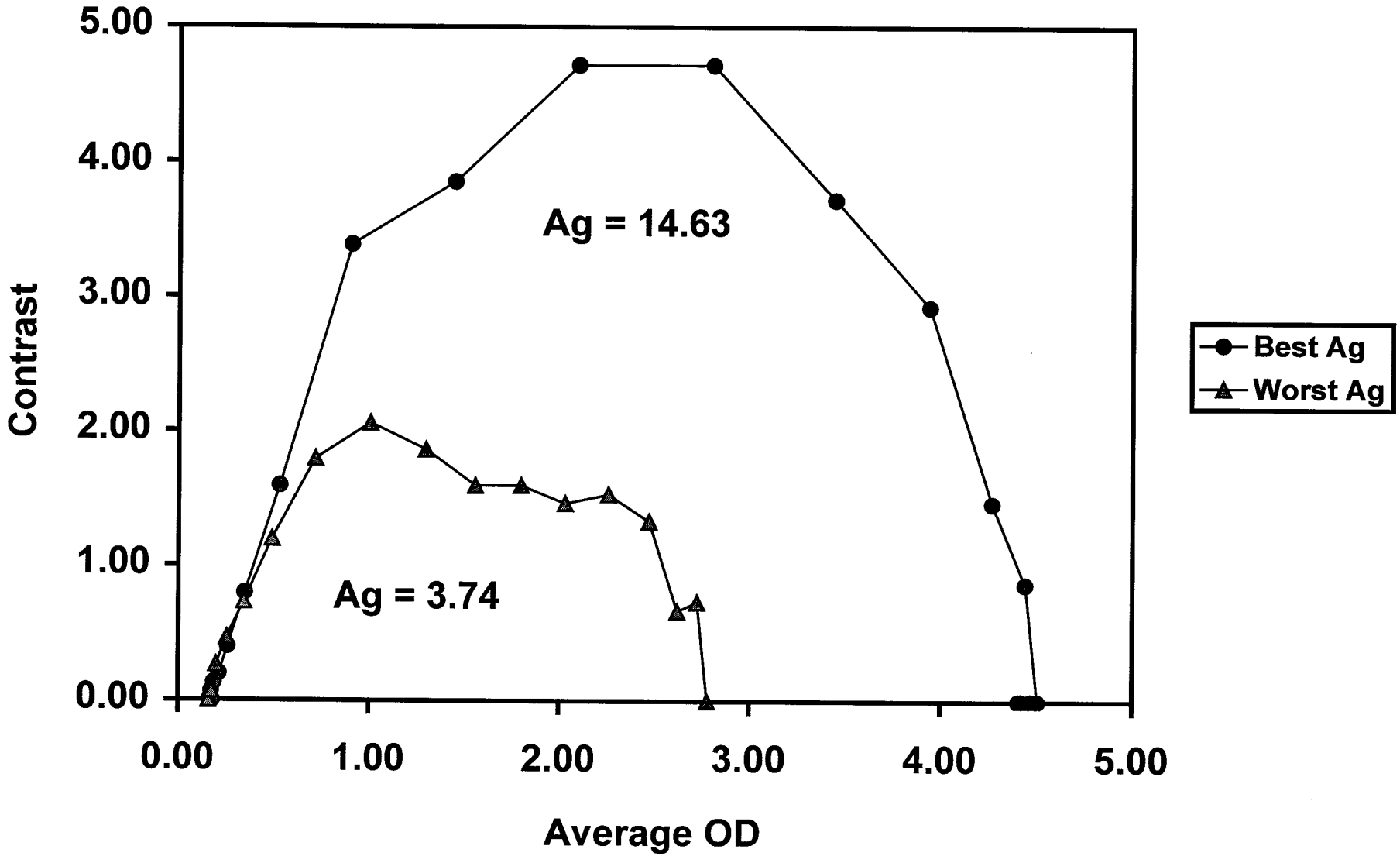
Best and Worst Film Contrast
For 207 Site Surveys
5.00
4.00
3.00
2.00
1.00
0.00
Contrast
Ag = 14.63
Ag = 3.74
0.00
1.00
2.00
3.00
4.00
5.00
Average OD
Best Ag
Worst Ag

Figure 7

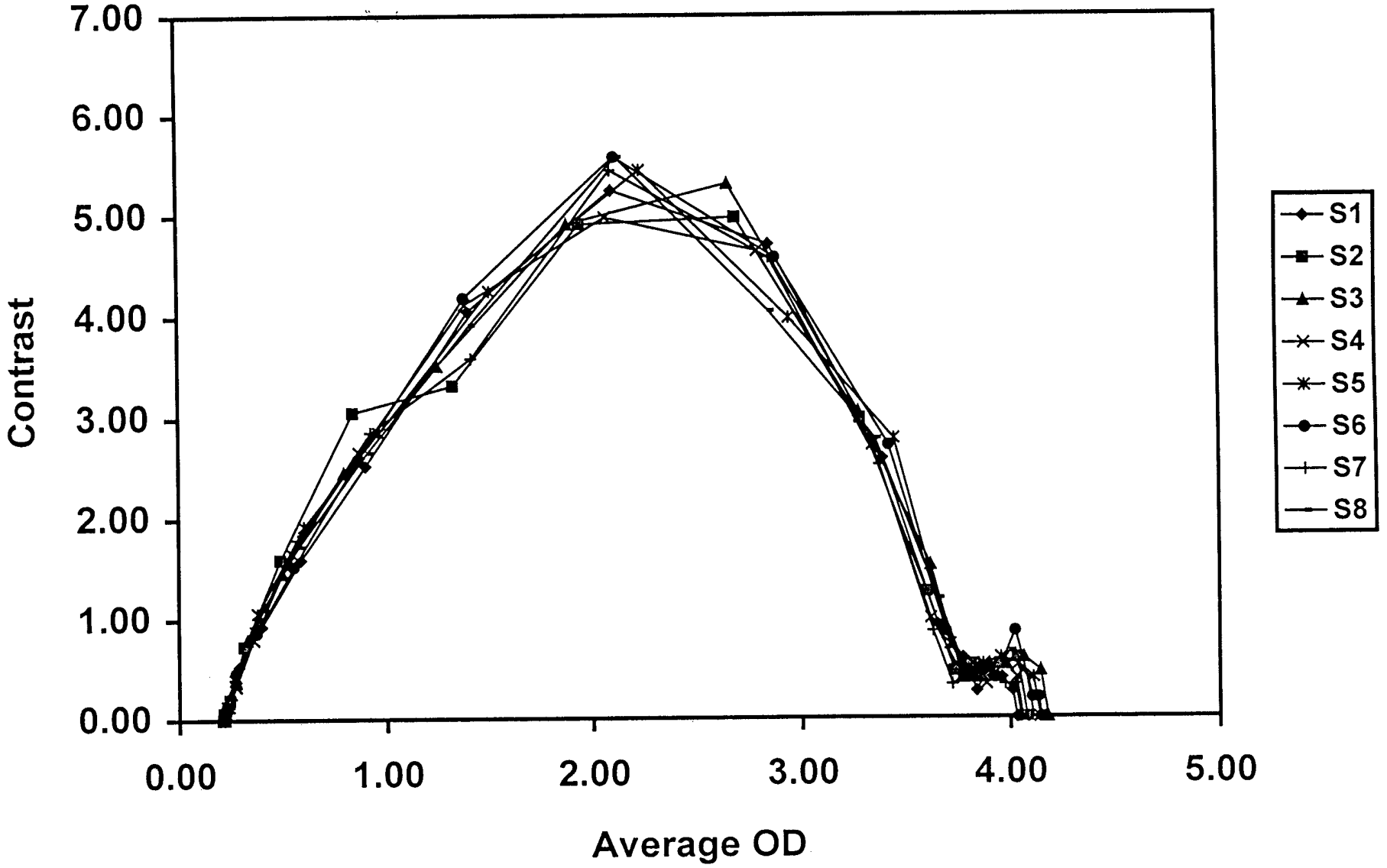
Sensitometer Comparison
7.00
6.00
5.00
4.00
3.00
2.00
1.00
0.00
Contrast
0.00
1.00
2.00
3.00
4.00
5.00
Average OD
S1
S2
S3
S4
S5
S6
S7
S8

Figure 8

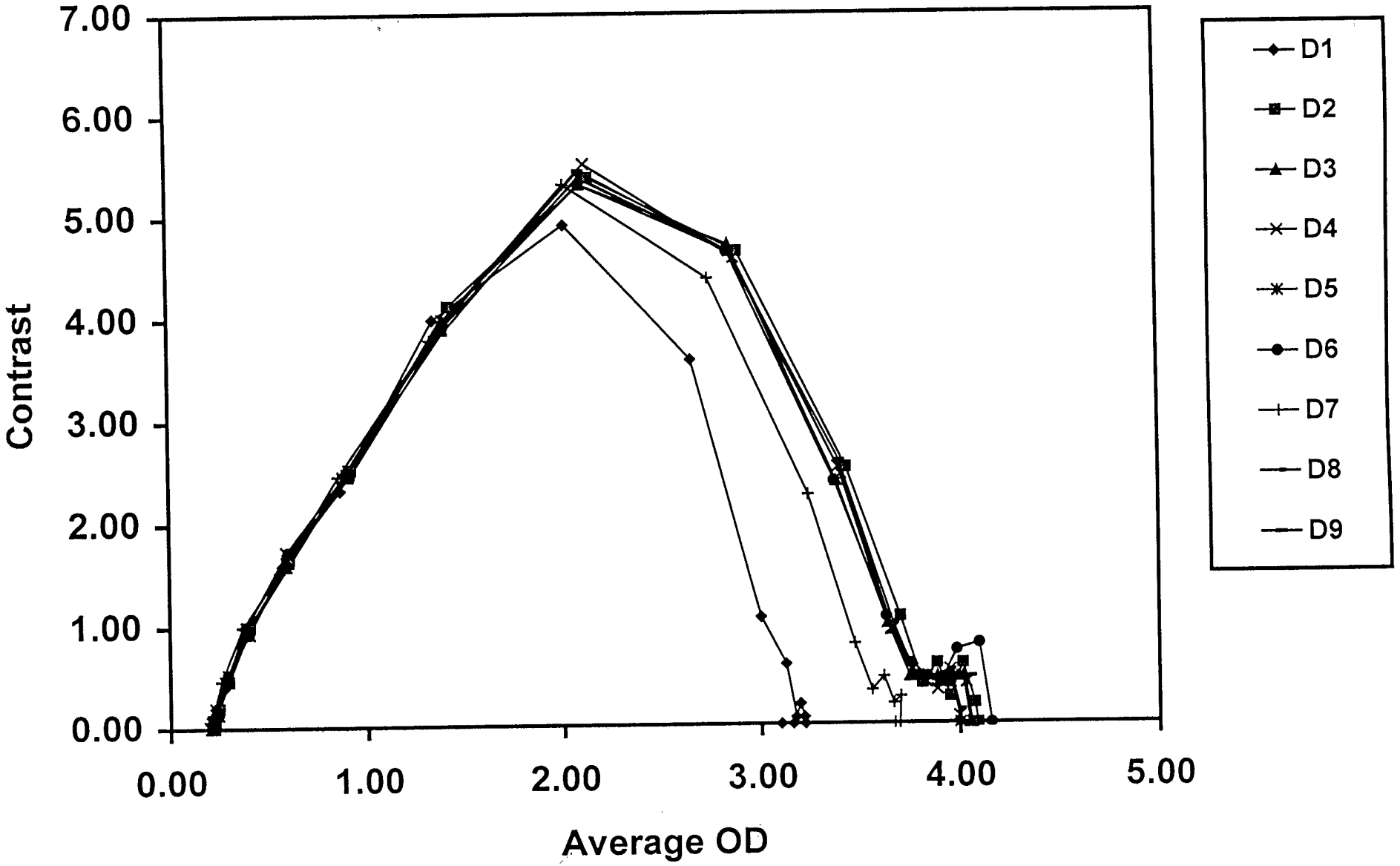
Densitometer Comparison
7.00
6.00
5.00
4.00
3.00
2.00
1.00
0.00
Contrast
0.00
1.00
2.00
3.00
4.00
5.00
Average OD
D1
D2
D3
D4
D5
D6
D7
D8
D9

Figure 9

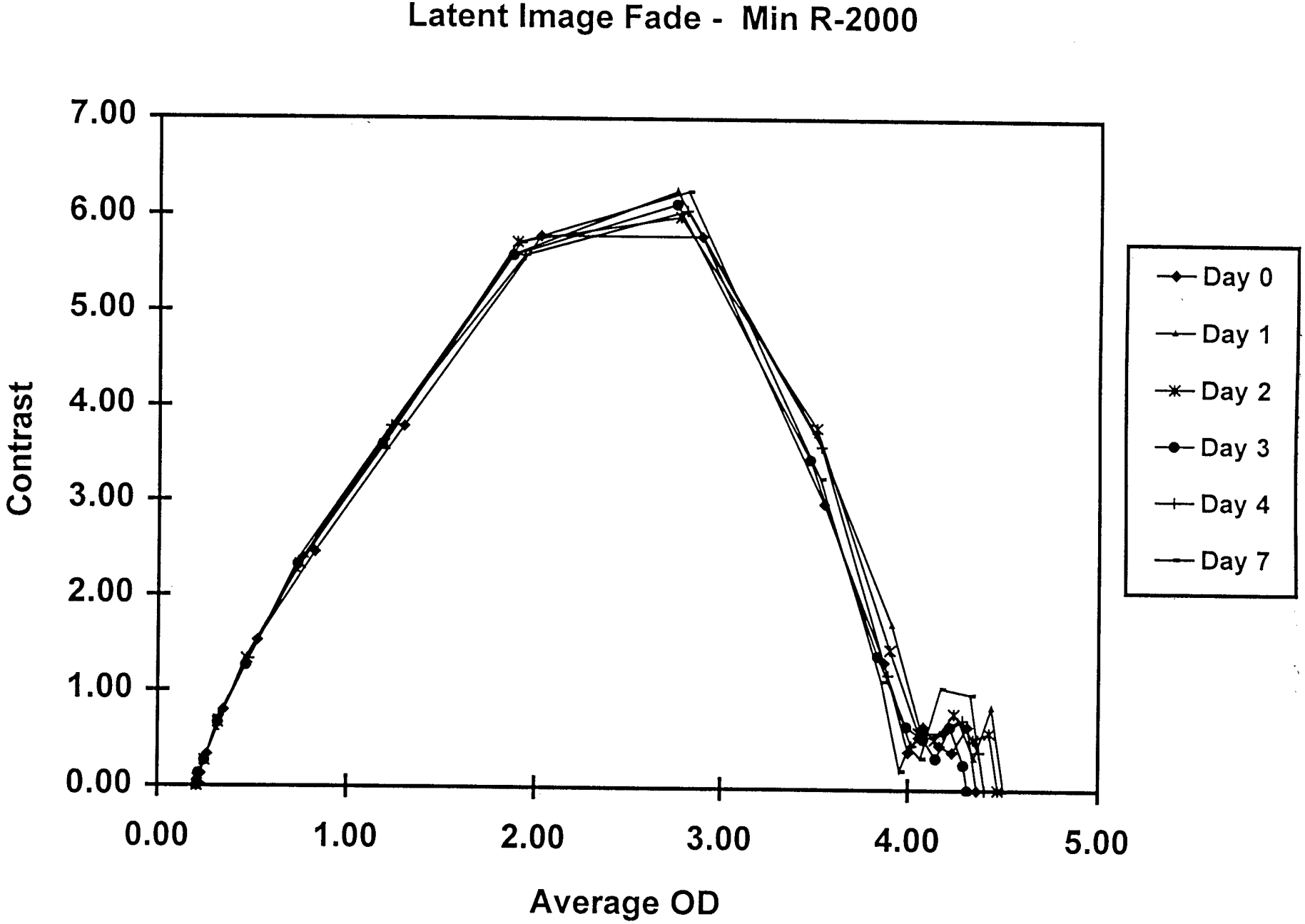
Latent Image Fade - Min R-2000
Contrast
7.00
6.00
5.00
4.00
3.00
2.00
1.00
0.00
0.00
1.00
2.00
3.00
4.00
5.00
Average OD
Day 0
Day 1
Day 2
Day 3
Day 4
Day 7

Figure 10

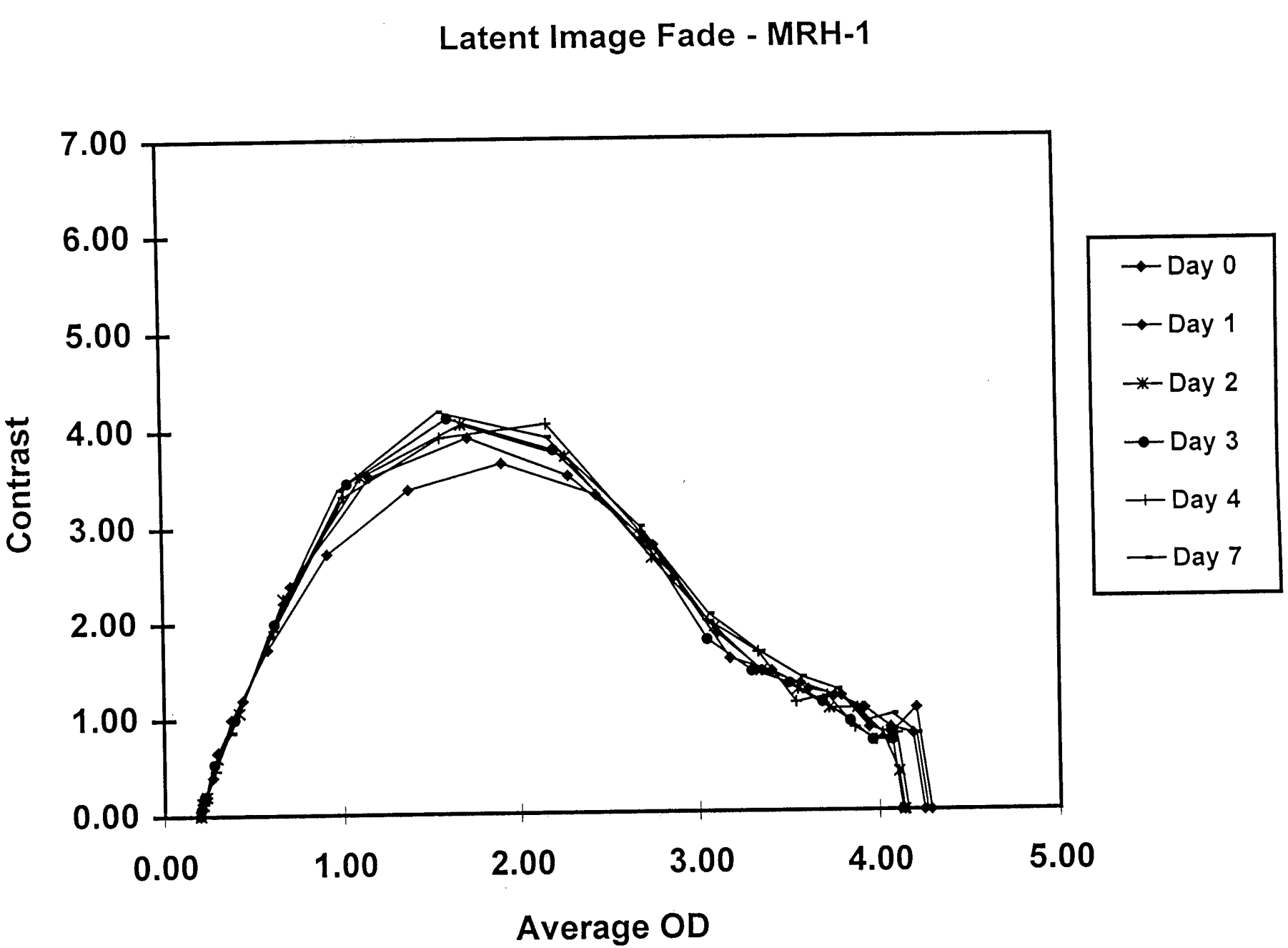
Latent Image Fade - MRH-1
7.00
6.00
5.00
4.00
3.00
2.00
1.00
0.00
Contrast
0.00
1.00
2.00
3.00
4.00
5.00
Average OD
Day 0
Day 1
Day 2
Day 3
Day 4
Day 7

Figure 11

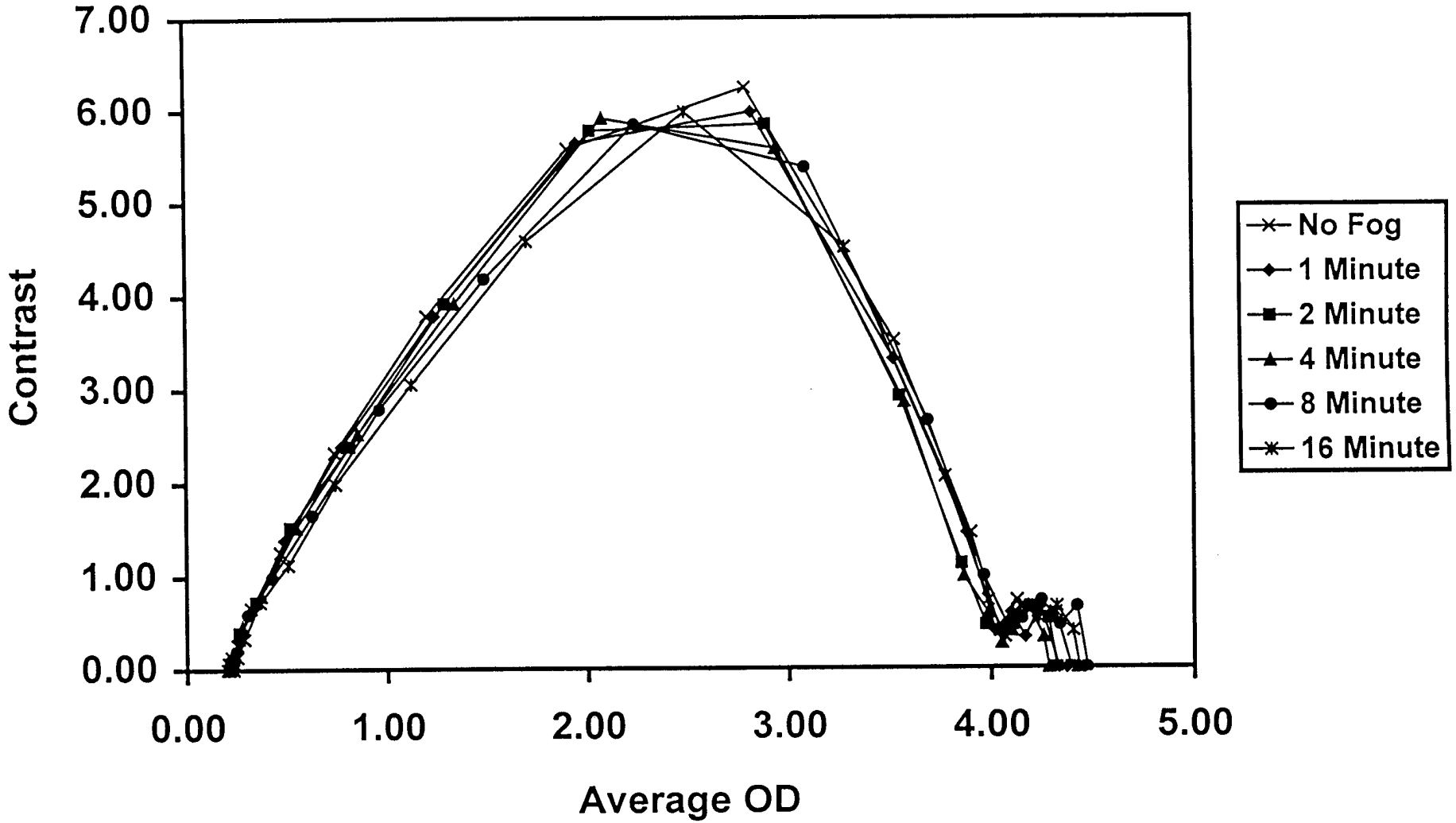
Fogged Films
7.00
6.00
5.00
4.00
3.00
2.00
1.00
0.00
Contrast
0.00
1.00
2.00
3.00
4.00
5.00
Average OD
No Fog
1 Minute
2 Minute
4 Minute
8 Minute
16 Minute

Figure 12

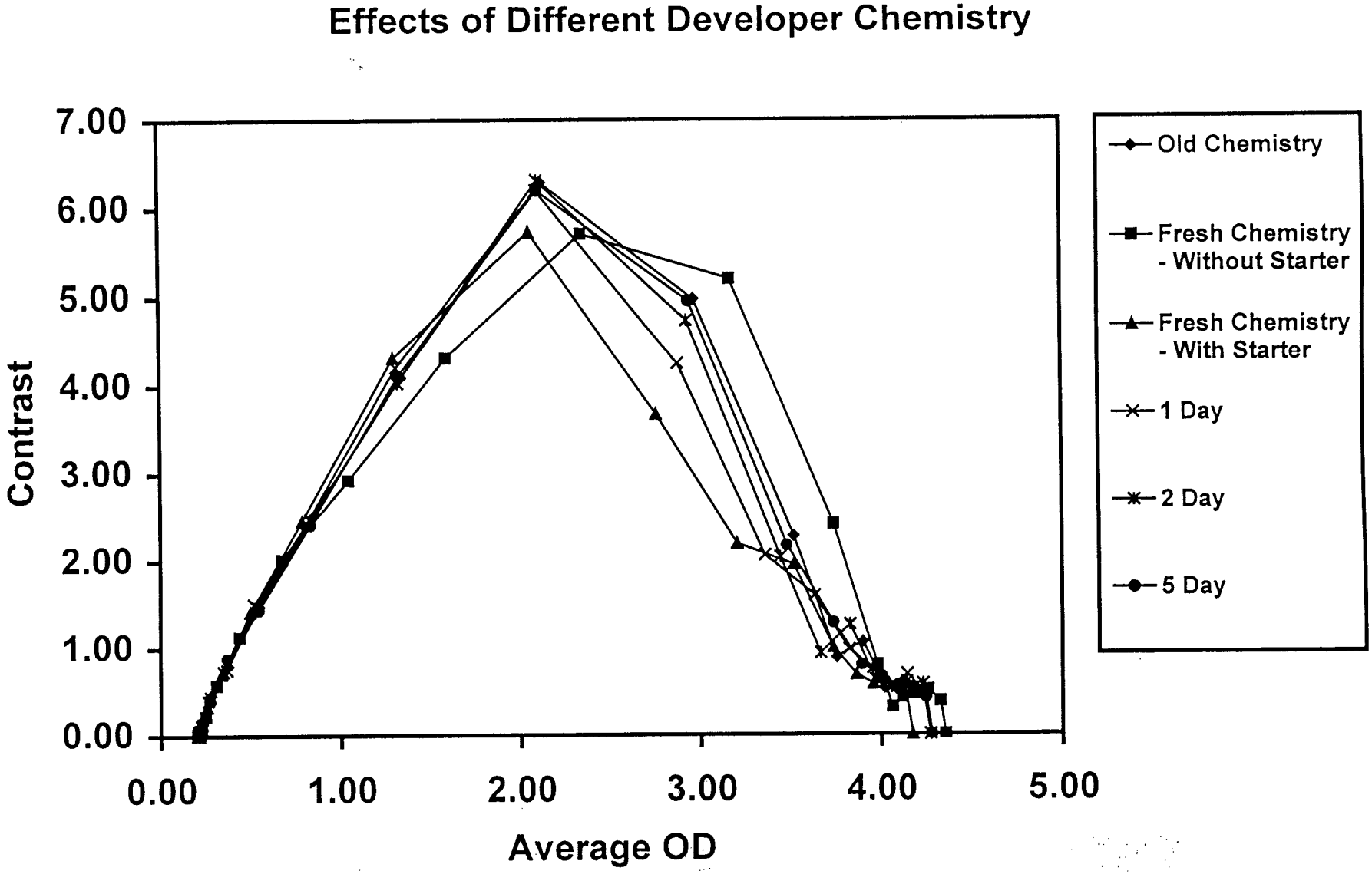
Effects of Different Developer Chemistry
Contrast
7.00
6.00
5.00
4.00
3.00
2.00
1.00
0.00
0.00
1.00
2.00
3.00
4.00
5.00
Average OD
Old Chemistry
Fresh Chemistry - Without Starter
Fresh Chemistry - With Starter
1 Day
2 Day
5 Day

Figure 13

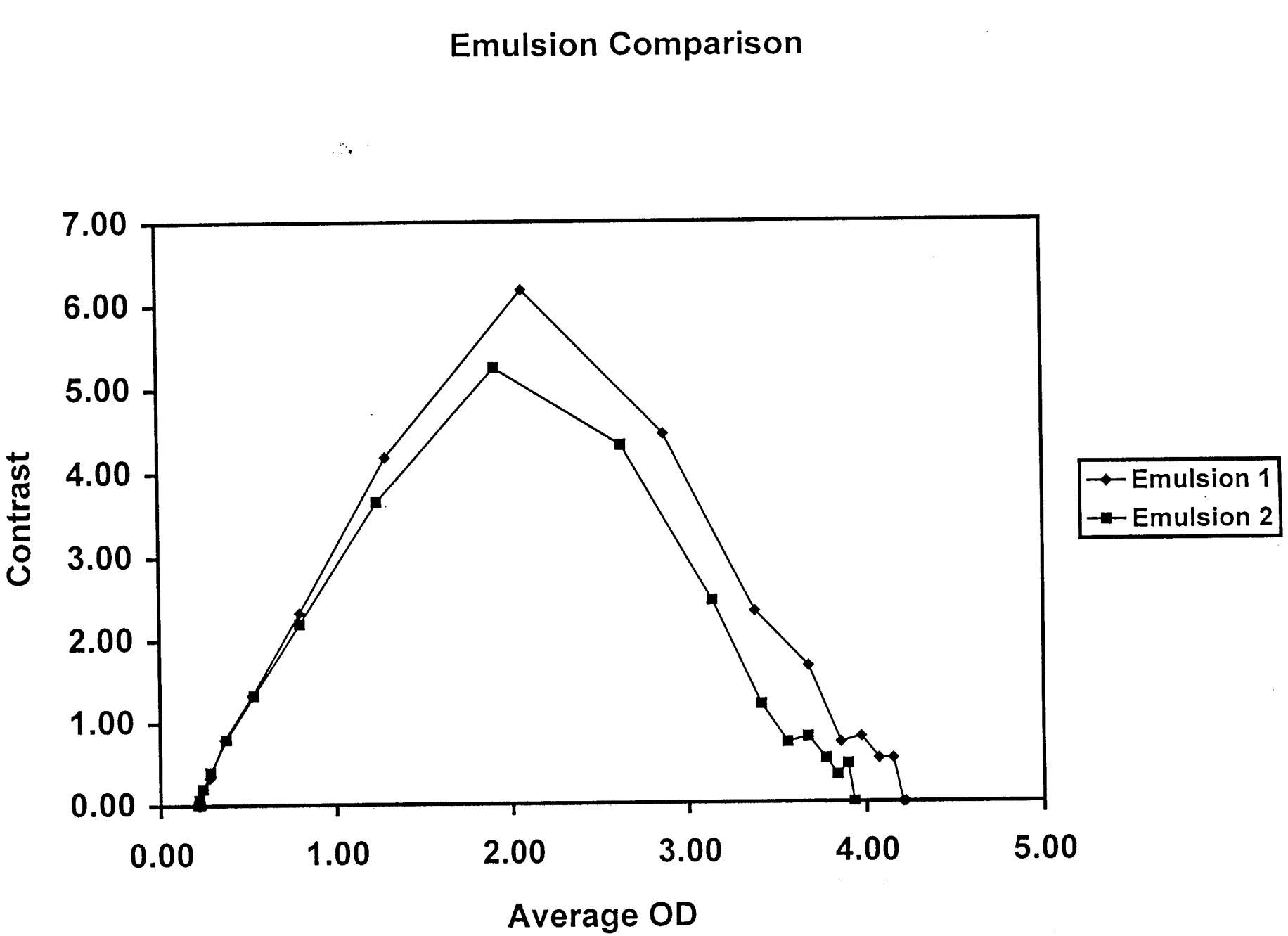
Emulsion Comparison
7.00
6.00
5.00
4.00
3.00
2.00
1.00
0.00
Contrast
0.00
1.00
2.00
3.00
4.00
5.00
Average OD
Emulsion 1
Emulsion 2

Figure 14

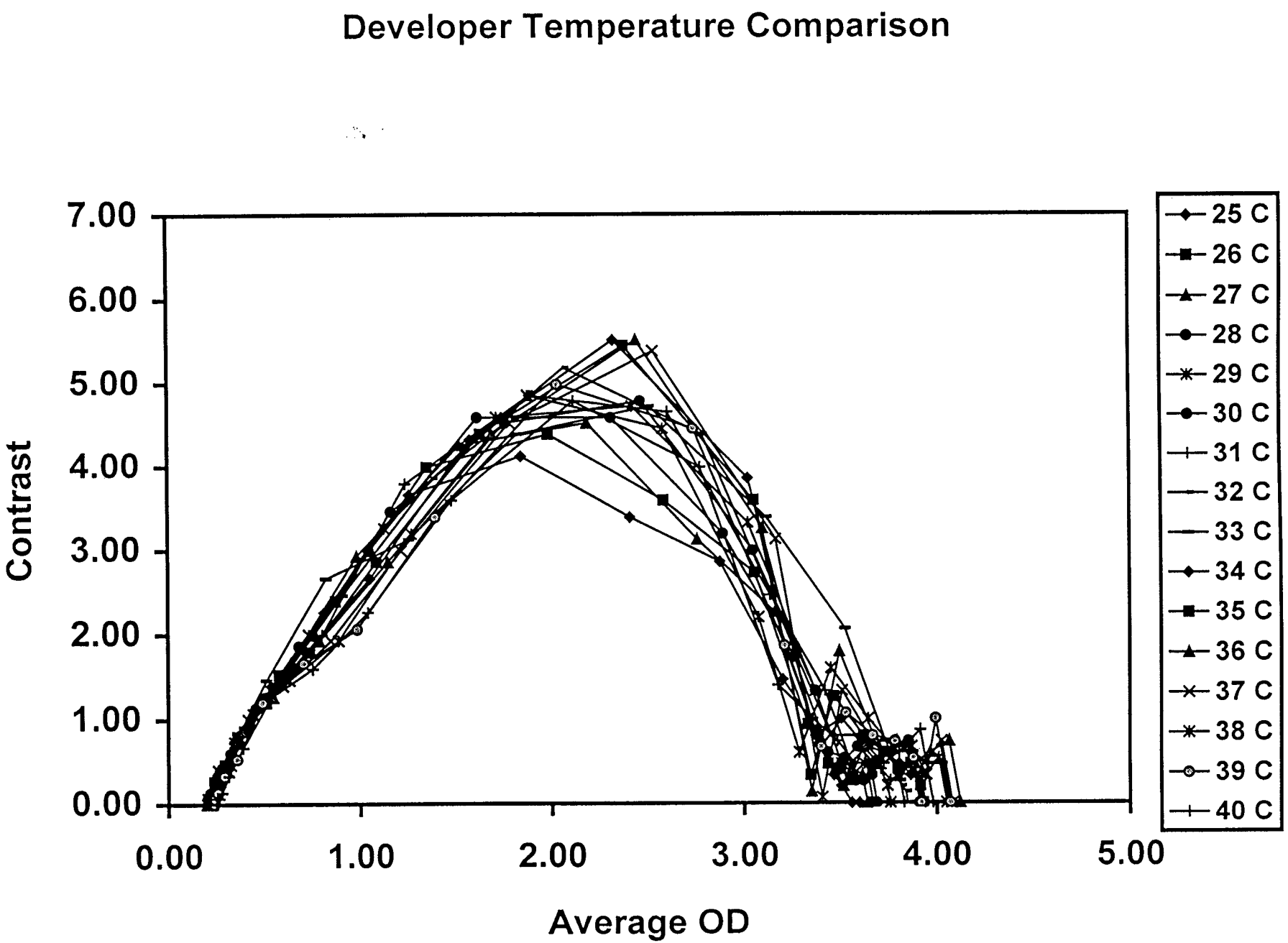
Developer Temperature Comparison
Contrast
7.00
6.00
5.00
4.00
3.00
2.00
1.00
0.00
0.00
1.00
2.00
3.00
4.00
5.00
Average OD
25 C
26 C
27 C
28 C
29 C
30 C
31 C
32 C
33 C
34 C
35 C
36 C
37 C
38 C
39 C
40 C

Figure 15

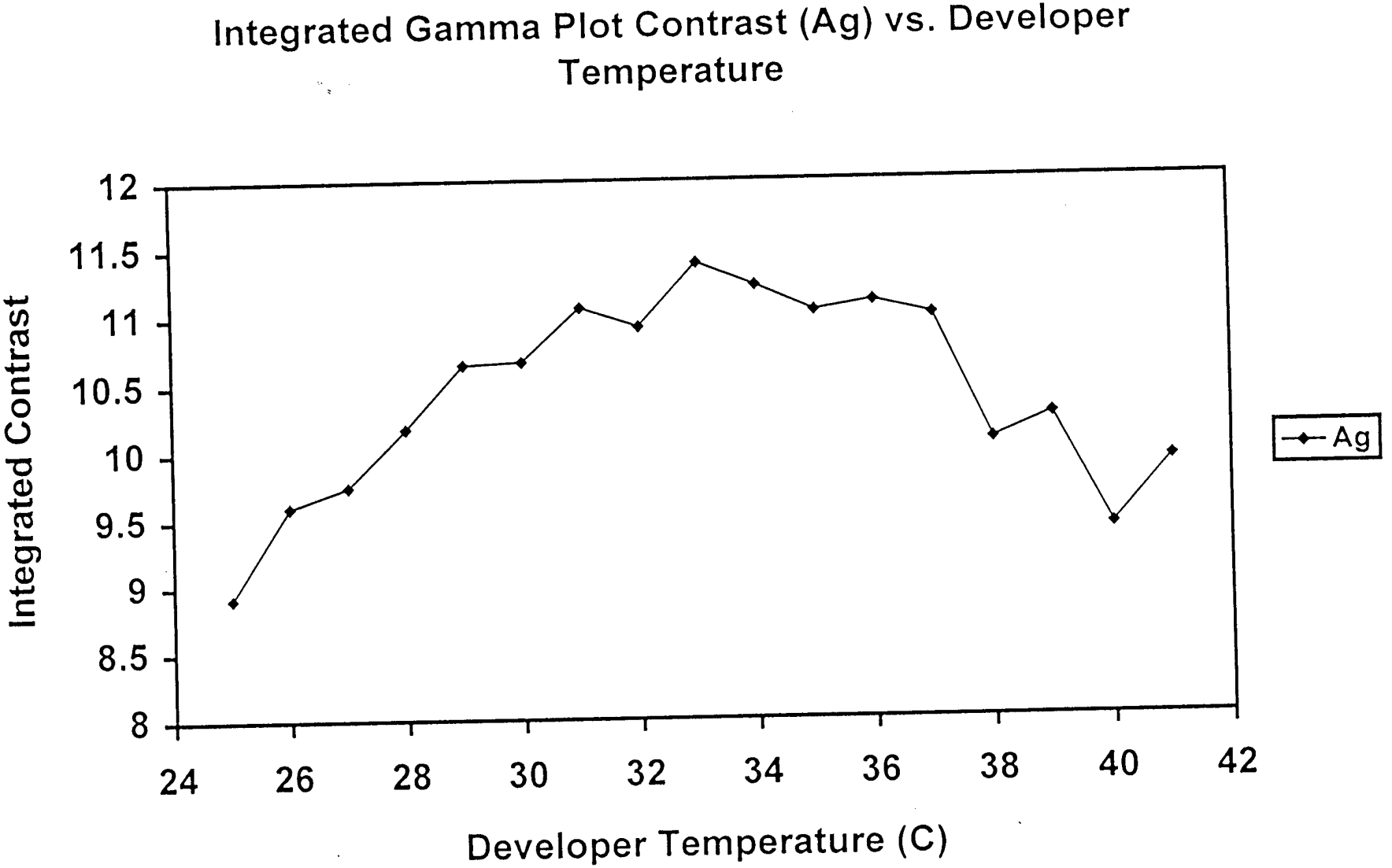
Integrated Gamma Plot Contrast (Ag) vs. Developer Temperature
Integrated Contrast
12
11.5
11
10.5
10
9.5
9
8.5
8
24
26
28
30
32
34
36
38
40
42
Developer Temperature (C)
Ag

Figure 16

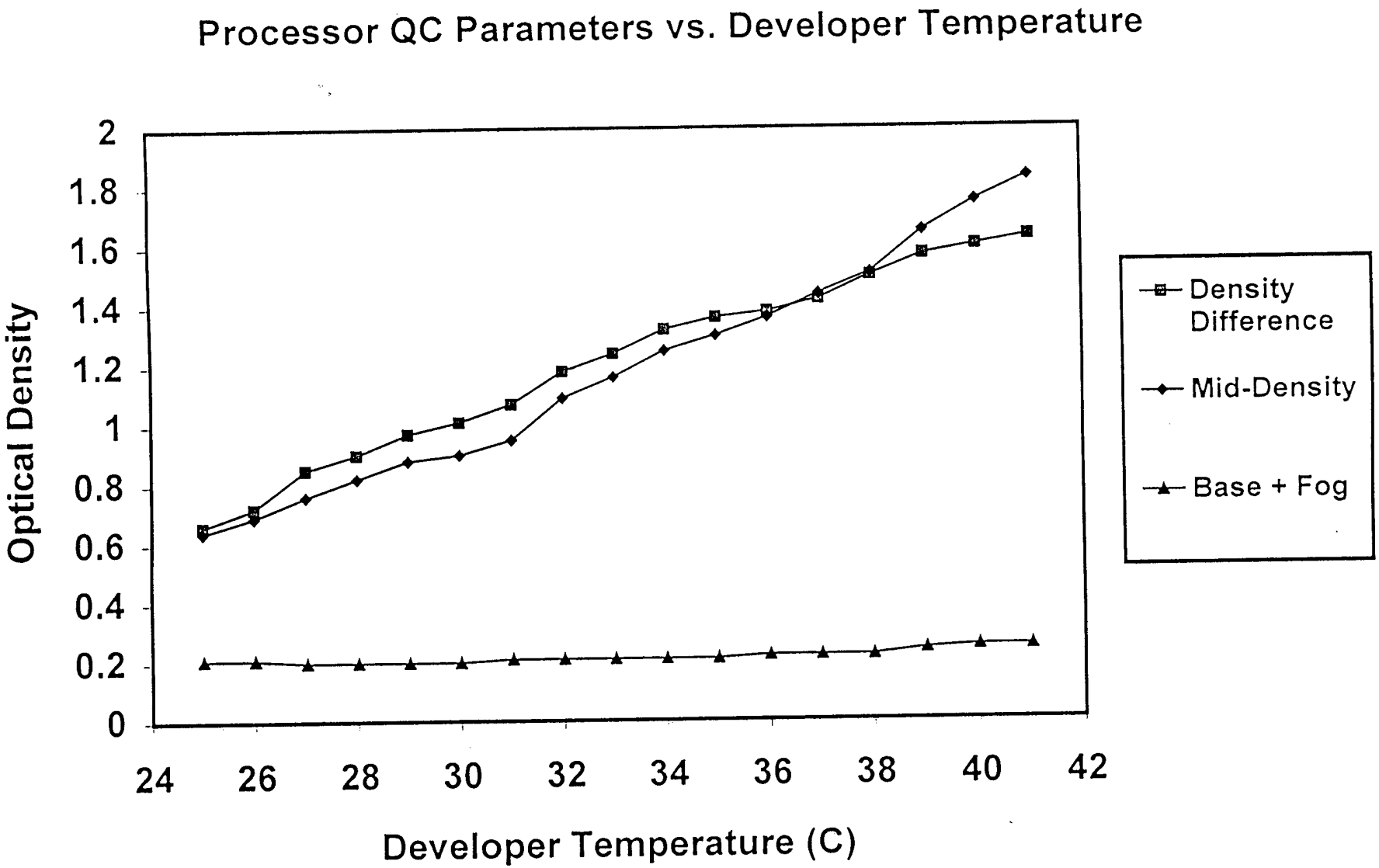
Processor QC Parameters vs. Developer Temperature
Optical Density
2
1.8
1.6
1.4
1.2
1
0.8
0.6
0.4
0.2
0
24
26
28
30
32
34
36
38
40
42
Developer Temperature (C)
Density Difference
Mid-Density
Base + Fog

Figure 17

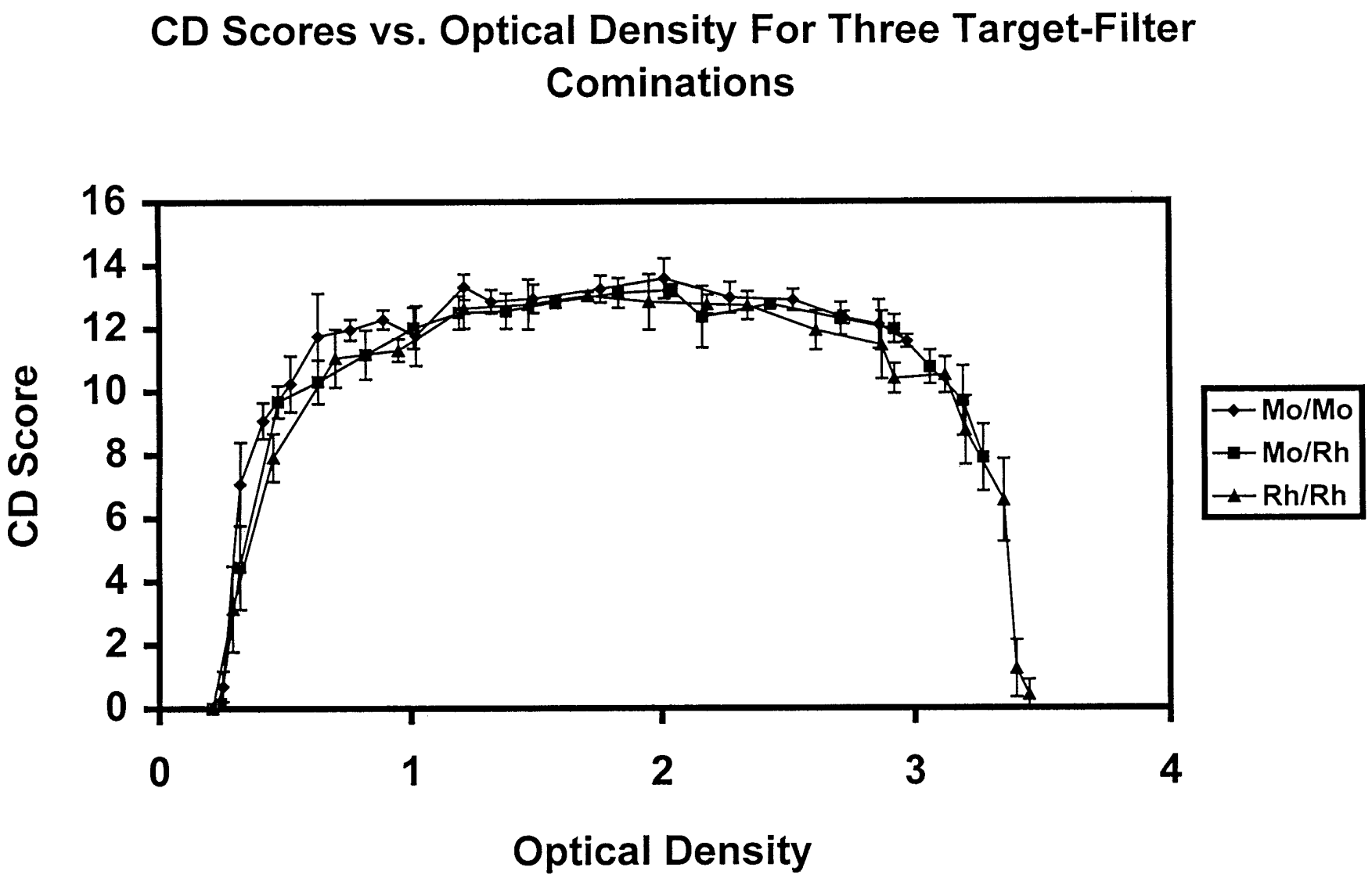
CD Scores vs. Optical Density For Three Target-Filter Cominations
CD Score
16
14
12
10
8
6
4
2
0
0
1
2
3
4
Optical Density
Mo/Mo
Mo/Rh
Rh/Rh

Figure 18

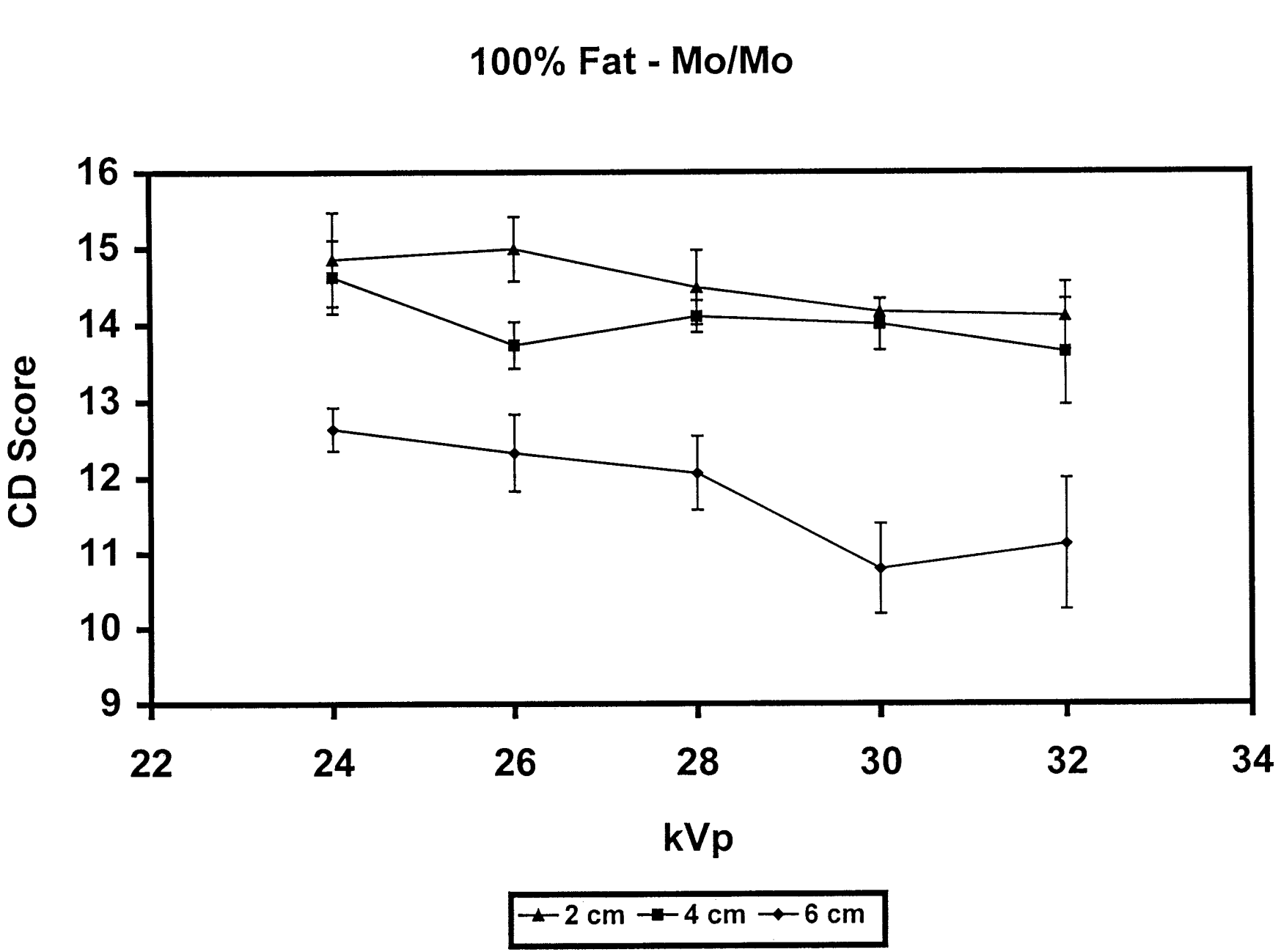
100% Fat - Mo/Mo
CD Score
16
15
14
13
12
11
10
9
22
24
26
28
30
32
34
kVp
2 cm
4 cm
6 cm

Figure 19A

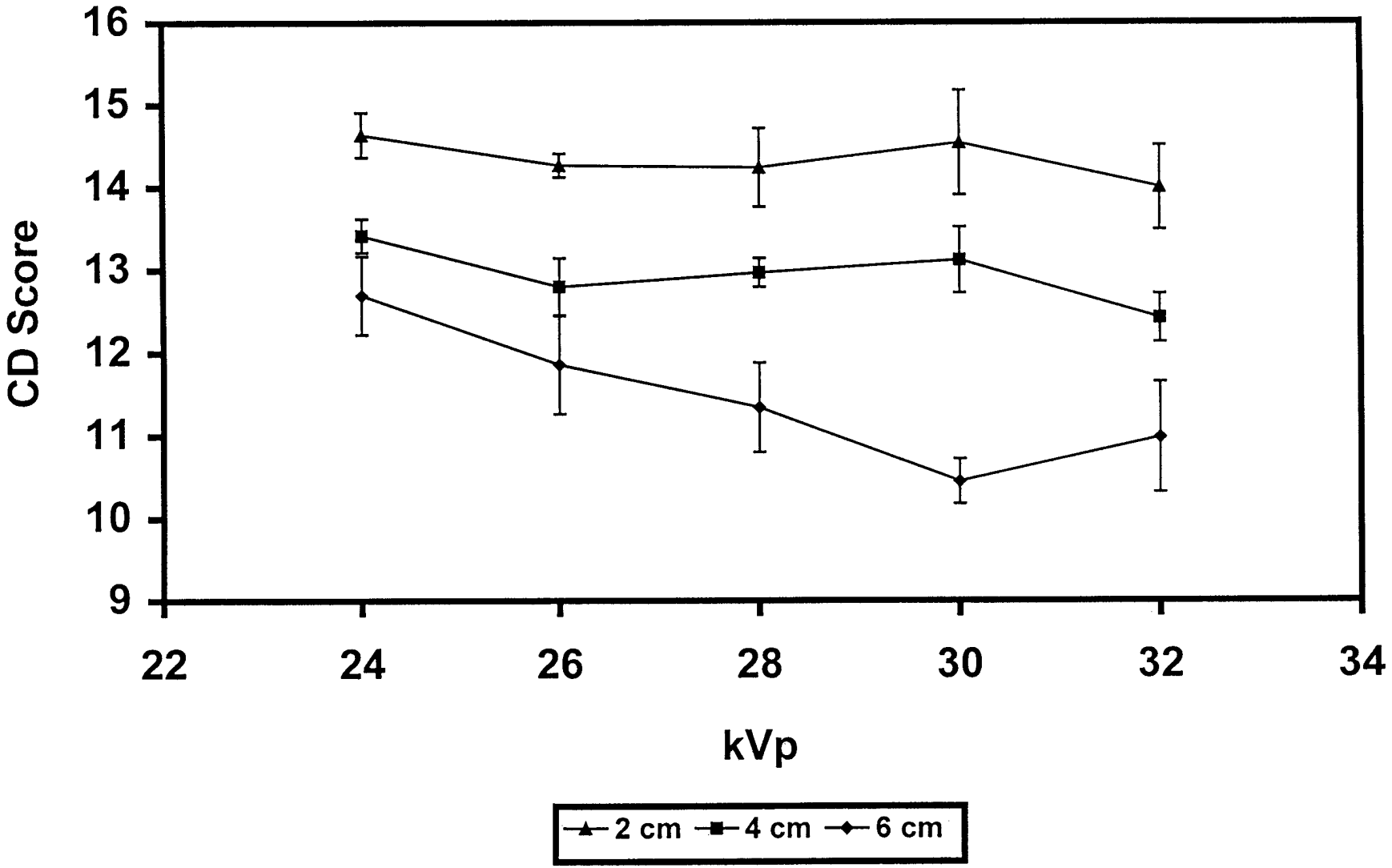
30% Glandular / 70% Fat - Mo/Mo
CD Score
16
15
14
13
12
11
10
9
22
24
26
28
30
32
34
kVp
2 cm
4 cm
6 cm

Figure 19B

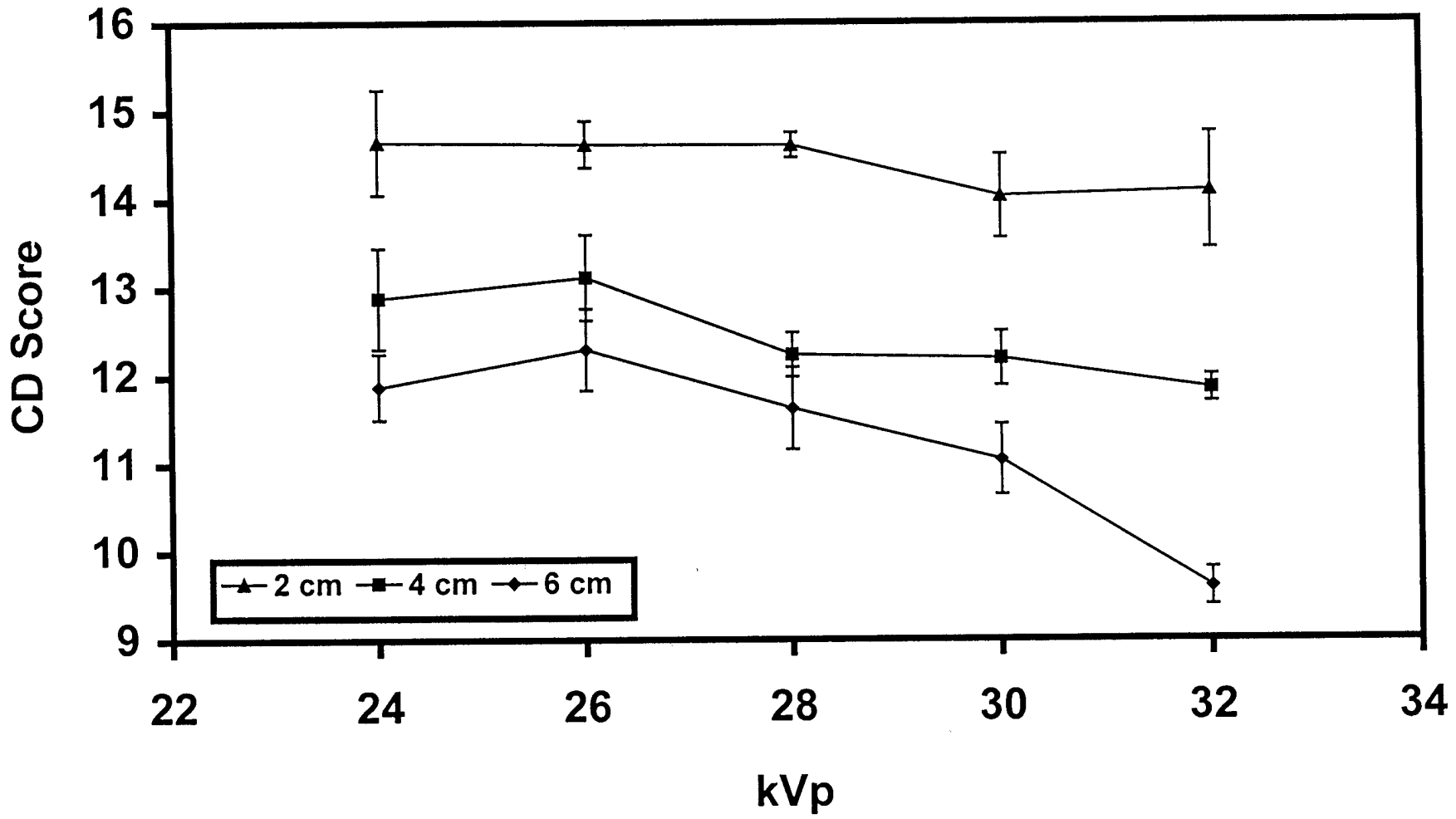
50% Glandular / 50% Fat - Mo/Mo
CD Score
16
15
14
13
12
11
10
9
22
24
26
28
30
32
34
kVp
2 cm
4 cm
6 cm

Figure 19C

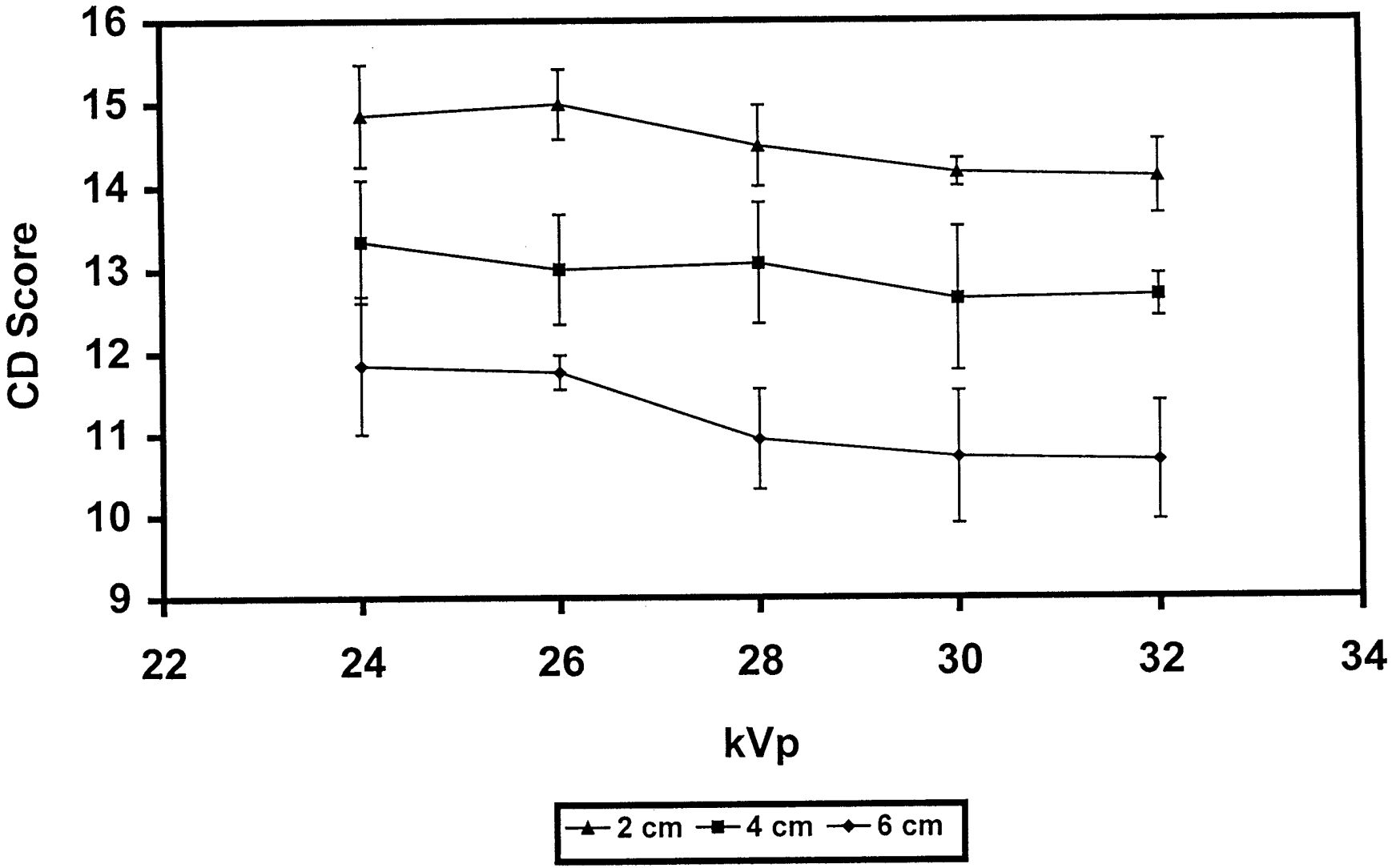
70% Glandular / 30% Fat - Mo/Mo
CD Score
16
15
14
13
12
11
10
9
22
24
26
28
30
32
34
kVp
2 cm
4 cm
6 cm

Figure 19D

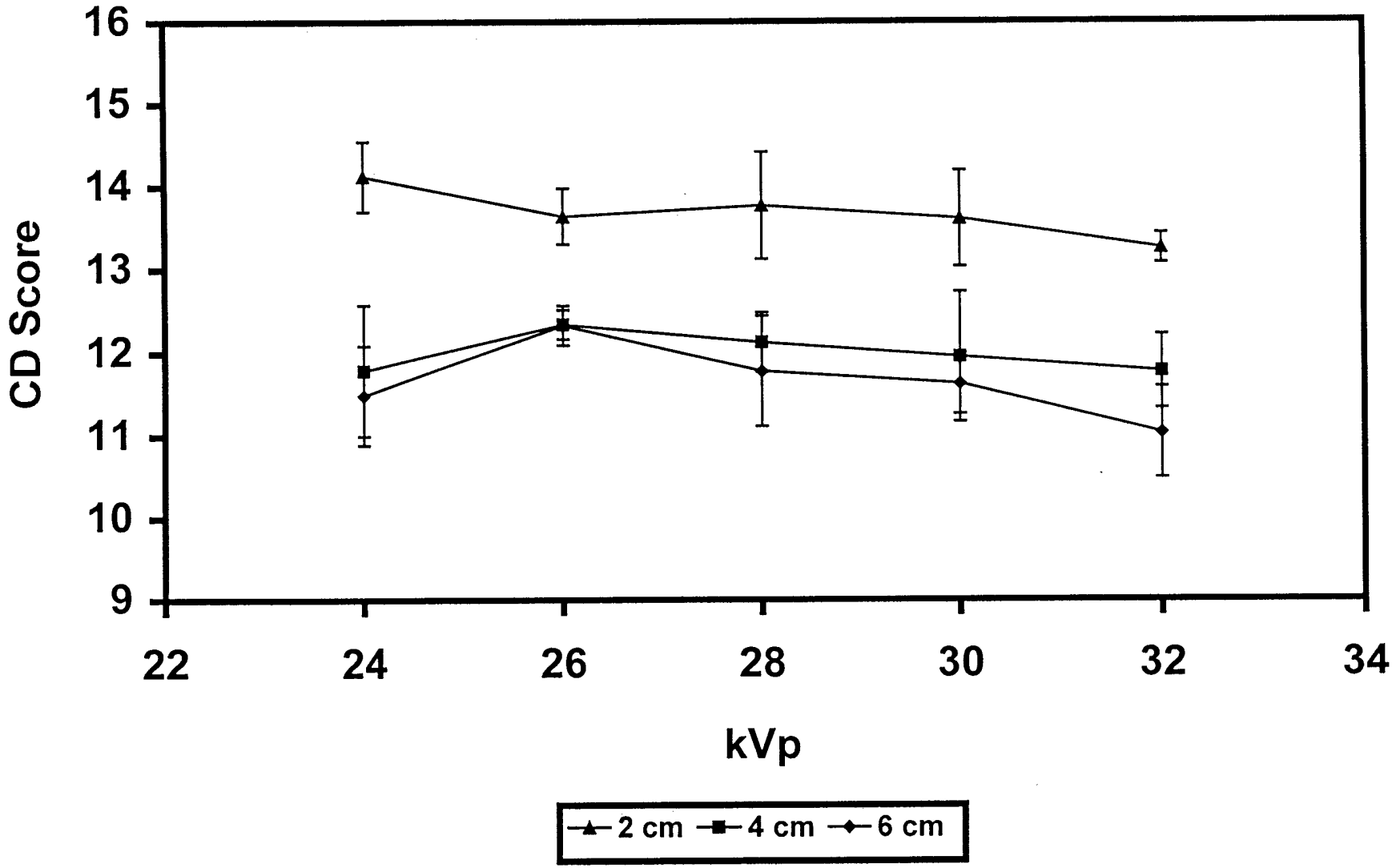
50% Glandular / 50% Fat - Mo/Rh
CD Score
16
15
14
13
12
11
10
9
22
24
26
28
30
32
34
kVp
2 cm
4 cm
6 cm

Figure 19E

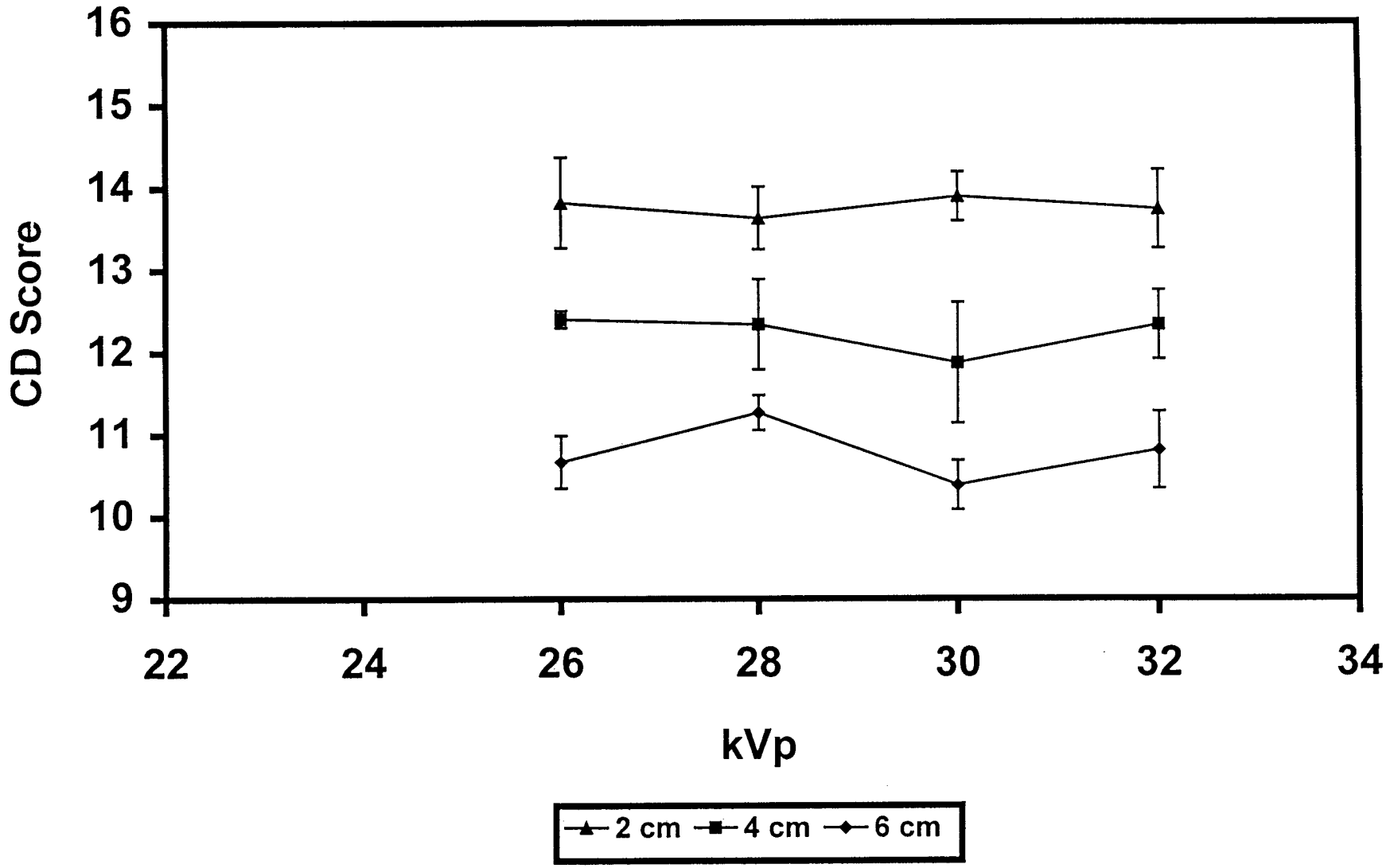
50% Glandular / 50% Fat - Rh/Rh
CD Score
16
15
14
13
12
11
10
9
22
24
26
28
30
32
34
kVp
2 cm
4 cm
6 cm

Figure 19F

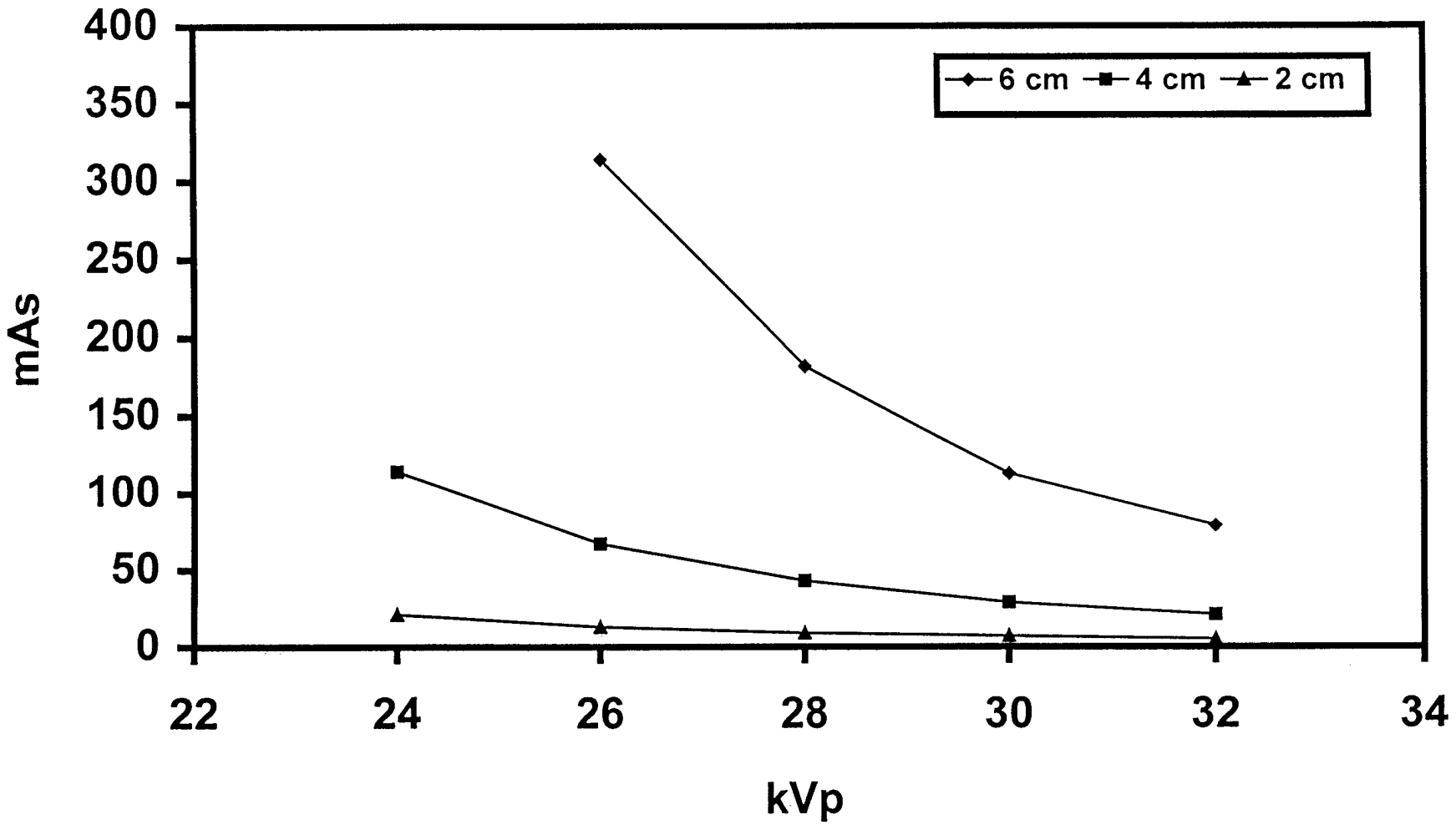
50% Glandular / 50% Fat - Mo/Mo
400
350
300
250
200
150
100
50
0
mAs
6 cm
4 cm
2 cm
22
24
26
28
30
32
34
kVp

Figure 20A

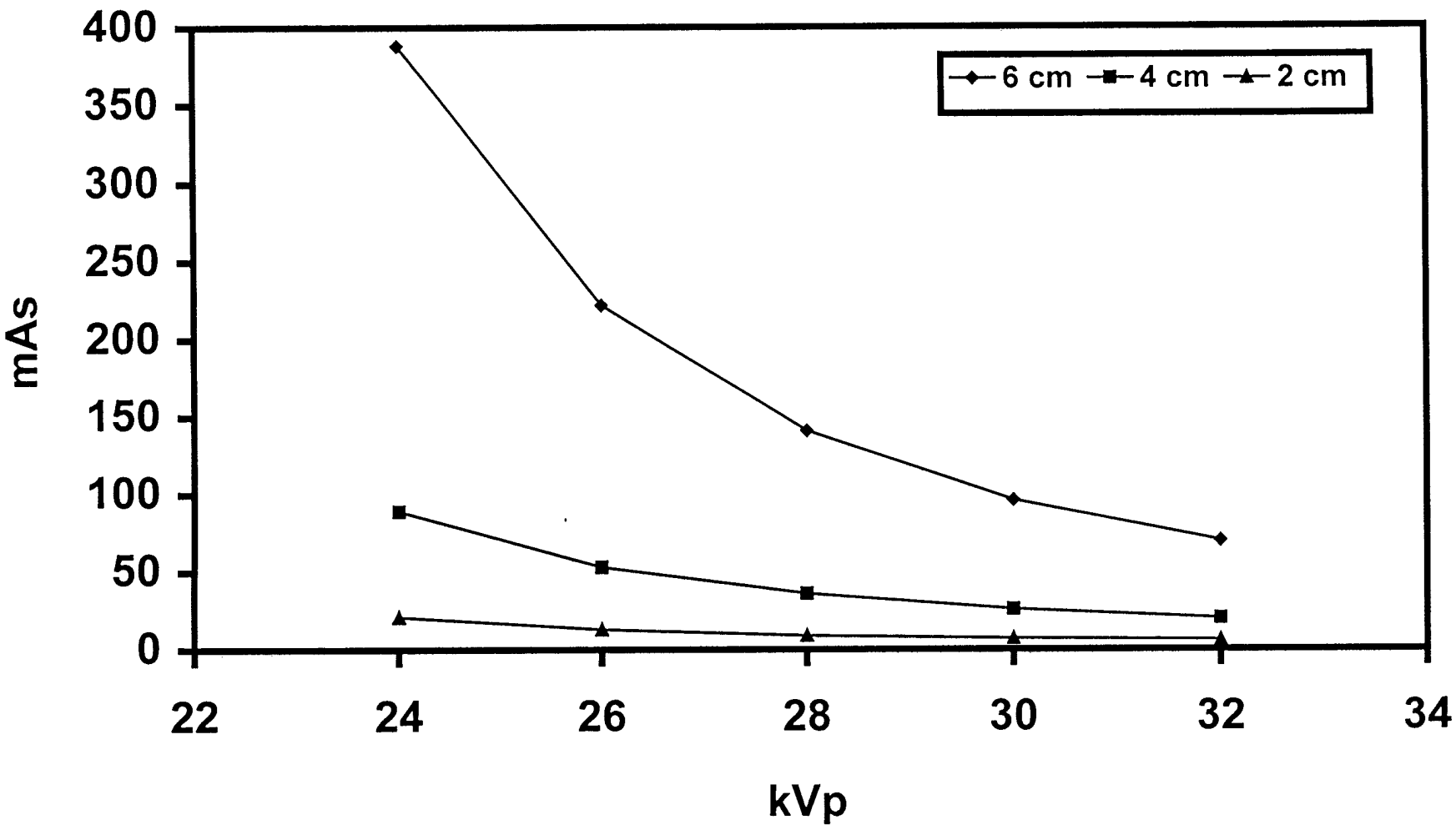
50% Glandular / 50% Fat - Mo/Rh
400
350
300
250
200
150
100
50
0
mAs
6 cm
4 cm
2 cm
22
24
26
28
30
32
34
kVp

Figure 20B

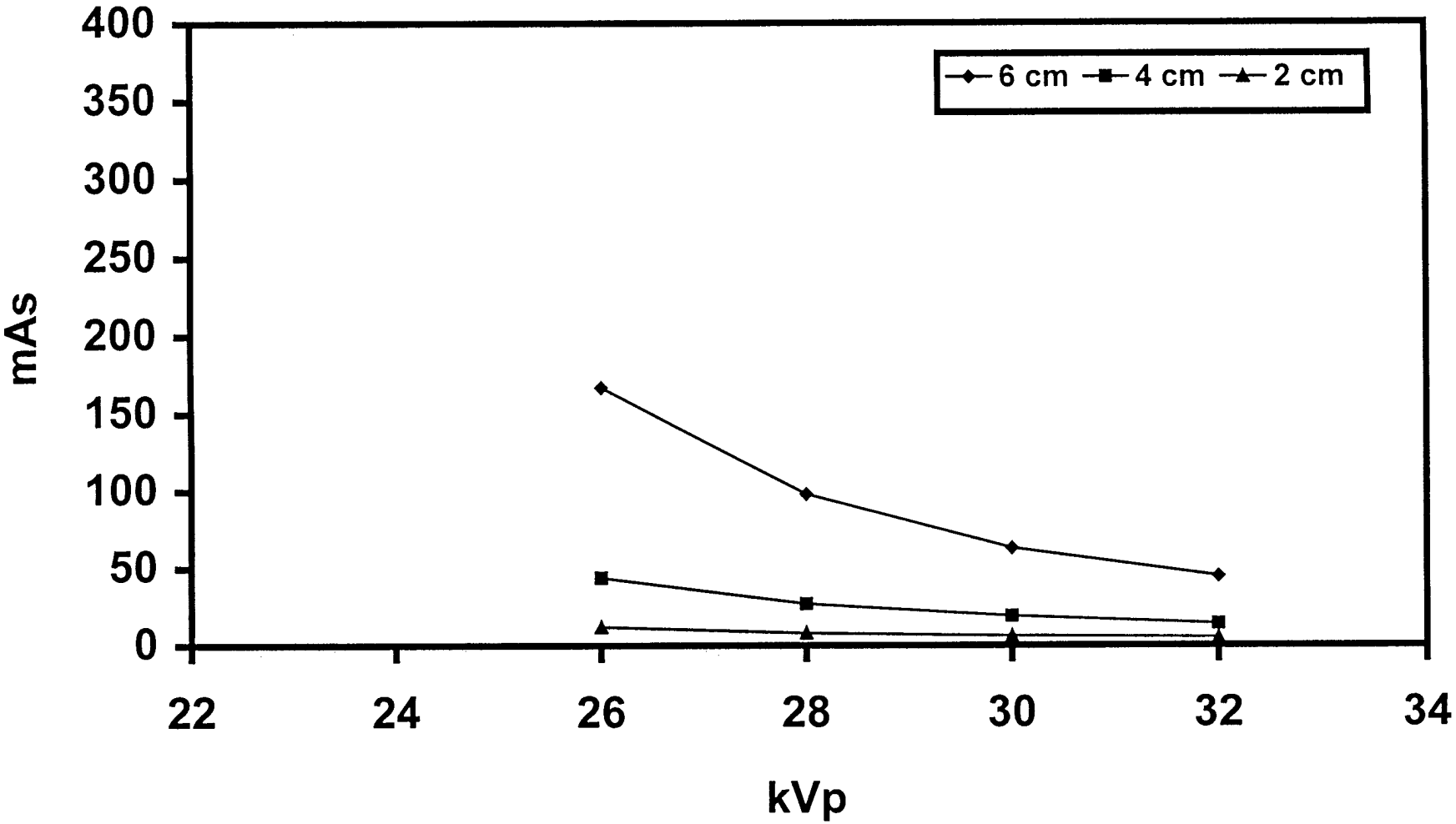
50% Glandular / 50% Fat - Rh/Rh
400
350
300
250
200
150
100
50
0
mAs
6 cm
4 cm
2 cm
22
24
26
28
30
32
34
kVp

Figure 20C

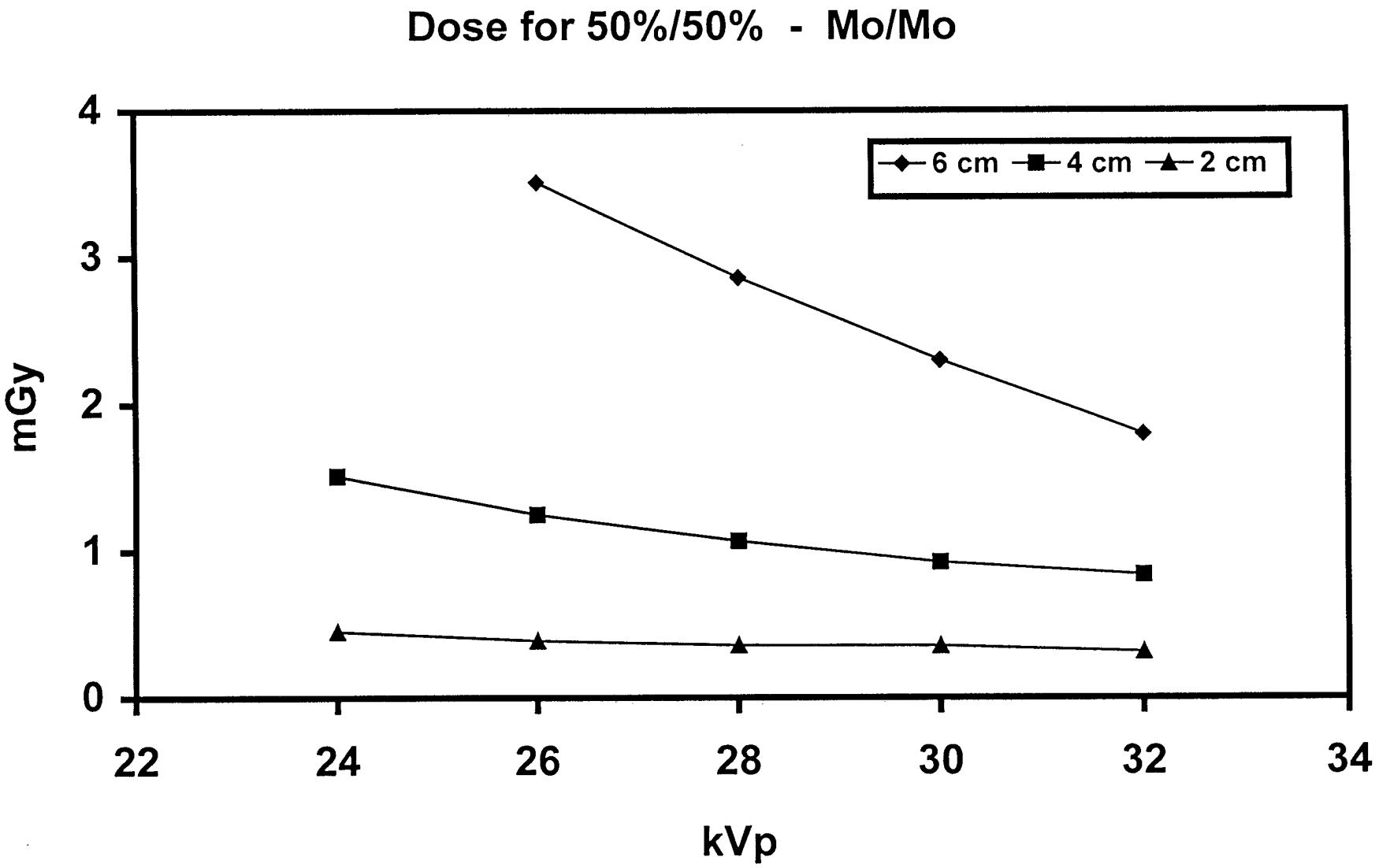

Figure 21A

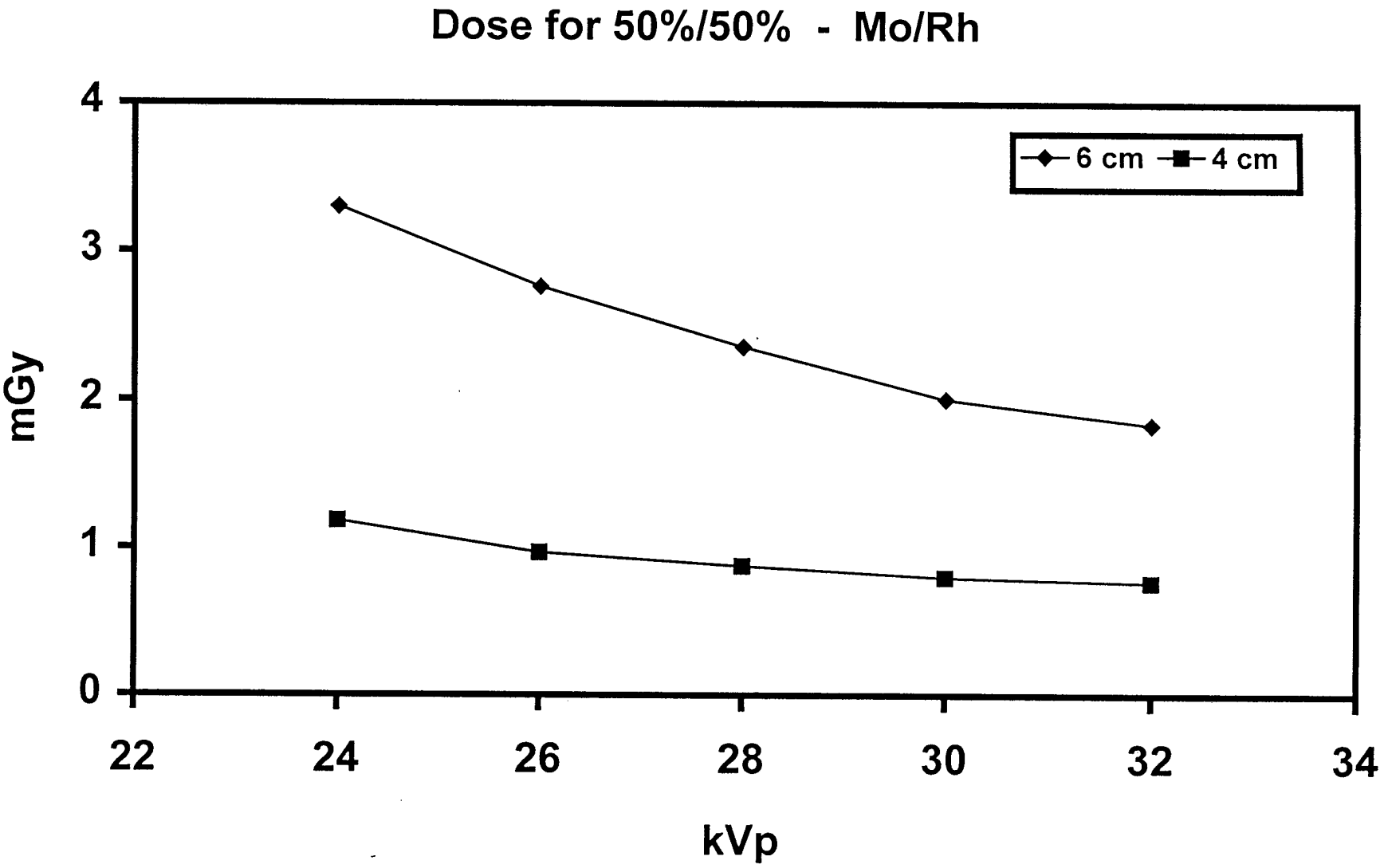

Figure 21B

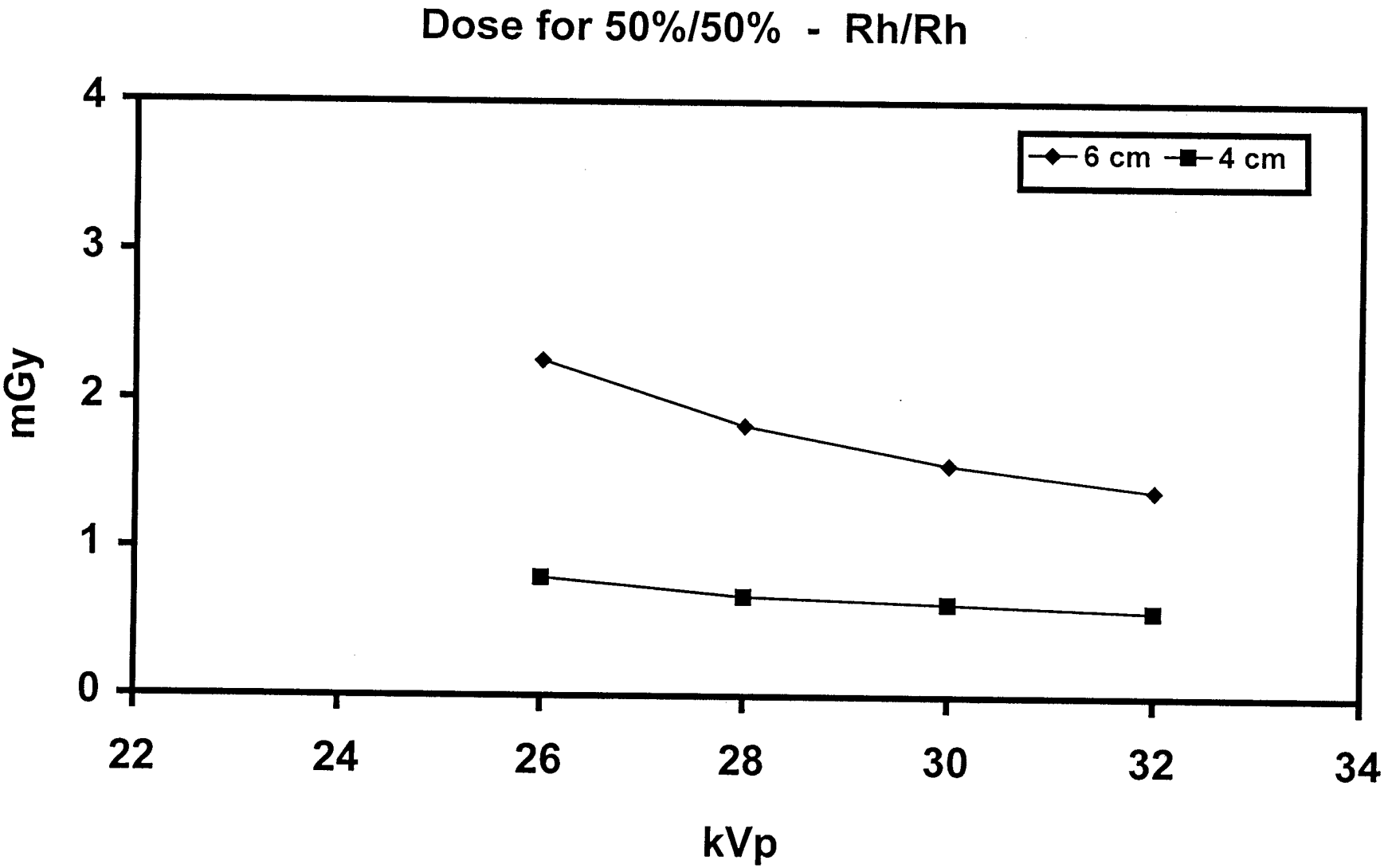

Figure 21C

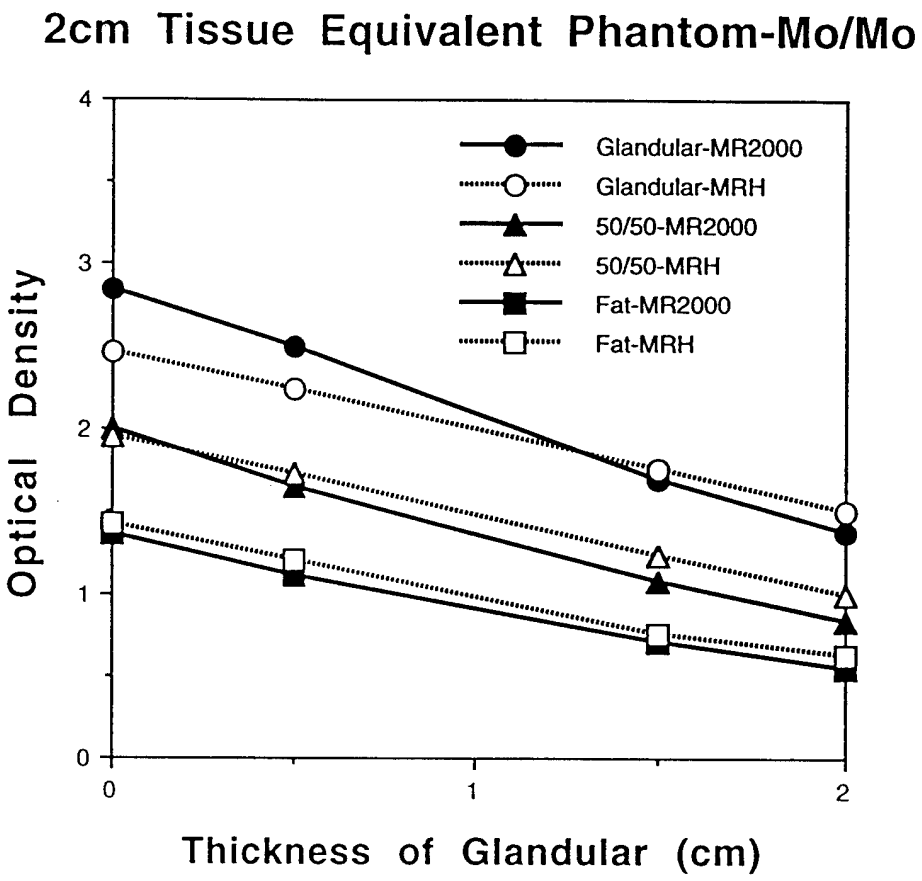
2cm Tissue Equivalent Phantom-Mo/Mo
Optical Density
Thickness of Glandular (cm)
Glandular-MR2000
Glandular-MRH
50/50-MR2000
50/50-MRH
Fat-MR2000
Fat-MRH
0
1
2
3
4
0
1
2

Figure 22A

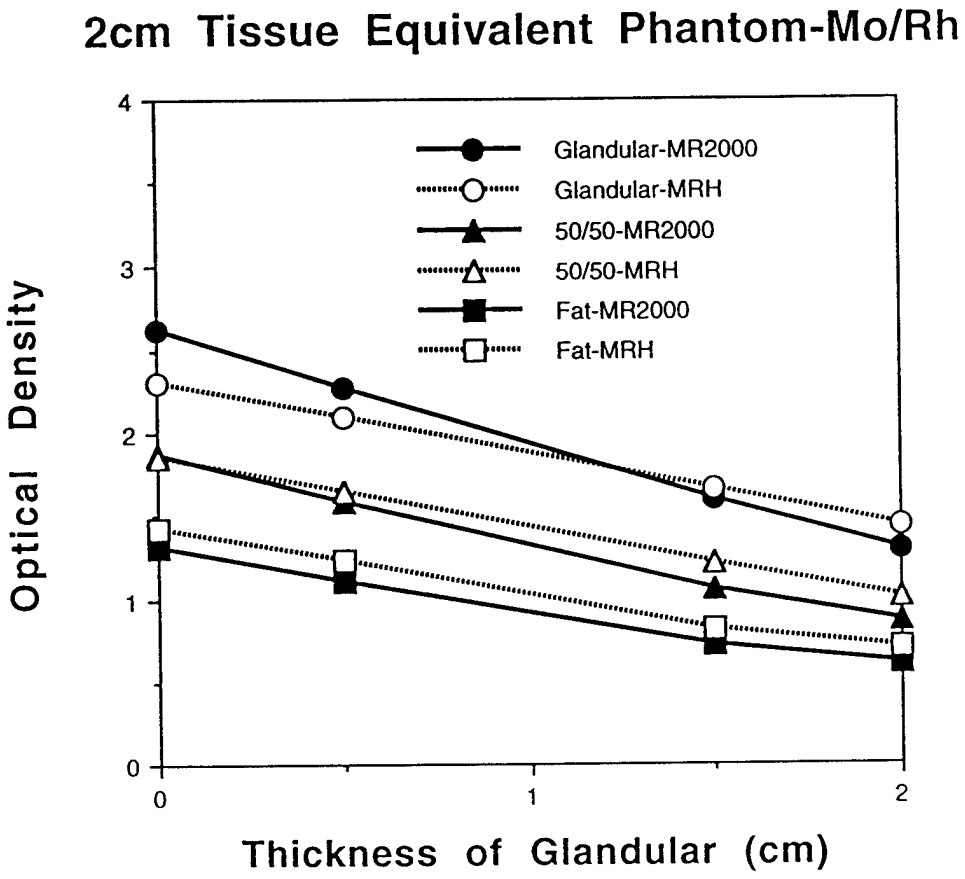
2cm Tissue Equivalent Phantom-Mo/Rh
Optical Density
Thickness of Glandular (cm)
Glandular-MR2000
Glandular-MRH
50/50-MR2000
50/50-MRH
Fat-MR2000
Fat-MRH
0
1
2
3
4
0
1
2

Figure 22B

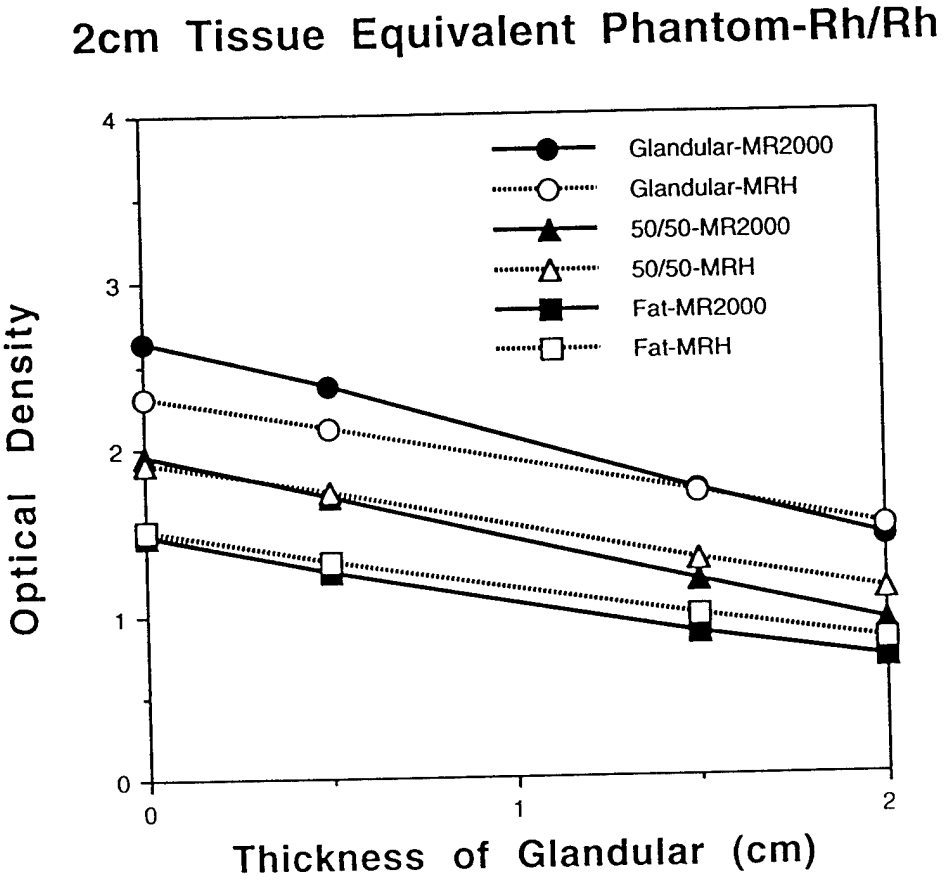
2cm Tissue Equivalent Phantom-Rh/Rh
Optical Density
Thickness of Glandular (cm)
Glandular-MR2000
Glandular-MRH
50/50-MR2000
50/50-MRH
Fat-MR2000
Fat-MRH
0
1
2
3
4
0
1
2

Figure 22C

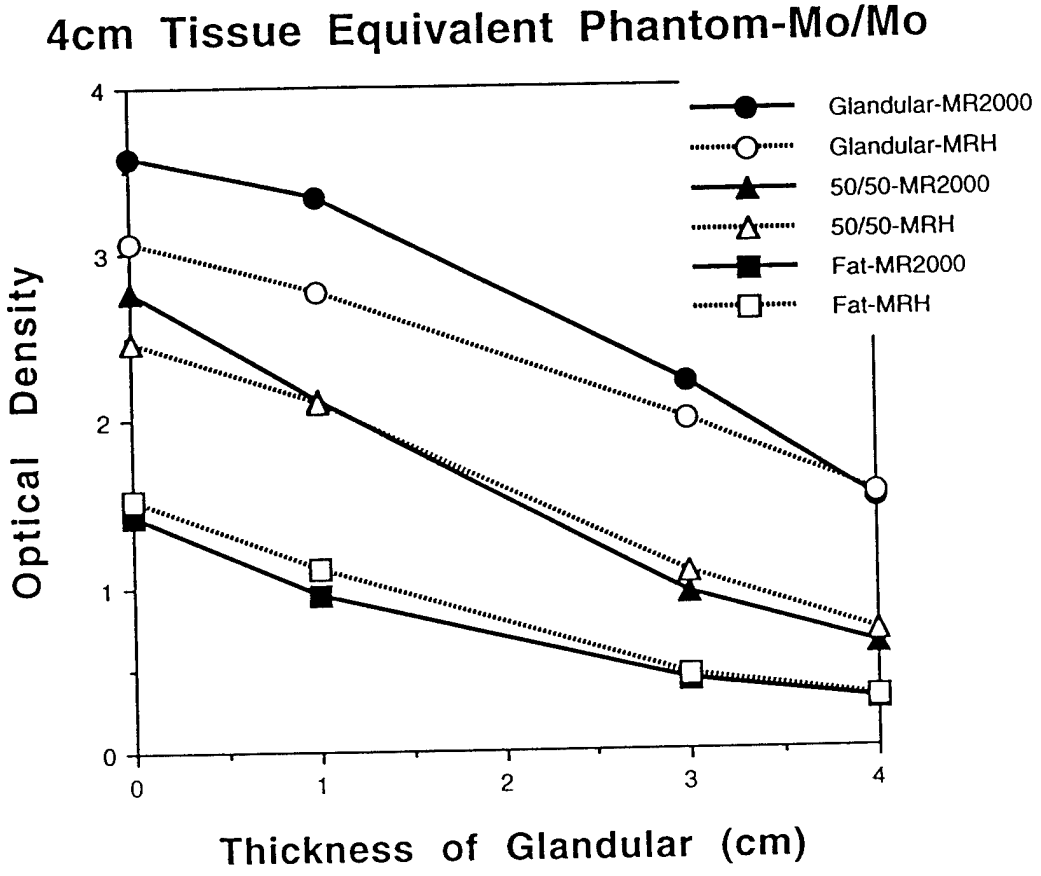
4cm Tissue Equivalent Phantom-Mo/Mo
Optical Density
Thickness of Glandular (cm)
Glandular-MR2000
Glandular-MRH
50/50-MR2000
50/50-MRH
Fat-MR2000
Fat-MRH
0
1
2
3
4

Figure 22D

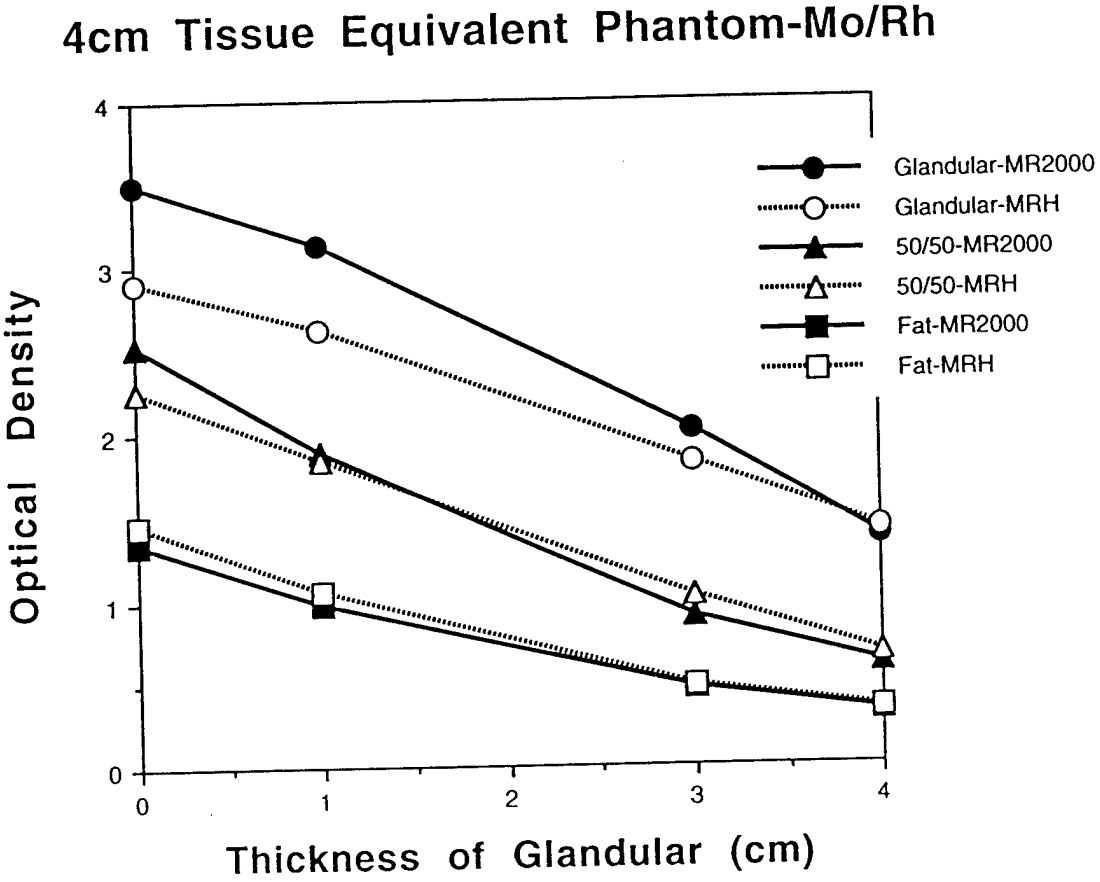
4cm Tissue Equivalent Phantom-Mo/Rh
Optical Density
Thickness of Glandular (cm)
0
1
2
3
4
Glandular-MR2000
Glandular-MRH
50/50-MR2000
50/50-MRH
Fat-MR2000
Fat-MRH

Figure 22E

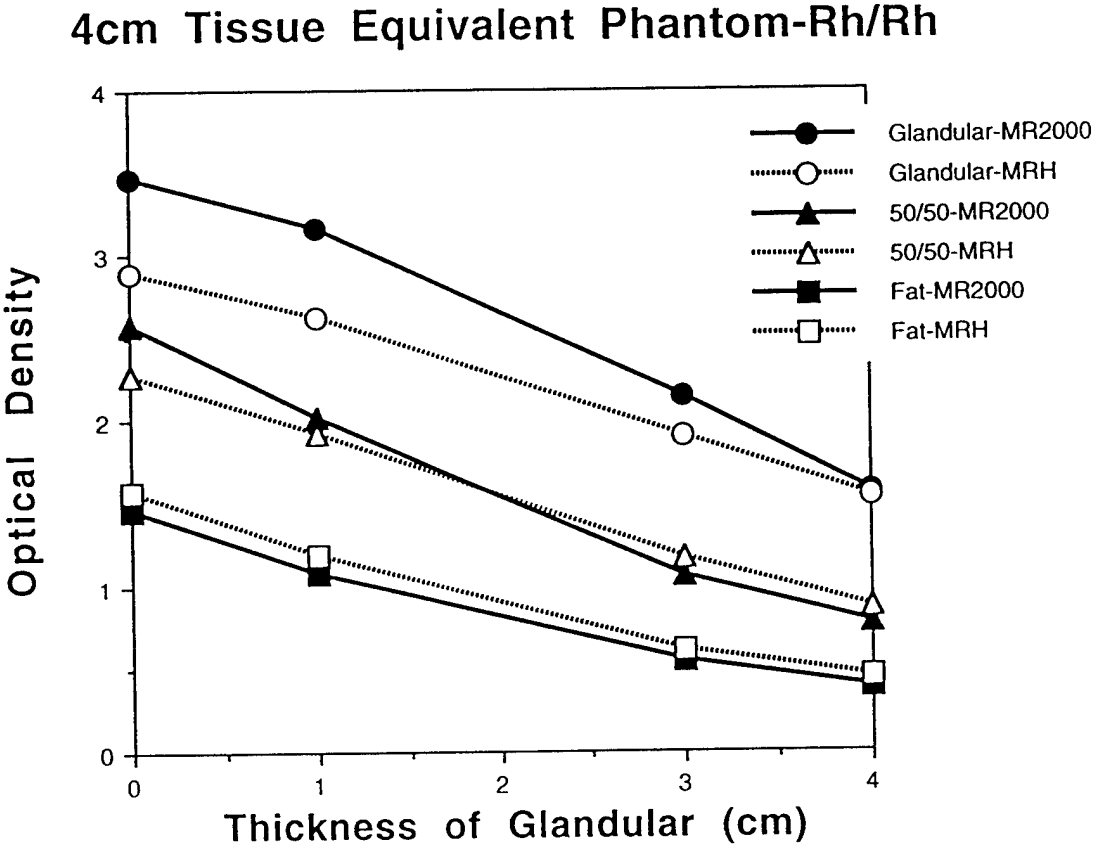
4cm Tissue Equivalent Phantom-Rh/Rh
Optical Density
Thickness of Glandular (cm)
0
1
2
3
4
Glandular-MR2000
Glandular-MRH
50/50-MR2000
50/50-MRH
Fat-MR2000
Fat-MRH

Figure 22F

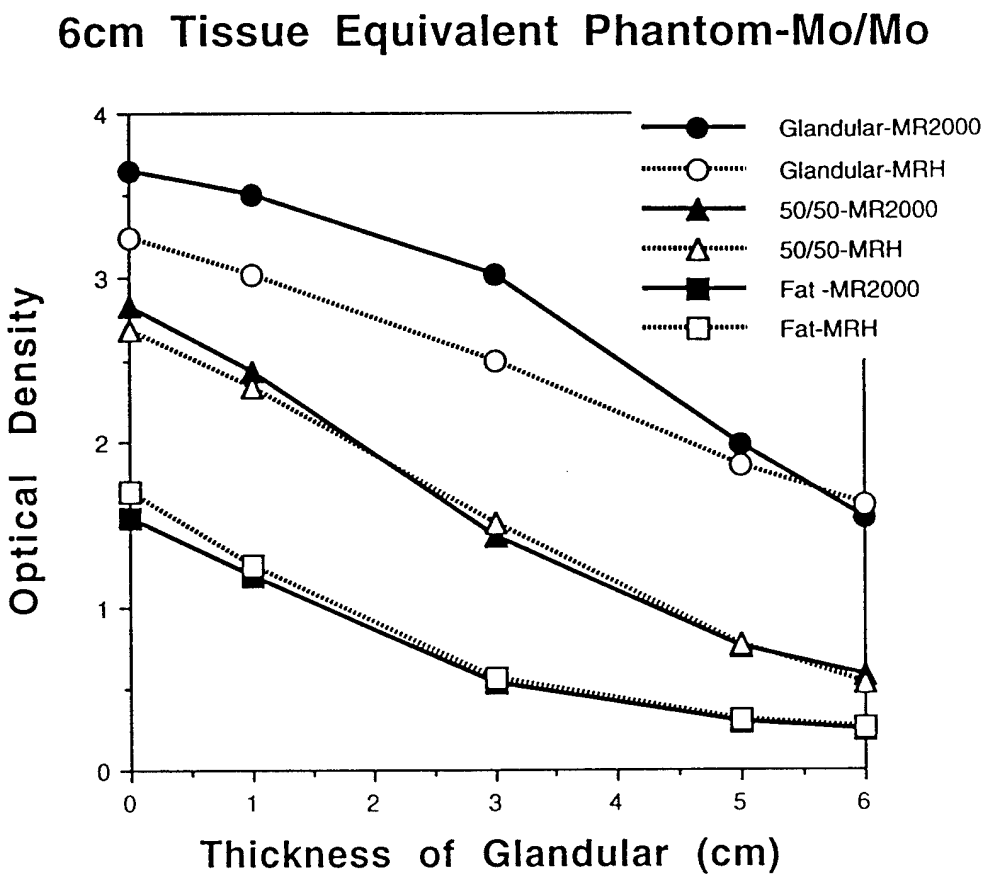
6cm Tissue Equivalent Phantom-Mo/Mo
Optical Density
Thickness of Glandular (cm)
Glandular-MR2000
Glandular-MRH
50/50-MR2000
50/50-MRH
Fat -MR2000
Fat-MRH
0
1
2
3
4
5
6

Figure 22G

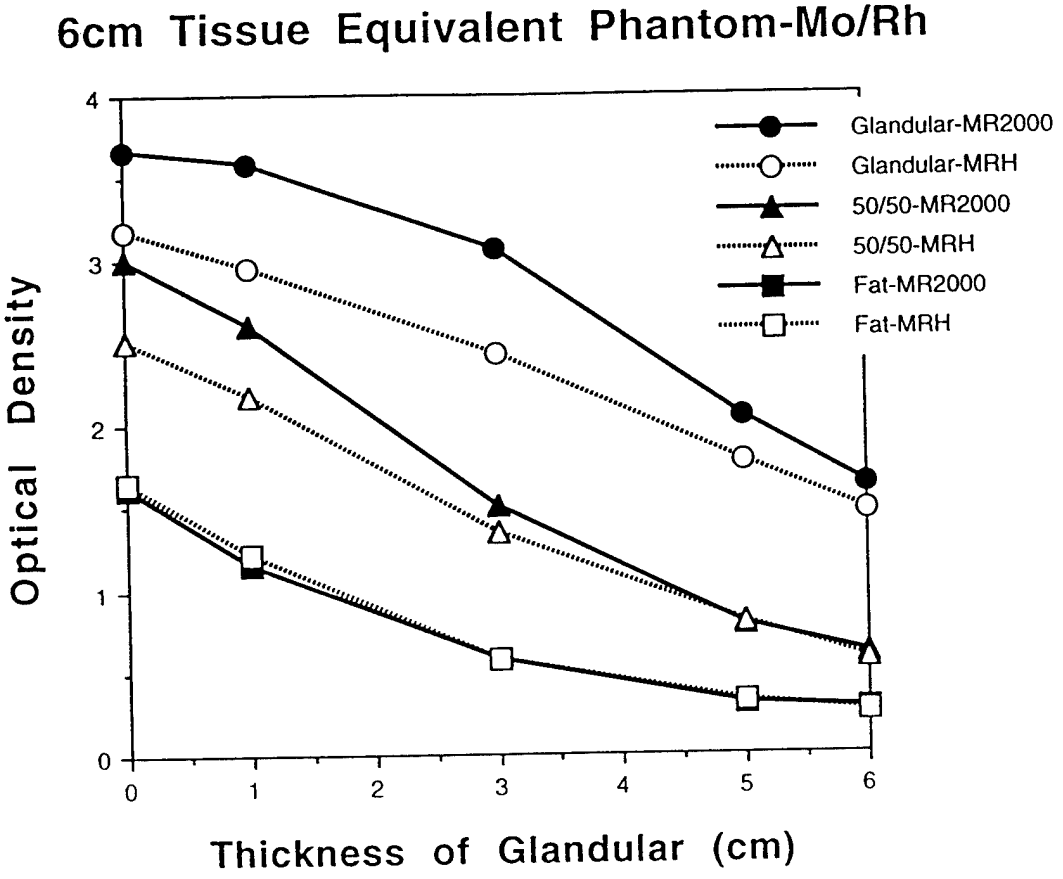
6cm Tissue Equivalent Phantom-Mo/Rh
Optical Density
Thickness of Glandular (cm)
Glandular-MR2000
Glandular-MRH
50/50-MR2000
50/50-MRH
Fat-MR2000
Fat-MRH
0
1
2
3
4
5
6

Figure 22H

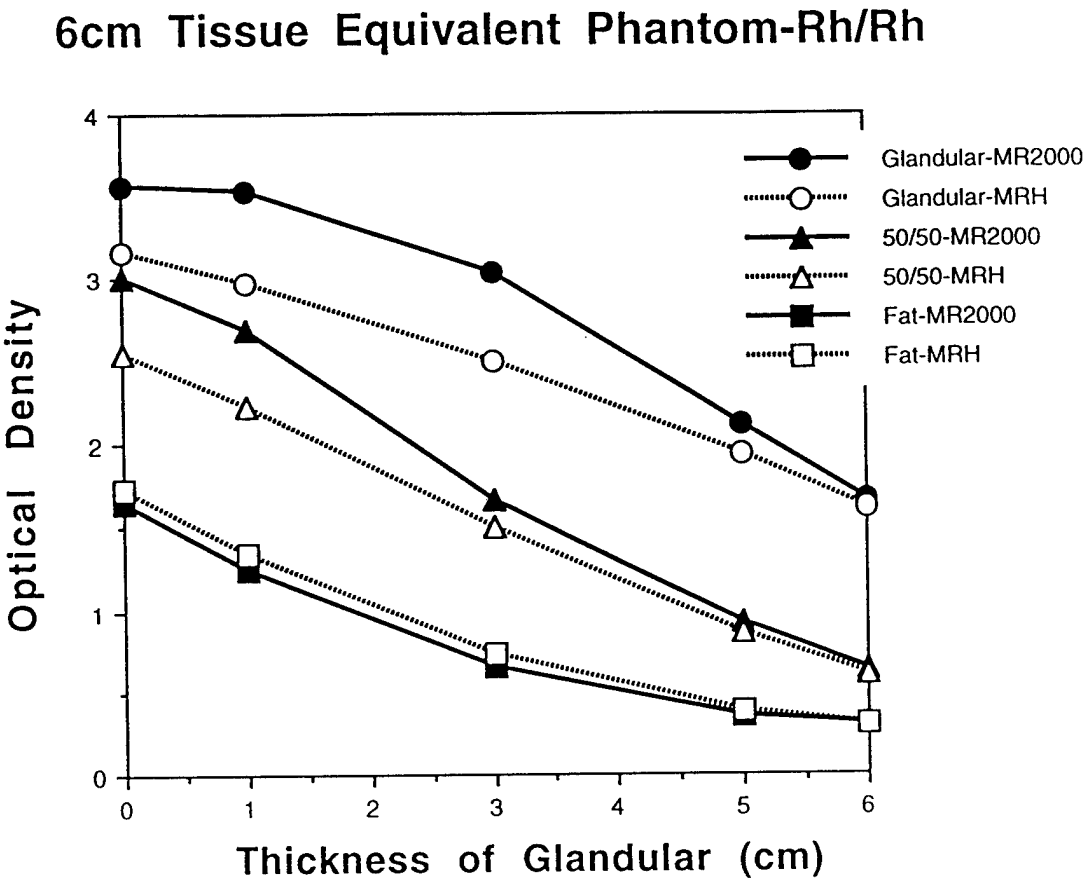
6cm Tissue Equivalent Phantom-Rh/Rh
Optical Density
Thickness of Glandular (cm)
Glandular-MR2000
Glandular-MRH
50/50-MR2000
50/50-MRH
Fat-MR2000
Fat-MRH
0
1
2
3
4
5
6

Figure 22I

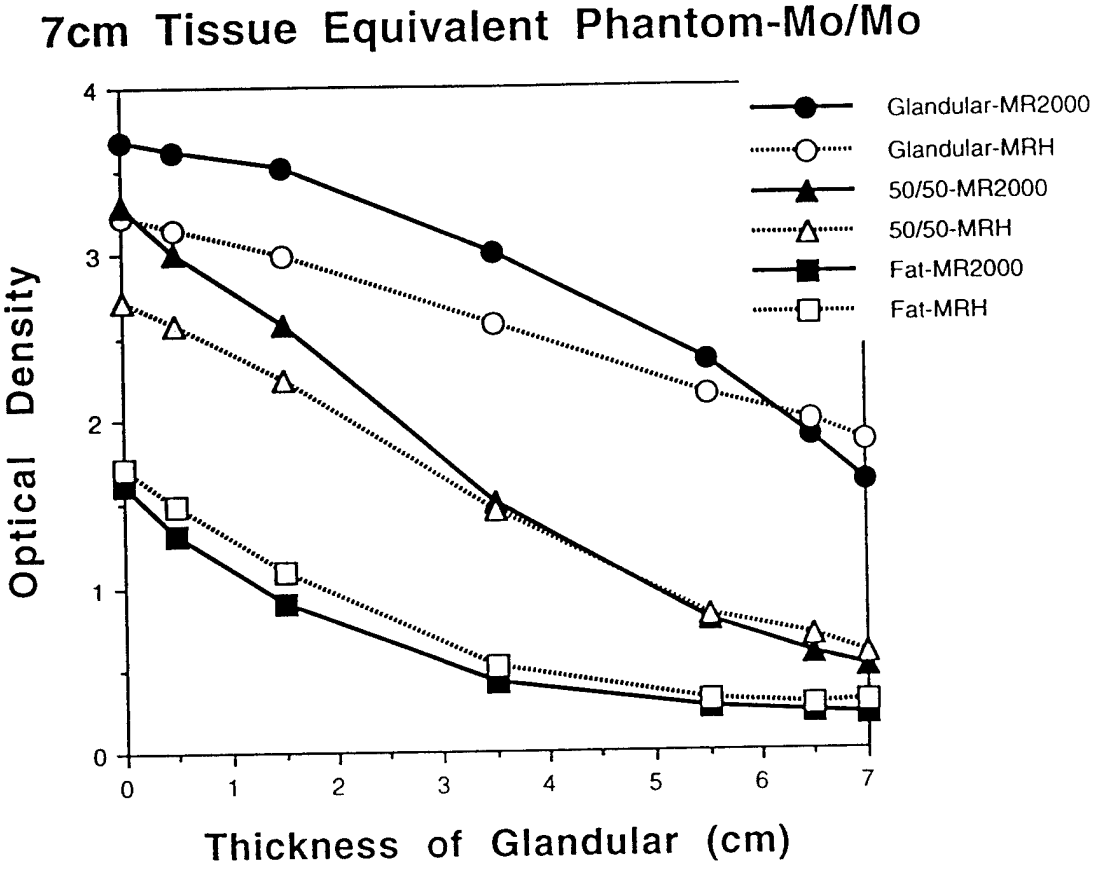
7cm Tissue Equivalent Phantom-Mo/Mo
Optical Density
Thickness of Glandular (cm)
Glandular-MR2000
Glandular-MRH
50/50-MR2000
50/50-MRH
Fat-MR2000
Fat-MRH
0
1
2
3
4
5
6
7

Figure 22J

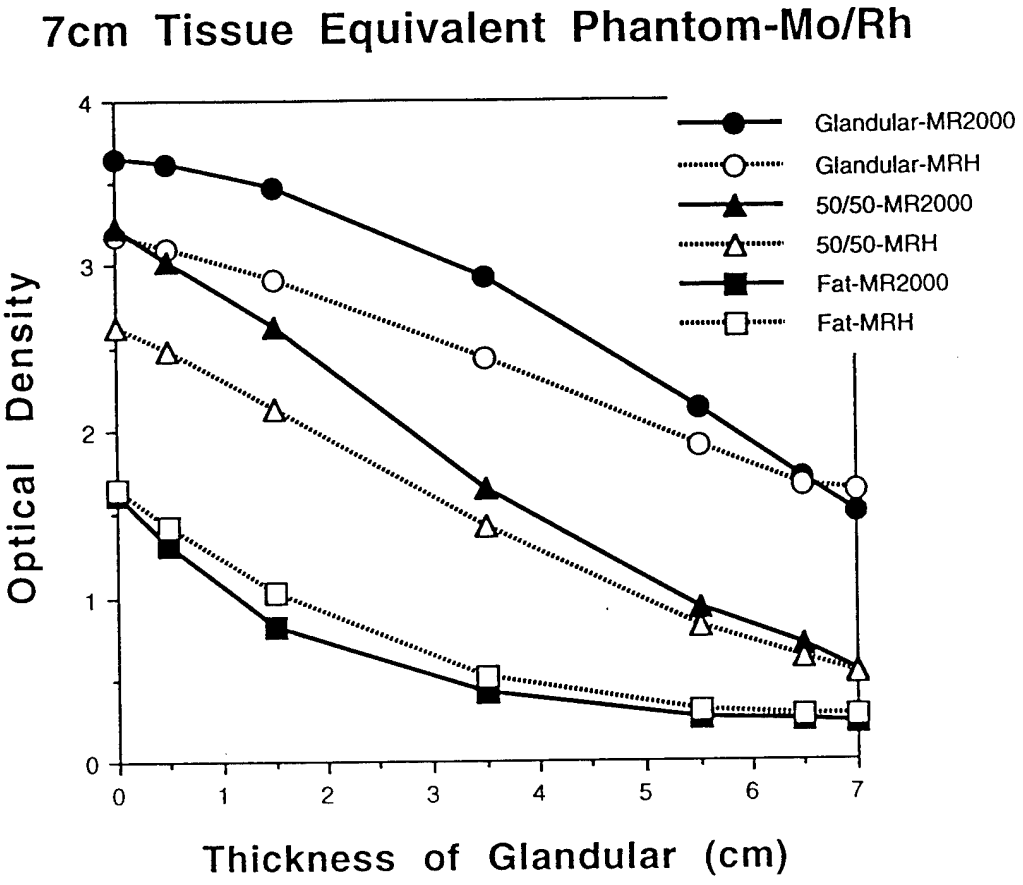
7cm Tissue Equivalent Phantom-Mo/Rh
Optical Density
Thickness of Glandular (cm)
Glandular-MR2000
Glandular-MRH
50/50-MR2000
50/50-MRH
Fat-MR2000
Fat-MRH
0
1
2
3
4
5
6
7

Figure 22K

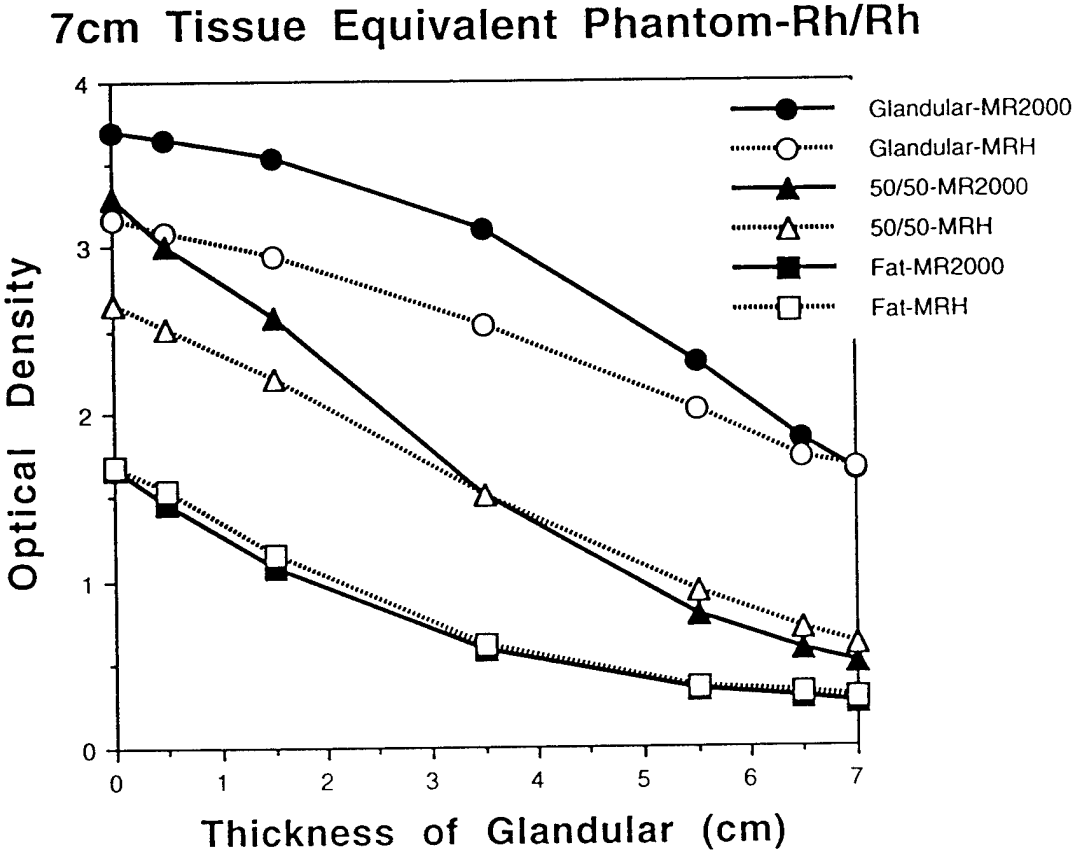
7cm Tissue Equivalent Phantom-Rh/Rh
Optical Density
Thickness of Glandular (cm)
Glandular-MR2000
Glandular-MRH
50/50-MR2000
50/50-MRH
Fat-MR2000
Fat-MRH
0
1
2
3
4
5
6
7

Figure 22L

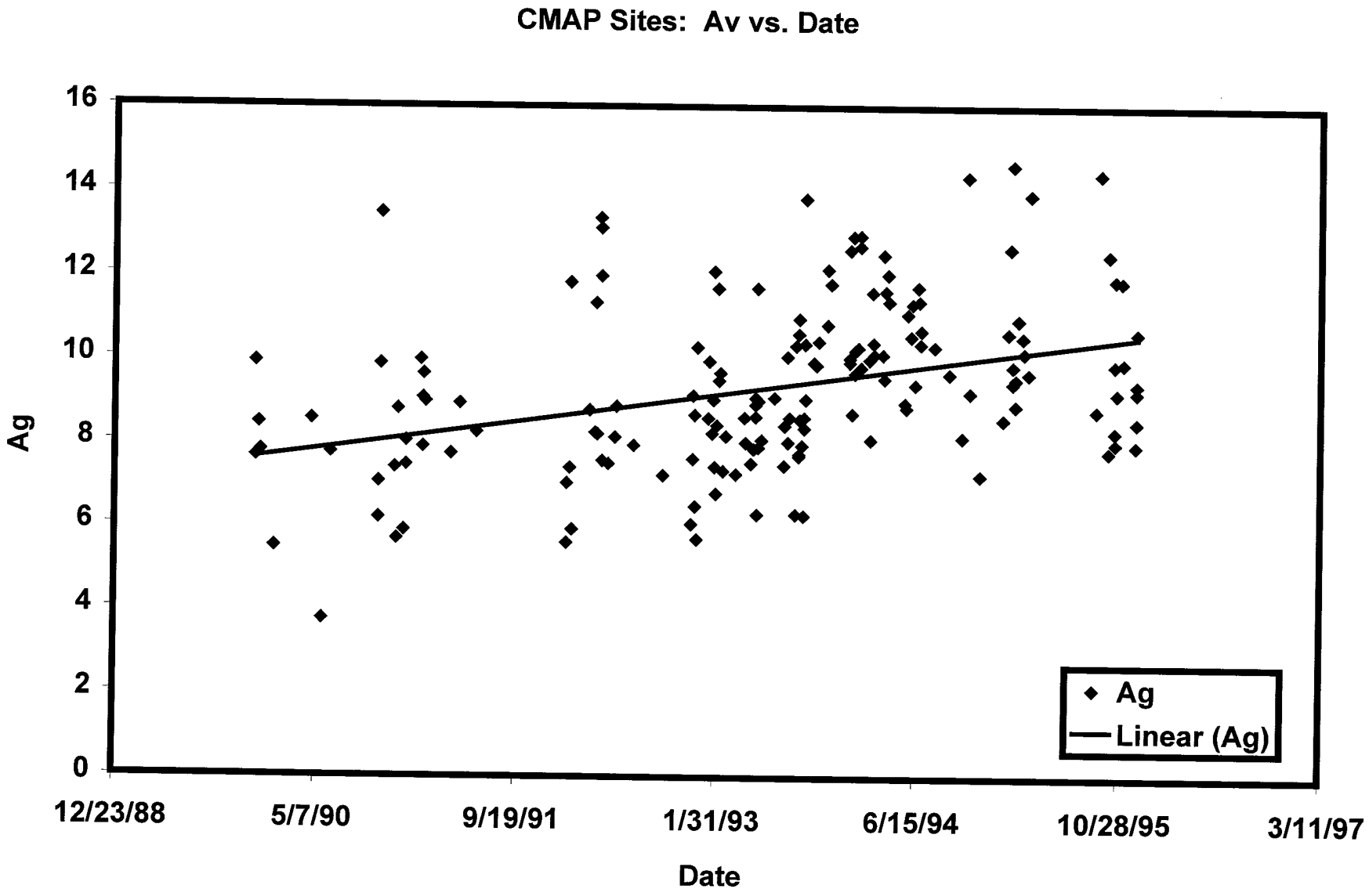
CMAP Sites: Av vs. Date
16
14
12
10
8
6
4
2
0
Ag
12/23/88
5/7/90
9/19/91
1/31/93
6/15/94
10/28/95
3/11/97
Date
Ag
Linear (Ag)

Figure 23A

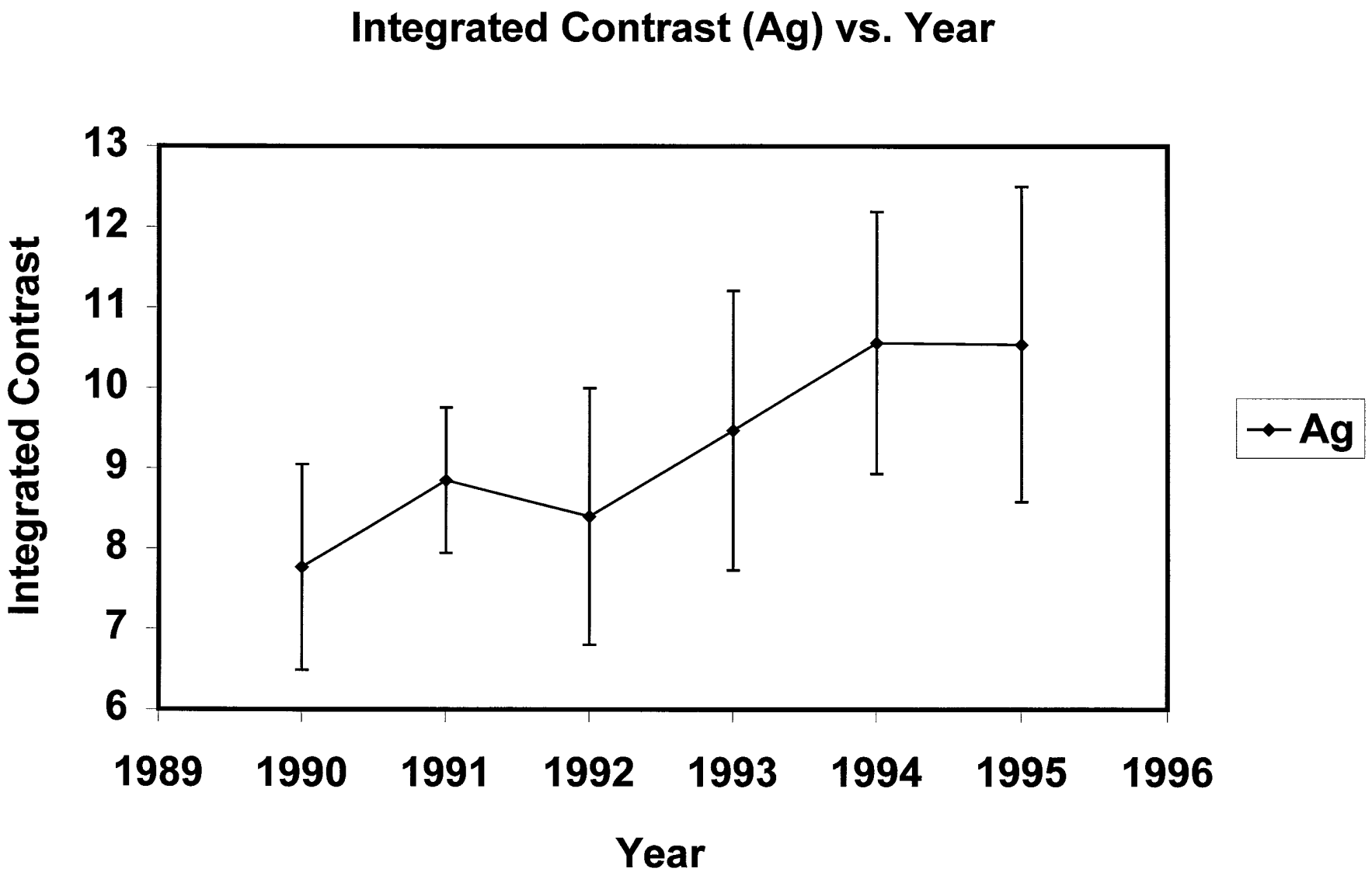
Integrated Contrast (Ag) vs. Year
Integrated Contrast
13
12
11
10
9
8
7
6
1989
1990
1991
1992
1993
1994
1995
1996
Year
Ag

Figure 23B

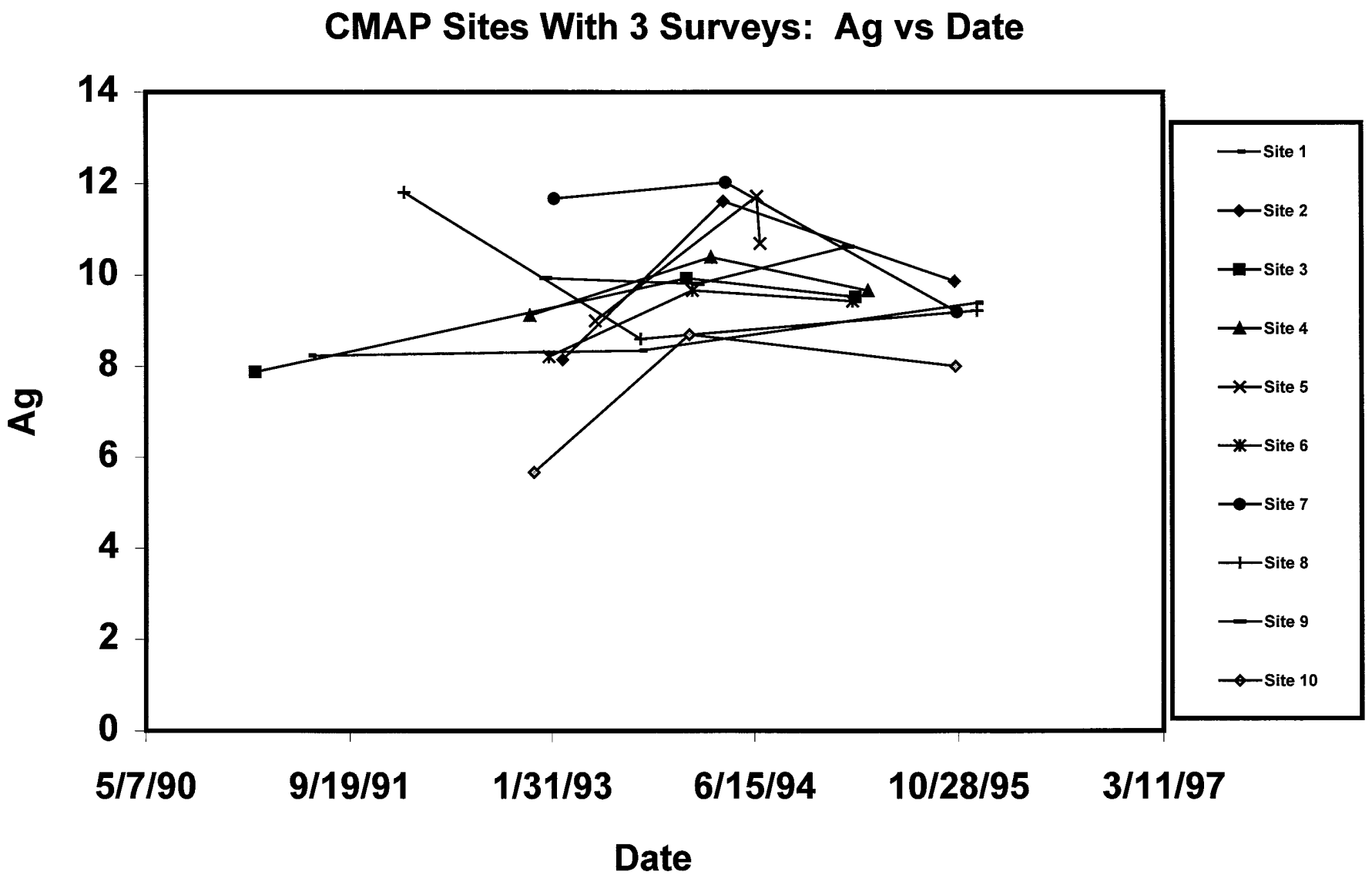
CMAP Sites With 3 Surveys: Ag vs Date
Ag
14
12
10
8
6
4
2
0
5/7/90
9/19/91
1/31/93
6/15/94
10/28/95
3/11/97
Date
Site 1
Site 2
Site 3
Site 4
Site 5
Site 6
Site 7
Site 8
Site 9
Site 10

Figure 23C

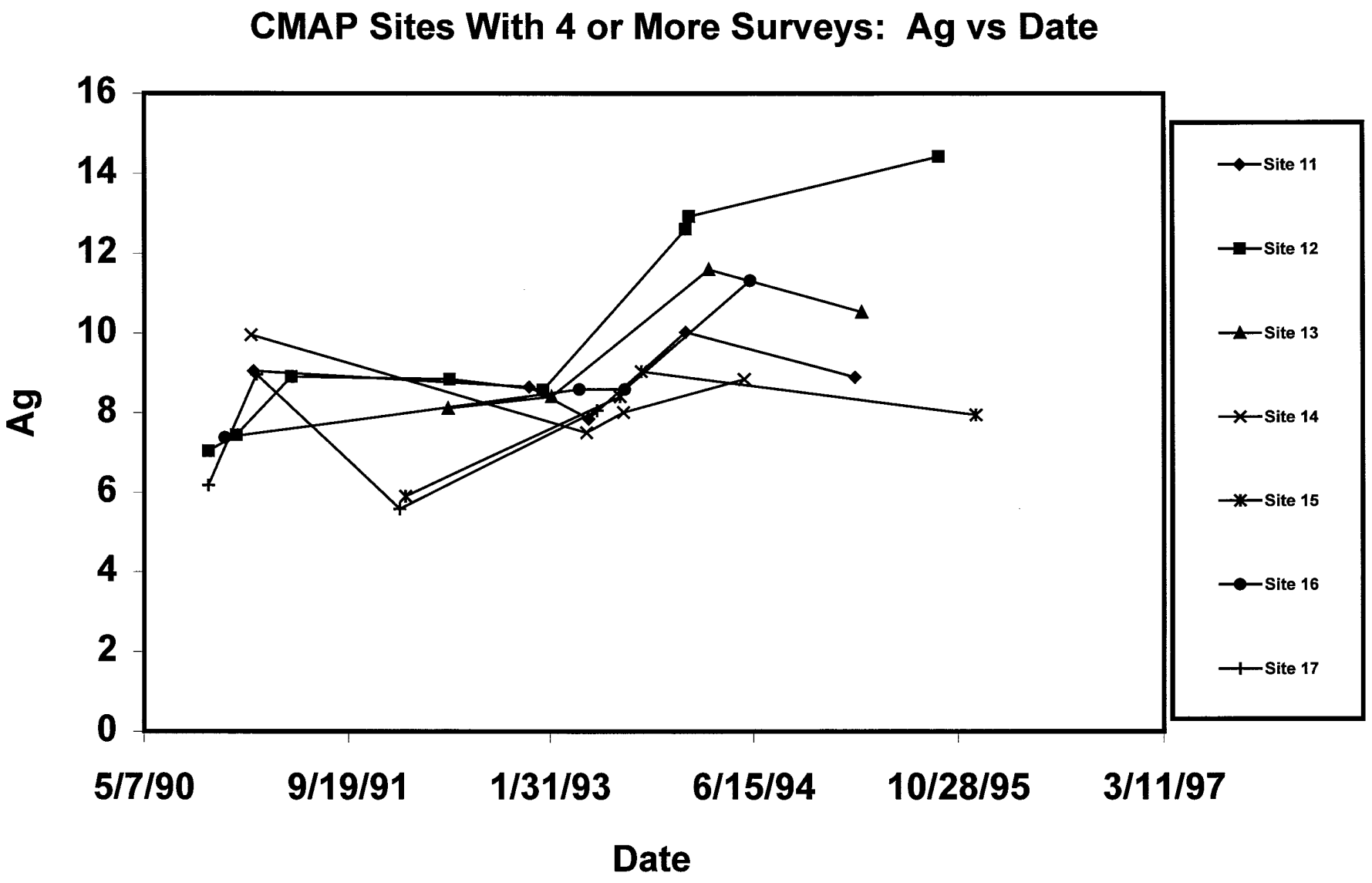
CMAP Sites With 4 or More Surveys: Ag vs Date
Ag
16
14
12
10
8
6
4
2
0
5/7/90
9/19/91
1/31/93
6/15/94
10/28/95
3/11/97
Date
Site 11
Site 12
Site 13
Site 14
Site 15
Site 16
Site 17

Figure 23D

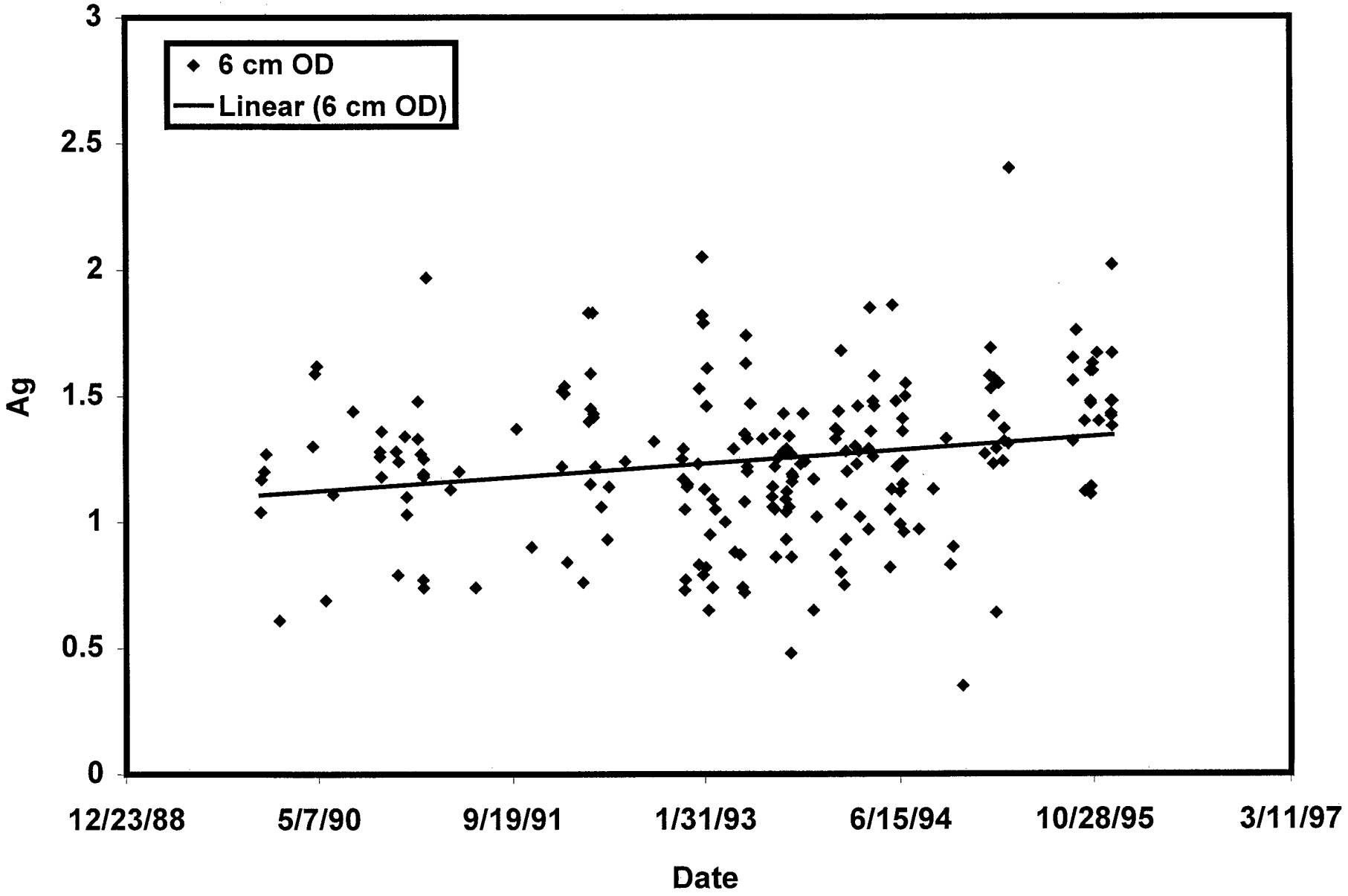
CMAP Sites: 6 cm OD vs. Date
6 cm OD
Linear (6 cm OD)
Ag
3
2.5
2
1.5
1
0.5
0
12/23/88
5/7/90
9/19/91
1/31/93
6/15/94
10/28/95
3/11/97
Date

Figure 24A

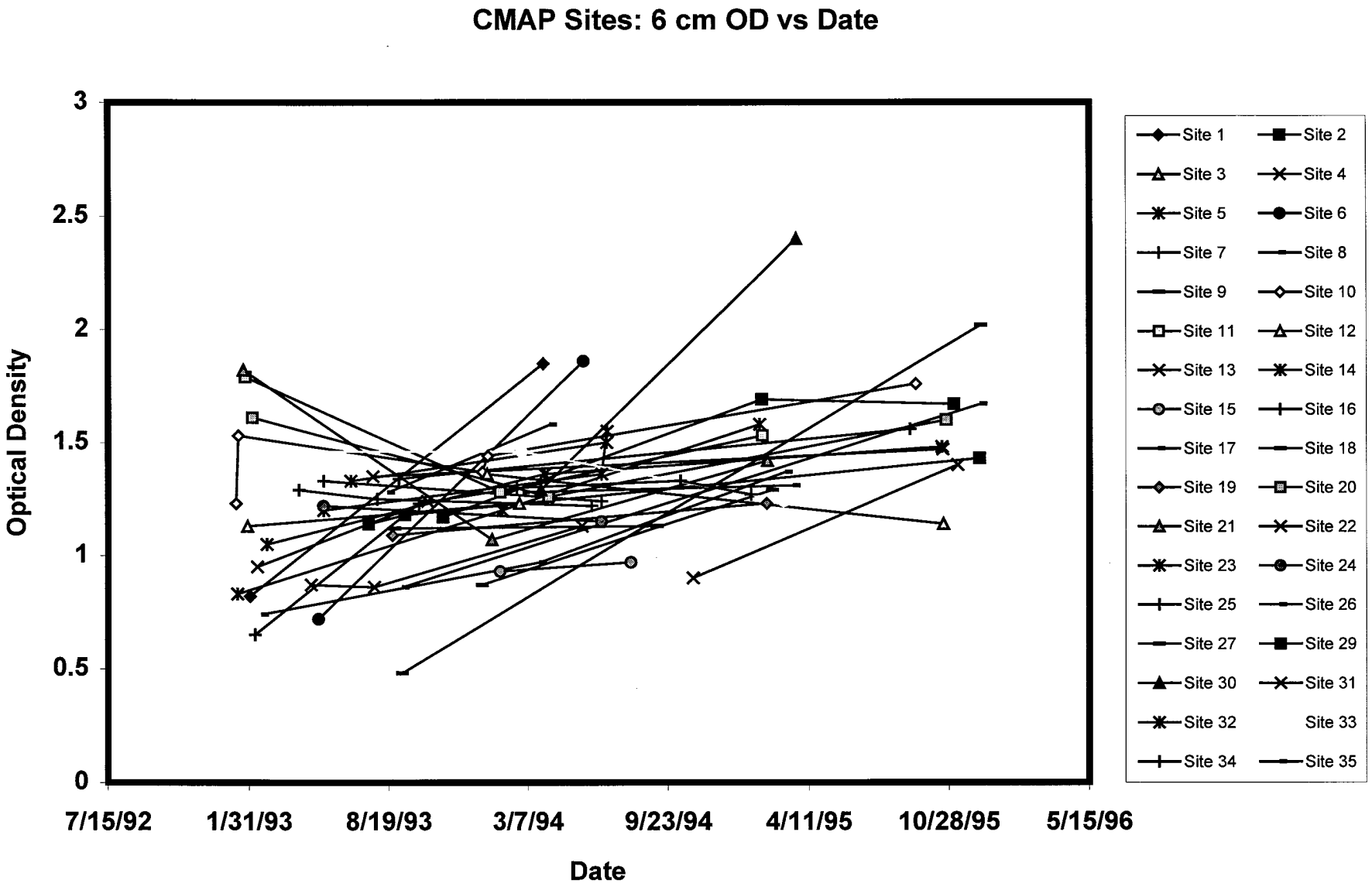
CMAP Sites: 6 cm OD vs Date
Optical Density
3
2.5
2
1.5
1
0.5
0
7/15/92
1/31/93
8/19/93
3/7/94
9/23/94
4/11/95
10/28/95
5/15/96
Date
Site 1
Site 2
Site 3
Site 4
Site 5
Site 6
Site 7
Site 8
Site 9
Site 10
Site 11
Site 12
Site 13
Site 14
Site 15
Site 16
Site 17
Site 18
Site 19
Site 20
Site 21
Site 22
Site 23
Site 24
Site 25
Site 26
Site 27
Site 29
Site 30
Site 31
Site 32
Site 33
Site 34
Site 35

Figure 24B

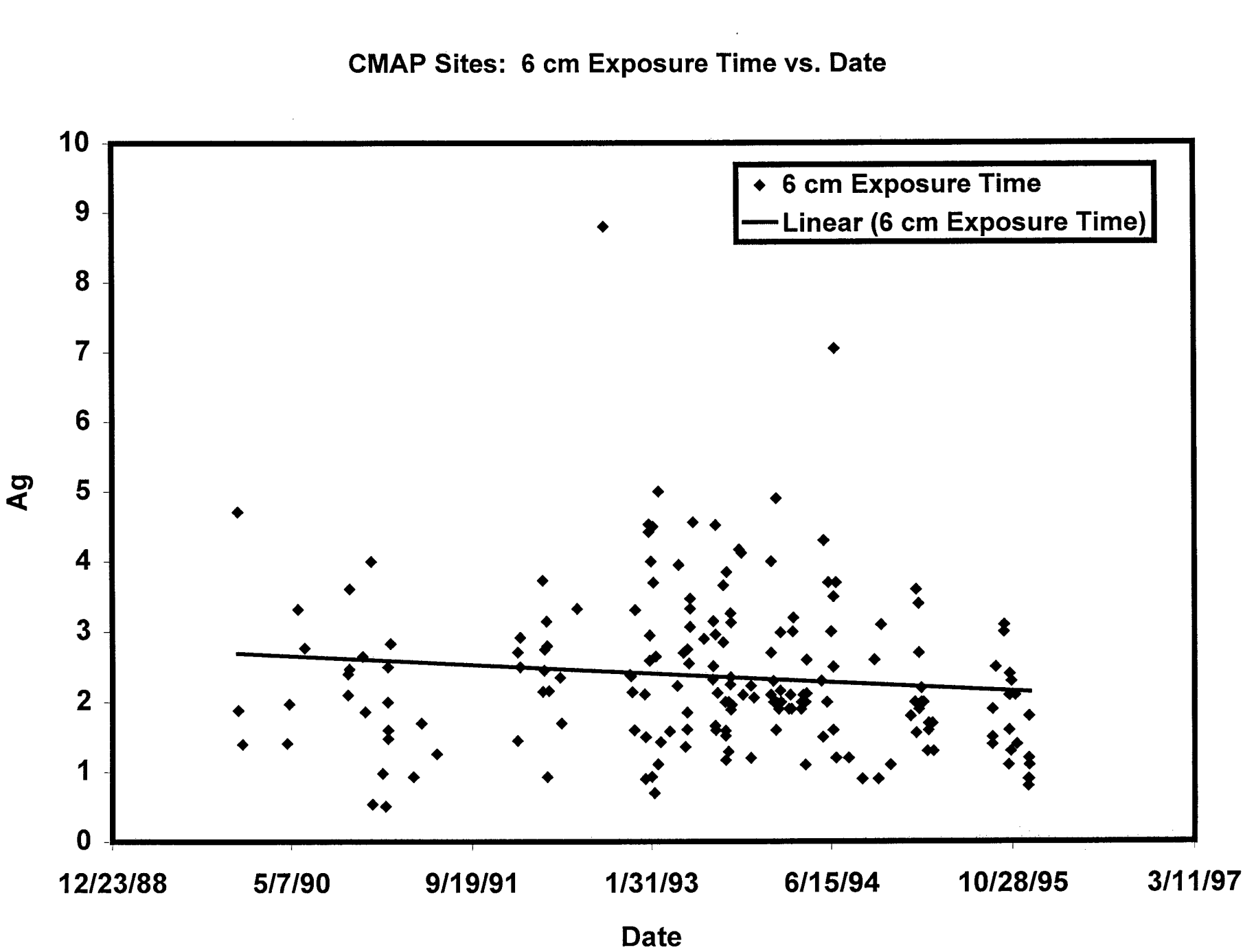
CMAP Sites: 6 cm Exposure Time vs. Date
6 cm Exposure Time
Linear (6 cm Exposure Time)
Ag
10
9
8
7
6
5
4
3
2
1
0
12/23/88
5/7/90
9/19/91
1/31/93
6/15/94
10/28/95
3/11/97
Date

Figure 25A

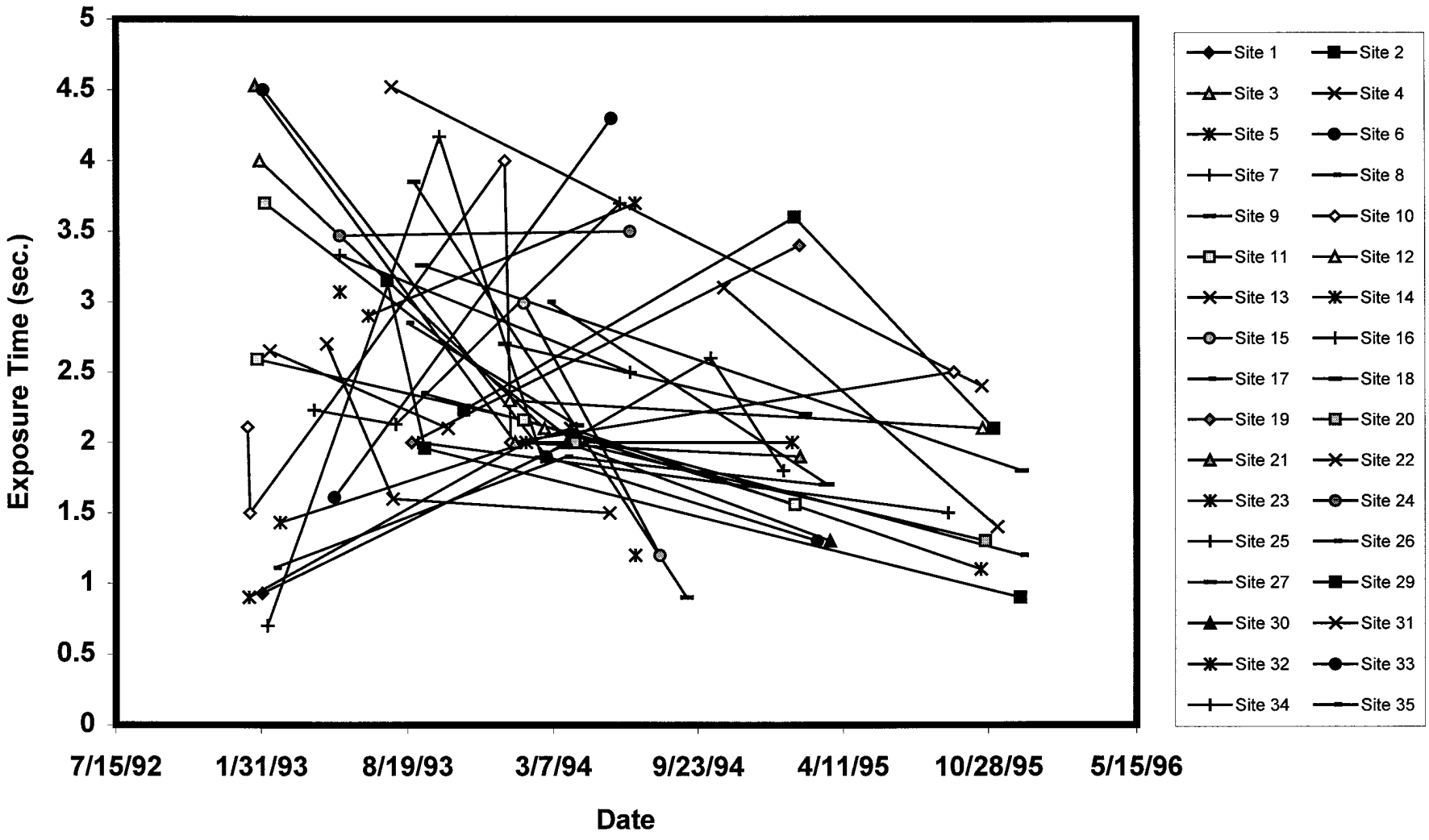
CMAP Sites: 6 cm Exposure Time vs Date
Exposure Time (sec.)
5
4.5
4
3.5
3
2.5
2
1.5
1
0.5
0
7/15/92
1/31/93
8/19/93
3/7/94
9/23/94
4/11/95
10/28/95
5/15/96
Date
Site 1
Site 2
Site 3
Site 4
Site 5
Site 6
Site 7
Site 8
Site 9
Site 10
Site 11
Site 12
Site 13
Site 14
Site 15
Site 16
Site 17
Site 18
Site 19
Site 20
Site 21
Site 22
Site 23
Site 24
Site 25
Site 26
Site 27
Site 29
Site 30
Site 31
Site 32
Site 33
Site 34
Site 35

Figure 25B